AD_____

Award Number: W81XWH-04-1-0301

TITLE: Exploiting Novel-Calcium-Mediated Apoptotic Processes for the Treatment of Human Breast Cancers with Elevated NQO1 Levels

PRINCIPAL INVESTIGATOR: Melissa S. Bentle, B.S.
David A. Boothman, Ph.D.

CONTRACTING ORGANIZATION: Case Western Reserve University
Cleveland OH 44106

REPORT DATE: March 2007

TYPE OF REPORT: Annual Summary

PREPARED FOR: U.S. Army Medical Research and Materiel Command
Fort Detrick, Maryland 21702-5012

REPORT DOCUMENTATION PAGE

Form Approved
OMB No. 0704-0188

1. REPORT DATE *(DD-MM-YYYY)*	**2. REPORT TYPE**	**3. DATES COVERED** *(From - To)*
01-03-2006	Annual Summary	06 Feb 04 - 05 Feb 07

4. TITLE AND SUBTITLE
Exploiting Novel-Calcium-Mediated Apoptotic Processes for the Treatment of Human Breast Cancers with Elevated NQO1 Levels

5a. CONTRACT NUMBER

5b. GRANT NUMBER
W81XWH-04-1-0301

5c. PROGRAM ELEMENT NUMBER

6. AUTHOR(S)
Melissa S. Bentle, B.S.; David A. Boothman, Ph.D.

E-Mail: melissa.bentle@case.edu

5d. PROJECT NUMBER

5e. TASK NUMBER

5f. WORK UNIT NUMBER

7. PERFORMING ORGANIZATION NAME(S) AND ADDRESS(ES)
Case Western Reserve University
Cleveland OH 44106

8. PERFORMING ORGANIZATION REPORT NUMBER

9. SPONSORING / MONITORING AGENCY NAME(S) AND ADDRESS(ES)
U.S. Army Medical Research and Materiel Command
Fort Detrick, Maryland 21702-5012

10. SPONSOR/MONITOR'S ACRONYM(S)

11. SPONSOR/MONITOR'S REPORT NUMBER(S)

12. DISTRIBUTION / AVAILABILITY STATEMENT
Approved for Public Release; Distribution Unlimited

13. SUPPLEMENTARY NOTES -Original contains colored plates: ALL DTIC reproductions will be in black and white.

14. ABSTRACT
None provided.

15. SUBJECT TERMS
Non-homologous end joining, homologous recombination, beta-lapachone, carcinogenesis, caspase-independent cell death, DNA damage

16. SECURITY CLASSIFICATION OF:			**17. LIMITATION OF ABSTRACT**	**18. NUMBER OF PAGES**	**19a. NAME OF RESPONSIBLE PERSON**
a. REPORT	**b. ABSTRACT**	**c. THIS PAGE**			**19b. TELEPHONE NUMBER** *(include area code)*
U	U	U	UU	64	USAMRMC

Standard Form 298 (Rev. 8-98)
Prescribed by ANSI Std. Z39.18

Table of Contents

Page

Introduction and Summary

β-lapachone (β-lap; a.k.a. ARQ 501) is currently in Phase II clinical trials for the treatment of pancreatic adenocarcinoma in combination with gemcitabine. β-Lap is a novel antitumor agent that is bio-activated by the two-electron oxidoreductase NAD(P)H quinone oxidoreductase-1 (NQO1) (E.C. 1.6.99.2). Since NQO1 is highly expressed in many human cancers (e.g. breast, lung, pancreatic, and prostate cancer) it is an attractive target for selective cancer chemotherapy by β-lap alone or in combination with IR (1-3). We previously reported that the initiation of β-lap-induced cell death is triggered by the NQO1-dependent oxidoreduction of β-lap (1). NQO1-mediated metabolism of β-lap results in a futile cycling event wherein β-lap is reduced to an unstable hydroquinone that reverts spontaneously back to its parent structure, using two molecules of oxygen (4). As a result, ROS are generated causing DNA damage, γ-H2AX foci formation, poly(ADP-ribose) polymerase-1 (PARP-1) hyperactivation, and subsequent loss of ATP and NAD^+ (5). This loss of ATP and NAD^+ was proposed to be the mechanism by which β-lap could enhance the sensitivities of a variety of chemotherapeutic therapies as well as IR (6). β-lap-induced cell death was unique in that PARP-1 and p53 were cleaved concomitant with μ-calpain activation, consistent with the fact that global caspase inhibitors had little effect on β-lap-induced proteolysis and lethality (1, 7). Interestingly, β-lap-mediated cell death exhibited classical features of apoptosis (e.g. DNA condensation, and terminal deoxynucleotidyl transferase-mediated dUTP nick-end labeling (TUNEL)-positive cells), but was not dependent on standard apoptotic mediators such as p53, Bax/Bak, or caspases (8).

Previous information from our laboratory demonstrated that β-lap caused DNA damage, γ-H2AX focus formation and PARP-1 hyperactivation selectively in NQO1-positive cells. To date, however, studies have not explored the contribution of DNA DSB repair in β-lap-induced cell death. We investigated whether β-lap exposure of NQO1-positive cancer cells activated HR and/or NHEJ, and explored the extent to which each of these repair systems influences drug resistance. To examine this, we utilized a variety of cell model systems with altered ATM, ATR, and DNA-PKcs functions as well as the use of selective inhibitors to these kinases. β-lap caused the delayed (10-15 min) but dose-dependent activation of the MRN complex, ATM, DNA-PKcs, as well as ATR monitored by Chk1-pSer345. Importantly, only inhibition of DNA-PKcs enhanced the potency of β-lap, indicating a predominant role for NHEJ in the repair of DSBs and resistance of cancer cells after sub-lethal doses of β-lap. Information gathered from these studies warrants the combinatorial usage of DNA repair inhibitors, particularly of NHEJ components, to enhance the toxicity of this agent in the treatment of human cancers that express elevated NQO1 levels.

Body

1. Identification of the transporter(s) responsible for endoplasmic reticulum (ER) Ca^{2+} release after β-lap treatment

Data from our lab has demonstrated that within 3-10 min after β-lap treatment of NQO1 positive cells release of intracellular Ca^{2+} from the endoplasmic reticulum was

observed, and that this release was comparable to thapsigargin (Tg) exposures. Furthermore, BAPTA-AM blocked this early increase in cytosolic Ca^{2+} and overall cell death. However, a number of attempts to recapitulate our previously published findings that Ca^{2+} is released from the ER have been unsuccessful. These findings were presented in last year's annual summary report.

We have therefore sought to examine the role of intranuclear calcium in the early upstream signaling events of β-lap-induced cell death and μ-calpain activation, which have been examined in relation to the modulation of PARP-1 activity (see below).

2. The role of PARP-1 in β-lapachone-induced cell death

** Please refer to the attached paper published in the *Journal of Biological Chemistry*, "Calcium-dependent modulation of PARP-1 alters cellular metabolism and DNA repair" by Bentle *et al.* for data pertaining to the following sections.

β-Lap-induced PARP-1 hyperactivation alters NAD^+ and ATP pools causing cell death

PARP-1 hyperactivation can elicit a dramatic depletion of cellular NAD^+ levels and cause cell death in situations of extreme DNA damage or ischemia-reperfusion (9, 10). Treatment of MCF-7 cells with doses of β-lap ≥5 μM resulted in a rapid and >80% decrease in NAD^+ and ATP levels 1 hr after exposure (Appended Figure 3A-C). To determine if NAD^+ and ATP losses were attributable to PARP-1 hyperactivation, MCF-7 cells were pretreated for 2 hr with PARP inhibitors 3-aminobenzamide (3-AB) or 3,4-dihydro-5[4-(1-piperindinyl)butoxy]-1(2H)-isoquinoline (DPQ), prior to 5 μM β-lap exposure. NAD^+ and ATP loss in β-lap-treated MCF-7 cells was partially abrogated by 3-AB or DPQ (Appended Figure 3B and 3C). Neither 3-AB nor DPQ (used at >2-fold doses than in the above experiments) altered NQO1 activity in *in vitro* enzyme assays. Finally, 3-AB did not affect β-lap-induced ROS formation.

To confirm the findings using PARP-1 inhibitors, we generated a MDA-MB-231 NQO1+ and NQO1- cell line that had PARP-1 protein levels knocked-down (KD) using shRNA. 231-NQ+ PARP-1-shRNA cells had lower levels of PAR accumulation after β-lap treatment then 231-NQ+ non-silencing-shRNA (ns-shRNA) cells (Appended Figure 4C). Furthermore, KD of PARP-1 protein levels was sufficient to protect cells from β-lap-induced apoptosis (Appendend Figure 4E).

Cumulatively, these data strongly suggest that Ca^{2+}-dependent PARP-1 hyperactivation caused NAD^+ and ATP loss in NQO1+ human breast cancer cell lines after β-lap treatment.

β-lap causes NQO1-dependent DNA damage

Since PARP-1 activation typically requires DNA damage, we examined cells exposed to β-lap for the presence and magnitude of DNA strand breaks, by measuring γ-H2AX. H2AX contains a highly conserved serine residue (ser139), which is rapidly phosphorylated upon DNA damage (11). Significant γ-H2AX foci formation was observed by 30 min, similar to that seen 15 min following 5 Gy ionizing radiation (IR) (Appended Figure 5A and 5B). Total H2AX and α-tubulin levels remained constant for the duration of the β-lap exposure. These results were confirmed by confocal microscopy.

Since Ca^{2+} chelation blocked both β-lap-induced PARP-1 hyperactivation and cell death, we tested the effects of BAPTA-AM on γ-H2AX foci formation. Similar to the immunoblot analyses and the PAR formation kinetics, β-lap-treated MCF-7 cells showed γ-H2AX foci at 30 min, with peak levels at 60 min. Importantly, β-lap-induced γ-H2AX foci formation was partially abrogated by BATPA-AM addition, with few γ-H2AX foci noted in 30-60 min (Appended Figure 5C).

Ca^{2+} chelation allows for DNA repair after β-lap treatment

We postulated that metabolism of β-lap by NQO1 would generate superoxide, peroxide, and other ROS (12). Since BAPTA-AM has moderate affinity for divalent cations other than Ca^{2+}, we explored the possibility that BAPTA-AM protected cells from DNA damage and subsequent cell death by interfering with Fenton chemistry. The oxidative state of MDA-MB-468-NQ+ cells was monitored after treatment with 4 μM β-lap in the presence or absence of 5 μM BAPTA-AM. β-Lap treatment caused an ~65% rise in disulfide glutathione (GSSG) levels, that persisted during drug exposure (Appended Figure 6A). Addition of BAPTA-AM did not alter the kinetics or levels of GSSG formation after β-lap exposure (Appended Figure 6A). These data suggest that the protective effects of BAPTA-AM on β-lap-treated NQO1+ cells were not due to interference with β-lap-induced ROS formation. Similar results were found in MCF-7 and 231-NQ+ cells.

To assess the effects of Ca^{2+} on DNA damage and repair, β-lap-treated MCF-7 cells were analyzed by alkaline comet assays to monitor total DNA strand breaks with or without BAPTA-AM addition. β-Lap-treated cells exhibited significant DNA strand breakage by 30 min, resembling the positive control (H_2O_2), and after 30 min, β-lap-induced DNA damage exceeded those levels. Cells pretreated with BAPTA-AM exhibited far less DNA damage compared to β-lap alone and their repair of DNA damage correlated well with their ability to survive (Appended Figure 6B *left panel*).

We then examined the kinetics of repair in MCF-7 cells following 2 hr β-lap exposures with or without BAPTA-AM addition. After β-lap exposure, DNA damage persisted and gradually increased over time, indicative of inhibition of DNA repair and consistent with the rapid drop in NAD^+ and ATP levels. In contrast, cells treated with β-lap and BAPTA-AM exhibited less DNA damage at 2 hr, and showed a time-dependent recovery (Appended Figure 6B *right panel*). Thus, NQO1-mediated metabolism of β-lap leads to the generation of ROS and subsequent DNA damage that hyperactivates PARP-1. Ca^{2+}-dependent PARP-1 hyperactivation drives the loss of NAD^+ and ATP levels, which suppresses DNA repair and survival.

Interestingly, we found that the mechanism of β-lap-induced cell death was similar to that of H_2O_2. These findings are discussed in further detail in the appended manuscript (Appended Figure 7).

3. The role of double-strand break repair in β-lapachone induced cell death

** Please refer to the attached manuscript entitled, "Non-homologous end joining is essential for cellular resistance to the novel antitumor agent, β-lapachone" by Bentle, *et al.* for data pertaining to the following sections.

The MRE11/Rad50/Nbs-1 (MRN) complex is activated by β-Lap.

Previously, we showed that exposure of NQO1-expressing cancer cells to β-lap caused ROS and DNA damage, measured by alkaline comet assay and γ-H2AX formation (5). Furthermore, activation of the MRN complex following β-lap exposure was recently reported in the yeast system *Saccharomyces cerevisiae* (13). Therefore, we wanted to determine if and which DSB repair pathways were activated in response to this agent by examining MRN complex recruitment to the break sites.

A marked increase in the organized localization of MRE-11 and Rad50 were observed in the nuclei of β-lap treated cells at 15 min and foci persisted through 60 min (Appended Fig. 1*A* and Fig. 1*B*). Similarly, nuclear foci for Nbs-1-p were also visible beginning at 15 minutes after drug exposure, similar to the kinetics of γ-H2AX (Appended Fig. 1*A* and Fig. 1*B*); both proteins are downstream targets of ATM activation (14). The appearance of these foci was delayed compared to foci observed after IR exposure, where prior studies have demonstrated γ-H2AX foci formation within 1-5 mins post-IR (15).

Dose-dependent activation of ATM and DNA-PK following β-lap treatment.

Since the MRN complex was recruited after exposure to β-lap, we tested for the activation of ATM; an HR-associated PI3K. To test for ATM activation, MCF-7 cells were mock-treated or exposed to varying doses of β-lap. Fixed cells were stained with a serine 1981 phospho-specific antibody to ATM (ATM-pSer1981). The activation of ATM occurred in a dose-dependent manner after β-lap treatment. Doses of β-lap (0-3 μM), resulted in few activated ATM molecules, consistent with the low level of DNA damage detected at these doses (Appended Supplementary Fig. 2 and Fig. 2*A*). In contrast, lethal doses of (≥4 μM) β-lap caused considerable ATM activation with an ~8 fold increase in the number of foci/cell, corresponding to the net increase in total damage (Appended Supplemental Fig. 2 and Fig 2*A* and 2*C*). These data suggest that the accumulation of large numbers of β-lap-induced SSBs leads to the creation of DSBs. These DSBs cause the activation of the canonical HR DSB repair pathway involving the MRN complex and ATM.

Due to the cell-cycle independence of NQO1-mediated bioactivation of β-lap (16) and generation of DNA damage, we examined DNA-PK activation, which is known to also be activated in a cell-cycle independent manner (8). MCF-7 cells were mock-treated or exposed to 1-5 μM β-lap for 30 min. Similar to ATM activation, DNA-PKcs-pThr2609 foci formed in a dose-dependent manner, wherein non-toxic doses of drug caused little DNA-PKcs-pThr2609 foci over background, whereas cytotoxic doses led to increases in DNA-PKcs-pThr2609 foci that co-localized with γ-H2AX (17) (Fig. 2*B*).

NHEJ is necessary for β-lap-induced cell death.

Due to the robust activation of DNA-PK, we examined the consequences of its inhibition on β-lap lethality. Glioblastoma cell lines, MO59K cells that contain DNA-PKcs and MO59J cells that lack DNA-PKcs were used (18). MO59J-NQ^+ and MO59K-NQ^+ were mock-treated or exposed to various doses of β-lap for 2 h, with or without DIC

cotreatment; a selective NQO1 inhibitor. DNA-PKcs-deficient MO59J-NQ^+ cells were significantly more sensitive to β-lap than their DNA-PKcs-proficient counterparts, MO59K-NQ^+ cells (Appended Fig. 3*A*). MO59J-NQ^+ cells required doses of ≥ 5 μM β-lap to elicit cell death whereas MO59K-NQ^+ cells were resistant to the drug, with only 30% cytotoxicity by 12 μM β-lap. In both cell lines, cytotoxicity was abrogated by inhibiting NQO1 activity with 40 μM DIC (Appended Fig. 3*A*). To assess the functionality of DNA-PKcs in the MO59K-NQ^+ cell line, we pretreated both MO59J-NQ^+ and MO59K-NQ^+ with the DNA-PKcs selective inhibitor Nu7026 prior to β-lap treatment. Nu7026 is a potent radiosensitizer in both proliferating and quiescent cells (19). As anticipated, Nu7026 had little effect on cell death in MO59J-NQ^+ cells, since they are devoid of DNA-PKcs activity. However, Nu7026 significantly sensitized MO59K-NQ^+ cells to β-lap (Appended Fig. 3*B*). Treatment with Nu7026 and 12 μM β-lap resulted in an ~80% ± 3.4 reduction in cell viability compared to ~5% ± 1.0 loss of survival in MO59K-NQ^+ cells that were not pretreated with Nu7026 (Appended Fig. 3*B*).

We previously demonstrated that β-lap-induced cell death was mediated by the hyperactivation of PARP-1 (5). Since a deficiency in DNA-PKcs, potentiated β-lap-induced cell death, we examined whether inhibition of NHEJ was accompanied by hyperactivation of PARP-1 at normally sub-lethal doses of β-lap. PARP-1 is associated with both DNA SSB and DSB repair. After binding to DNA breaks, PARP-1 converts β-NAD^+ into polymers of branched or linear poly(ADP-ribose) (PAR) units and attaches them to various nuclear receptor proteins, including PARP-1 itself as part of its autoregulation (20). MO59J-NQ^+ and MO59K-NQ^+ cells were treated with varying doses of β-lap and cell extracts were taken after 20 min. Lethal doses of β-lap in MO59J-NQ^+ cells resulted in considerable PAR accumulation, while the same dose that was found to be non-toxic in the MO59K-NQ^+ cells resulted in little PAR accumulation (Appended Fig. 3*E*). Increasing amounts of PAR polymers were noted in the MO59K-NQ^+ cells with increasing ≥5 μM β-lap doses (Appended Fig. 3*E*).

The HR-associated PI3K ATM is not necessary for β-lap-induced cell death.

Since ATM autophosphorylation was also observed following β-lap treatment in NQO1-proficient cancer cells, we investigated whether loss of ATM would alter β-lap-mediated cytotoxicity. Isogenic NQO1-positive human immortalized fibroblasts from A-T patients deficient in ATM ($AT^{-/-}$) or proficient via ectopic ATM expression ($AT^{+/+}$) were used (21). $AT^{+/+}$ and $AT^{-/-}$ cells were mock-treated or exposed to varying doses of β-lap in the presence or absence of DIC for 4 h. There was no observable difference in β-lap-induced lethality between NQO1-proficient $AT^{+/+}$ or $AT^{-/-}$ cells. Furthermore, both cells were protected from lethality via DIC cotreatment (Appended Fig. 6*A*).

To corroborate these findings, MCF-7 cells were mock-treated or exposed to sub-lethal-to-lethal doses of β-lap in the presence or absence of the ATM kinase inhibitor KU55933 or the general ATM/ATR inhibitor AAI for 2 h or 4 h (22). Although weak ATM activation was observed after sub-lethal doses of β-lap, inhibition of ATM by KU55933 or AAI had little effect on the lethality of β-lap when treated for either 2 h or 4 h (Appended Fig. 2*A* and 4*B*-*C*).

ATR activation after β-lap exposure.

In addition to ATM, HR can also be mediated via ATR, which is recruited to single-stranded DNA regions, which primarily arise in response to replication fork arrest or during the processing of bulky lesions such as UV photoproducts (23). Since β-lap causes ROS generation, we postulate that the DNA SSBs are the primary lesions formed. However, because of the robust DNA DSB damage responses, DSBs could be formed as a result of stalled replication forks. Therefore, we wanted to examine the activation of ATR in response to β-lap treatment by utilizing a set of stable cell lines derived from U2OS cells (human osteosarcoma). ATR activation after β-lap treatment was confirmed by monitoring Chk1-pSer345 levels in WT U2OS cells after treatment with both UVC or β-lap (Appended Fig. 5*A*). However, in U2OS KD-ATR cells, Chk1-pSer345 was muted after both UVC and β-lap exposure (Appended Fig. 5*A*). Furthermore, neither expression of wild-type ATR nor inhibition of ATR (by KD-ATR expression) affected the survival of NQO1-proficient U2OS cells following β-lap exposure (Appended Fig. 5*B*). Furthermore, administration of DIC abrogated β-lap-induced lethality in both cells lines; confirming its role as the key determinant in β-lap-mediated cytotoxicity (Appended Fig. 5*B*).

ATR activation argues for the presence of DNA SSBs at arrested replication forks. To elucidate the type of DNA damage created by β-lap, NQO1-positive MCF-7 cells were treated with lethal (5 μM) as well as sub-lethal (0-2 μM) doses of β-lap and the formation of total DNA strand breaks (measured by alkaline comet assays) as well as DSBs (monitored by neutral comet assays) were assessed. Sub-lethal doses of β-lap resulted in little to no strand breakage over time, consistent with their survival at these same doses (Appended Supplementary Fig. 2) (5). In contrast, lethal doses of β-lap resulted in a significant increase in total DNA breaks, occurring minutes after drug exposure (Appended Fig. 5*C*) and surpassing the positive control, 500 μM H_2O_2 30 min thereafter (Appended Supplementary Fig. 4). Further analyses indicated that ROS formation and DNA damage were detected within ≤ 5 min after drug addition (5). The amount of DNA strand breaks increased over time after 5 μM β-lap treatment, suggesting that the lethal event may be related to the total amount of DNA breaks generated[2]. Interestingly, when cells were analyzed using neutral conditions, under the same conditions, little to no DSBs were observed, in contrast to ETO treatment (Appended Fig. 5*C* and Supplemental Fig. 4). As expected, H_2O_2 treatment caused few DNA DSBs, similar to what was observed after β-lap exposure (Appended Supplemental Fig. 4). The formation of DNA breaks after β-lap exposure was NQO1-dependent as coadminstration with DIC prevented any damage (5). These studies indicate that the majority of DNA damage caused by the NQO1-mediated metabolism of β-lap was SSBs, consistent with the genesis of "long-lived" ROS (e.g. H_2O_2).

Key Research Accomplishments:

- β-Lap causes Ca^{2+}-mediated PARP-1 hyperactivation at lethal doses
- Ca^{2+} chelation allows for DNA repair after β-lap treatment
- β-Lap causes NQO1-dependent DNA damage
- DSB repair pathways are activated after treatment with β-Lap (HR and NHEJ)

- Inhibition of NHEJ potentiates β-Lap-induced cell death at sub-lethal doses

Reportable Outcomes:

- **Bentle, M.S.,** Bey, E.A., Dong, Y., Reinicke, K.E., and Boothman, D.A. New Tricks for Old Drugs: The Anticarcinogenic Potential of DNA Repair Inhibitors. (2006) *The Journal of Molecular Histology*, **37**(5-7), 203-218.
- **Bentle, M.S**., Reinicke, K.E., Bey, E.A., Spitz, D.R., and Boothman, D.A. Calcium-dependent modulation of poly(ADP-ribose) polymerase-1 alters cellular metabolism and DNA repair. (2006) *Journal of Biological Chemistry*, **281**, 33684-33696
- **Bentle, M.S**., Reinicke, K.E., Dong, Y., and Boothman, D.A. Non-homologous end joining is essential for cellular resistance to the novel antitumor agent, β-lapachone. (2006) *Cancer Research*, submitted.
- Meeting Abstracts and Presentations:
  - **Bentle, M.S.** and Boothman, D.A. Calcium-mediated poly(ADP-ribose) polymerase hyperactivation in β-lapachone-induced programmed necrosis. Department of Pharmacology Retreat, Case Western Reserve University, Cleveland, OH, October, 2006.
  - **Bentle, M.S.** and Boothman, D.A. Calcium-mediated poly(ADP-ribose) polymerase hyperactivation in β-lapachone-induced programmed necrosis. Keystone Symposium on Metabolomics, Snow Bird, UT April 2006.
  - **Bentle, M.S.,** and Boothman, D.A. The role of calcium release and poly(ADP-ribose) polymerase-1 activation in β-lapachone-mediated cell death. Biomedical Graduate Student Symposium, Case Western Reserve University, Cleveland, OH, April, 2006.
- Associate Member, American Association for Cancer Research
- The Marcus Singer Poster Award, Biomedical Graduate Student Symposium, Case Western Reserve University, Cleveland, OH for presentation entitled, "The role of calcium release and poly(ADP-ribose) polymerase-1 activation in β-lapachone-mediated cell death" April, 2006

Conclusions

Scientific findings…

Here we demonstrate that PARP-1 hyperactivation occurs shortly after β-lap exposure in an NQO1-dependent manner. Hyperactivation of PARP-1 is consistent with the presence of DNA strand breaks as detected by both γ-H2AX foci formation and alkaline comet assays. Inhibition of PARP-1 activity either by protein knock-down using shRNA to PARP-1 or chemical inhibition abrogated β-lap-induced apoptosis, NAD^+, and ATP pool depletion. Chelation of intracellular Ca^{2+} using BAPTA-AM prevented PARP-1 hyperactivation, γ-H2AX, μ-calpain activation, cell death but not comet formation.

In addition to SSB-induced DNA repair pathways, β-lap causes the activation of a variety of DSB repair pathways. In particular, NEHJ was found to be key to the survival

of cells exposed β-lap, since inhibition of NHEJ caused a PARP-1-mediated cell death after treatment with sub-lethal doses of β-lap. In summary, these data warrant the combinatorial use of β-lap with inhibitors of NHEJ thereby increasing the therapeutic efficacy of this compound by targeting two distinct repair mechanisms.

As a breast cancer researcher in training…
As the primary researcher driving these studies, I have had the first-hand opportunity to experience the molecular problems affecting breast cancer treatment and pathogenesis at both the molecular and clinical levels. Investigating the molecular mechanisms of β-lap has given me a strong foundation in basic research, which is paramount to achieving my career goals as both an educator and an independent primary breast cancer researcher. As a result of these experiences, I was able to contribute to the scientific community, via publication in peer-reviewed journals, knowledge on another promising breast cancer chemotherapeutic agent, β-lap (a.k.a. ARQ 501) that is currently under PhaseI/II clinical trials.

References

1. Pink, J. J., Planchon, S. M., Tagliarino, C., Varnes, M. E., Siegel, D., and Boothman, D. A. NAD(P)H:Quinone oxidoreductase activity is the principal determinant of beta-lapachone cytotoxicity. J Biol Chem, *275:* 5416-5424, 2000.
2. Boothman, D. A. and Pardee, A. B. Inhibition of radiation-induced neoplastic transformation by beta-lapachone. Proc Natl Acad Sci U S A, *86:* 4963-4967, 1989.
3. Suzuki, M., Amano, M., Choi, J., Park, H. J., Williams, B. W., Ono, K., and Song, C. W. Synergistic effects of radiation and beta-lapachone in DU-145 human prostate cancer cells in vitro. Radiat Res, *165:* 525-531, 2006.
4. Bentle, M. S., Bey, E. A., Dong, Y., Reinicke, K. E., and Boothman, D. A. New tricks for old drugs: the anticarcinogenic potential of DNA repair inhibitors. J Mol Histol, *37:* 203-218, 2006.
5. Bentle, M. S., Reinicke, K. E., Bey, E. A., Spitz, D. R., and Boothman, D. A. Calcium-dependent modulation of poly(ADP-ribose) polymerase-1 alters cellular metabolism and DNA repair. J Biol Chem, *281:* 33684-33696, 2006.
6. Wang, A., Li, C. J., Reddy, P. V., and Pardee, A. B. Cancer chemotherapy by deoxynucleotide depletion and E2F-1 elevation. Cancer Res, *65:* 7809-7814, 2005.
7. Tagliarino, C., Pink, J. J., Reinicke, K. E., Simmers, S. M., Wuerzberger-Davis, S. M., and Boothman, D. A. Mu-calpain activation in beta-lapachone-mediated apoptosis. Cancer Biol Ther, *2:* 141-152, 2003.
8. Wuerzberger, S. M., Pink, J. J., Planchon, S. M., Byers, K. L., Bornmann, W. G., and Boothman, D. A. Induction of apoptosis in MCF-7:WS8 breast cancer cells by beta-lapachone. Cancer Res, *58:* 1876-1885, 1998.
9. Szabo, C. and Dawson, V. L. Role of poly(ADP-ribose) synthetase in inflammation and ischaemia-reperfusion. Trends Pharmacol Sci, *19:* 287-298, 1998.

10. Pieper, A. A., Verma, A., Zhang, J., and Snyder, S. H. Poly (ADP-ribose) polymerase, nitric oxide and cell death. Trends Pharmacol Sci, *20:* 171-181, 1999.
11. Rogakou, E. P., Pilch, D. R., Orr, A. H., Ivanova, V. S., and Bonner, W. M. DNA double-stranded breaks induce histone H2AX phosphorylation on serine 139. J Biol Chem, *273:* 5858-5868, 1998.
12. Reinicke, K. E., Bey, E. A., Bentle, M. S., Pink, J. J., Ingalls, S. T., Hoppel, C. L., Misico, R. I., Arzac, G. M., Burton, G., Bornmann, W. G., Sutton, D., Gao, J., and Boothman, D. A. Development of beta-lapachone prodrugs for therapy against human cancer cells with elevated NAD(P)H:quinone oxidoreductase 1 levels. Clin Cancer Res, *11:* 3055-3064, 2005.
13. Menacho-Marquez, M. and Murguia, J. R. beta-lapachone Activates a Mre11p-Tel1p G1/S Checkpoint in Budding Yeast. Cell Cycle, *5*, 2006.
14. Kurz, E. U. and Lees-Miller, S. P. DNA damage-induced activation of ATM and ATM-dependent signaling pathways. DNA Repair (Amst), *3:* 889-900, 2004.
15. Rothkamm, K. and Lobrich, M. Evidence for a lack of DNA double-strand break repair in human cells exposed to very low x-ray doses. Proc Natl Acad Sci U S A, *100:* 5057-5062, 2003.
16. Pink, J. J., Wuerzberger-Davis, S., Tagliarino, C., Planchon, S. M., Yang, X., Froelich, C. J., and Boothman, D. A. Activation of a cysteine protease in MCF-7 and T47D breast cancer cells during beta-lapachone-mediated apoptosis. Exp Cell Res, *255:* 144-155, 2000.
17. Chan, D. W., Chen, B. P., Prithivirajsingh, S., Kurimasa, A., Story, M. D., Qin, J., and Chen, D. J. Autophosphorylation of the DNA-dependent protein kinase catalytic subunit is required for rejoining of DNA double-strand breaks. Genes Dev, *16:* 2333-2338, 2002.
18. Allalunis-Turner, M. J., Barron, G. M., Day, R. S., 3rd, Dobler, K. D., and Mirzayans, R. Isolation of two cell lines from a human malignant glioma specimen differing in sensitivity to radiation and chemotherapeutic drugs. Radiat Res, *134:* 349-354, 1993.
19. Veuger, S. J., Curtin, N. J., Richardson, C. J., Smith, G. C., and Durkacz, B. W. Radiosensitization and DNA repair inhibition by the combined use of novel inhibitors of DNA-dependent protein kinase and poly(ADP-ribose) polymerase-1. Cancer Res, *63:* 6008-6015, 2003.
20. Kim, M. Y., Zhang, T., and Kraus, W. L. Poly(ADP-ribosyl)ation by PARP-1: 'PAR-laying' NAD+ into a nuclear signal. Genes Dev, *19:* 1951-1967, 2005.
21. Ziv, Y., Bar-Shira, A., Pecker, I., Russell, P., Jorgensen, T. J., Tsarfati, I., and Shiloh, Y. Recombinant ATM protein complements the cellular A-T phenotype. Oncogene, *15:* 159-167, 1997.
22. Hickson, I., Zhao, Y., Richardson, C. J., Green, S. J., Martin, N. M., Orr, A. I., Reaper, P. M., Jackson, S. P., Curtin, N. J., and Smith, G. C. Identification and characterization of a novel and specific inhibitor of the ataxia-telangiectasia mutated kinase ATM. Cancer Res, *64:* 9152-9159, 2004.
23. Cortez, D., Guntuku, S., Qin, J., and Elledge, S. J. ATR and ATRIP: partners in checkpoint signaling. Science, *294:* 1713-1716, 2001.

Appendices

1. Bentle, M.S., Reinicke, K.E., Bey, E.A., Spitz, D.R., and Boothman, D.A. Calcium-dependent modulation of poly(ADP-ribose) polymerase-1 alters cellular metabolism and DNA repair. (2006) *Journal of Biological Chemistry*, **281**, 33684-33696

2. Bentle, M.S., Reinicke, K.E., Dong, Y., and Boothman, D.A. Non-homologous end joining is essential for cellular resistance to the novel antitumor agent, β-lapachone. (2006) *Cancer Research*, submitted.

THE JOURNAL OF BIOLOGICAL CHEMISTRY VOL. 281, NO. 44, pp. 33684–33696, November 3, 2006

Calcium-dependent Modulation of Poly(ADP-ribose) Polymerase-1 Alters Cellular Metabolism and DNA Repair*[S]

Received for publication, April 17, 2006, and in revised form, August 17, 2006 Published, JBC Papers in Press, August 17, 2006, DOI 10.1074/jbc.M603678200

Melissa S. Bentle[‡], Kathryn E. Reinicke[§], Erik A. Bey[¶], Douglas R. Spitz[‖], and David A. Boothman[‡§¶1]

From the Departments of [‡]Pharmacology and [§]Biochemistry, Case Western Reserve University, Cleveland, Ohio 44106, the [¶]Department of Pharmacology, Laboratory of Molecular Stress Responses, and the Simmons Comprehensive Cancer Center, University of Texas Southwestern Medical Center, Dallas, Texas 75390, and the [‖]Department of Radiation Oncology, Free Radical and Radiation Biology Program, Holden Comprehensive Cancer Center, University of Iowa, Iowa City, Iowa 52242

After genotoxic stress poly(ADP-ribose) polymerase-1 (PARP-1) can be hyperactivated, causing (ADP-ribosyl)ation of nuclear proteins (including itself), resulting in NAD^+ and ATP depletion and cell death. Mechanisms of PARP-1-mediated cell death and downstream proteolysis remain enigmatic. β-lapachone (β-lap) is the first chemotherapeutic agent to elicit a Ca^{2+}-mediated cell death by PARP-1 hyperactivation at clinically relevent doses in cancer cells expressing elevated NAD(P)H:quinone oxidoreductase 1 (NQO1) levels. β-lap induces the generation of NQO1-dependent reactive oxygen species (ROS), DNA breaks, and triggers Ca^{2+}-dependent γ-H2AX formation and PARP-1 hyperactivation. Subsequent NAD^+ and ATP losses suppress DNA repair and cause cell death. Reduction of PARP-1 activity or Ca^{2+} chelation protects cells. Interestingly, Ca^{2+} chelation abrogates hydrogen peroxide (H_2O_2), but not *N*-Methyl-*N*′-nitro-*N*-nitrosoguanidine (MNNG)-induced PARP-1 hyperactivation and cell death. Thus, Ca^{2+} appears to be an important co-factor in PARP-1 hyperactivation after ROS-induced DNA damage, which alters cellular metabolism and DNA repair.

Alterations in the initiation and regulation of caspase-mediated apoptosis are associated with an array of pathological disease states, including chemotherapy resistance in cancer (1). Therefore, elucidating mechanisms that initiate non-caspase-mediated cell death are crucial for the development and use of novel anticancer agents.

A growing number of chemotherapeutic approaches focus on targeting specific DNA repair enzymes. In particular, inhibitors of poly(ADP-ribose) polymerase-1 (PARP-1)[2] that sensitize cells to DNA-damaging agents are under extensive investigation (2). PARP-1 functions as a DNA damage sensor that responds to both single- and/or double-strand DNA breaks (SSBs, DSBs), facilitating DNA repair and cell survival. After binding to DNA breaks, PARP-1 converts β-NAD^+ (NAD^+) into polymers of branched or linear poly(ADP-ribose) units (PAR) and attaches them to various nuclear acceptor proteins, including XRCC1, histones, and PARP-1 for its autoregulation (3). However, in response to extensive DNA damage, PARP-1 can be hyperactivated, eliciting rapid cellular NAD^+ and ATP pool depletion. PARP-1-mediated NAD^+ and ATP losses have affects on mitochondrial function by decreasing the levels of pyruvate and NADH. Loss of mitochondrial membrane potential (MMP) ensues, causing caspase-independent cell death by as yet unknown mechanisms (3). PARP-1 hyperactivation was documented in the cellular response to trauma, such as ischemia-reperfusion, myocardial infarction, and reactive oxygen species (ROS)-induced injury (3). In each case, inhibition of PARP-1 was necessary for the long-term survival of damaged cells (4).

β-lapachone (β-lap) elicits a unique cell death process in various human breast, lung, and prostate cancers that have elevated levels of the two-electron oxidoreductase, NAD(P)H:quinone oxidoreductase 1 (NQO1) (EC 1.6.99.2) (5). β-lap induces an NQO1-dependent form of cell death wherein PARP-1 and p53 proteolytic cleavage fragments were noted (6), concomitant with μ-calpain activation (7). β-lap-induced lethality and proteolysis were abrogated by dicoumarol (an NQO1 inhibitor), and were muted in cells deficient in NQO1

* This work was supported in part by National Institutes of Health/NCI Grant 1R01CA10279201 (to D. A. B.), 1R01CA100045 (to D. R. S.), CWRU Core Grants P30CA43703 and P30CA43703-12, as well as Department of Defense Breast Cancer Program Predoctoral Fellowships, W81XWH-04-1-0301 and W81XWH-05-1-0248 (to M. S. B. and K. E. R.), respectively. This is manuscript CSCN 001 from the Cell Stress and Cancer Nanomedicine program in the Simmons Comprehensive Cancer Center at the University of Texas Southwestern Medical Center at Dallas. The costs of publication of this article were defrayed in part by the payment of page charges. This article must therefore be hereby marked "*advertisement*" in accordance with 18 U.S.C. Section 1734 solely to indicate this fact.

[S] The on-line version of this article (available at http://www.jbc.org) contains supplemental experimental procedures, Figs. S1–S5, and Table S1.

[1] To whom correspondence should be addressed: Dept. of Pharmacology, Laboratory of Molecular Stress Responses, and the Simmons Comprehensive Cancer Center, UT Southwestern Medical Center, 5323 Harry Hines Blvd, Dallas, TX 75390. Tel.: 214-648-9255; Fax: 214-648-0264; E-mail: David.Boothman@UTSouthwestern.edu.

[2] The abbreviations used are: PARP-1, poly(ADP-ribose) polymerase-1; β-lap, β-lapachone (3,4-dihydro-2,2-dimethyl-2*H*-naphthol[1,2b]pyran-5,6-dione); ROS, reactive oxygen species; H_2O_2, hydrogen peroxide; MNNG, *N*-methyl-*N*′-nitro-*N*-nitrosoguanidine; SSBs/DSBs, single/double-stranded DNA breaks; PAR, poly(ADP-ribose); MMP, mitochondrial membrane potential; NQO1, NAD(P)H:quinone oxidoreductase 1; STS, staurosporine; TUNEL, terminal deoxynucleotidyl transferase-mediated dUTP nick-end labeling; BAPTA-AM, (1,2-bis-(2-aminophenoxy)ethane-*N*,*N*,*N*′,*N*′-tetraacetic acid tetra-(acetoxymethyl ester)); Me_2SO, dimethyl sulfoxide; DIC, dicoumarol; 3-AB, 3-aminobenzamide; DPQ, (3,4-dihydro-5[4-(1-piperindinyl)butoxy]-1(2H)-isoquinoline); DCF, 6-carboxy-2′7′-dichlorodihydrofluorescin diacetate, di(acetoxymethyl ester); 231, MDA-MB-231; ns-shRNA, non-silencing shRNA; ER, endoplasmic reticulum; 231-NQ−, MDA-MB-231-NQO1-negative; 231-NQ+, MDA-MB-231-NQO1-positive; PARG, poly(ADP-ribose) glycohydrolase; IR, ionizing radiation; Topo, topoisomerase; MOMP, mitochondrial outer membrane permeabilization; PP2A, protein phosphatase 2A; PMCA, plasma membrane Ca^{2+}-ATPase; SERCA, sarcoplasmic/endoplasmic reticulum ATPase; TRMP, transient receptor potential-melastatin-like; AIF, apoptosis-inducing factor.

enzymatic activity (5). Restoration of NQO1 caused increases in drug sensitivity (5). In contrast to staurosporine (STS), global caspase inhibitors had little effect on β-lap lethality (5). β-lap-mediated cell death exhibited classical features of apoptosis (*e.g.* DNA condensation, trypan blue exclusion, sub-G_0-G_1 cells, and terminal deoxynucleotidyl transferase-mediated dUTP nick-end labeling (TUNEL)-positive cells). β-lap cell death was not, however, dependent on typical apoptotic mediators, such as p53 or caspases (8). To date, the mechanisms responsible for the initiation of this unique cell death have not been delineated.

We report that β-lap induces an NQO1-dependent, PARP-1-mediated cell death pathway involving changes in cellular metabolism leading to cell death. NQO1-dependent reduction of β-lap results in a futile redox cycle between the parent β-lap molecule and its hydroquinone form (5), wherein ROS generation causes extensive DNA damage, H2AX phosphorylation (γ-H2AX) and PARP-1 hyperactivation. Drastic decreases in NAD^+ and ATP pools, in turn, inhibit DNA repair and accelerate cell death. In addition, chelation of intracellular Ca^{2+} by 1,2-bis-(2-aminophenoxy)ethane-*N*,*N*,*N*′,*N*′-tetraacetic acid tetra-acetoxymethyl ester (BAPTA-AM) abrogates β-lap-induced: (i) γ-H2AX formation, (ii) PARP-1 hyperactivation, (iii) atypical PARP-1 and p53 proteolysis, and (iv) cytotoxicity without affecting NQO1-dependent ROS production. A similar Ca^{2+}-sensitive cell death is observed after hydrogen peroxide (H_2O_2) exposure. Interestingly, *N*-methyl-*N*′-nitro-*N*-nitrosoguanidine (MNNG)-induced PARP-1 hyperactivation is not sensitive to BAPTA-AM. These data support a critical role for Ca^{2+} as a regulator of cellular metabolism in response to ROS-induced DNA damage.

EXPERIMENTAL PROCEDURES

Reagents—β-lap was synthesized by Dr. William G. Bornmann (MD Anderson), dissolved in dimethyl sulfoxide (Me_2SO) at 40 mM, and the concentration verified by spectrophotometric analyses (8). β-lap stocks were stored at −80 °C. Hoechst 33258, 3-aminobenzamide (3-AB), dicoumarol (DIC), H_2O_2, STS, and MNNG were obtained from Sigma. BAPTA-AM was dissolved in Me_2SO and used at 5 μM unless otherwise stated. DPQ (3,4-dihydro-5[4-(1-piperindinyl)butoxy]-1(2*H*)-isoquinoline) was dissolved in Me_2SO and used at 20 μM. DPQ and BAPTA-AM were obtained from Calbiochem (La Jolla, CA). Z-VAD-fmk was obtained from Enzyme Systems Products (Dublin, CA), diluted in Me_2SO and used at 50 μM. DCF was dissolved in Me_2SO and used at 5 μM to monitor ROS formation. DCF was obtained from Molecular Probes (Eugene, OR).

Cell Culture—Human MCF-7 and MDA-MB-468-NQ+ breast cancer cells were maintained and used as described (5). Human MDA-MB-231 (231) breast cancer cells that contain a 609C>T polymorphism in NQO1 (9) and are deficient in enzyme activity, were obtained from the American Type Culture Collection (Manassas, VA). Cells were stably transfected with a CMV-driven NQO1 cDNA or the pcDNA3 vector alone as described (5). All cells were grown in high glucose-containing RPMI 1640 tissue culture medium containing 5% fetal bovine serum, 2 mM L-glutamine, 100 units/ml penicillin, and 100 mg/ml streptomycin at 37 °C in a 5% CO_2, 95% air humidified atmosphere (6). 231-NQO1+ (NQ+) and −NQO1 (NQ−) cells were maintained in medium containing 400 μg/ml geneticin (8), but all experiments were performed without selection. All tissue culture components were purchased from Invitrogen (Carlsbad, CA) unless otherwise stated. All cells were routinely tested and found free of mycoplasma contamination.

PARP-1 Knockdown—A puromycin-selectable-pSHAG-MAGIC2 retroviral vector containing a short hairpin small interfering RNA against PARP-1 (PARP-1-shRNA) and a non-silencing sequence (ns-shRNA) control were used to infect both NQ+ and NQ− 231 cells (Open Biosystems, Huntsville, AL). Cells were then selected and grown in 0.5 μg/ml puromycin and screened for PARP-1 protein expression and NQO1 enzymatic activity.

Relative Survival Assays—Relative survival assays were performed as previously described (5). MCF-7 cells were pretreated or not with BAPTA-AM (5 μM, 30 min) then treated with or without 2-h pulses of β-lap at the doses indicated, in the presence or absence of 40 μM dicoumarol. In some experiments, cells were exposed to 5 μM β-lap followed by delayed ($t = 0–2$ h) addition of 5 μM BAPTA-AM. After drug addition, media were removed and drug-free media added. Cells were then allowed to grow for an additional 6 days and relative survival, based on DNA content (Hoechst 33258 staining), was determined (5). Prior studies using β-lap showed that relative survival assays correlated directly with colony forming ability assays (5). Data were expressed as treated/control (T/C) from separate triplicate experiments (means, ± S.E.), and comparisons analyzed using a two-tailed Student's *t* test for paired samples.

Immunoblotting and Confocal Microscopy—Western blots were prepared as previously described (8). α-PARP (sc-8007) and α-p53 (DO-1) antibodies were utilized at dilutions of 1:1000 (Santa Cruz Biotechnology). The α-PAR antibody was used at 1:2000 dilution (BD-Pharmingen, San Jose, CA). Antibodies to total levels of H2AX or γ-H2AX were used at dilutions of 1:100–1:500 and purchased from Bethyl Laboratories (Montgomery, TX) and Upstate (Charlottesville, VA), respectively. An NQO1 antibody was generated and used directly for immunoblot analyses in medium containing 10% fetal bovine serum, 1× phosphate-buffered saline, and 0.2% Tween 20 (10).

Confocal microscopy was performed as previously described (7). Cells were fixed in methanol/acetone (1:1) and incubated with α-PAR (10H; Alexis, San Diego, CA) or α-γ-H2AX (Trevigen, Gaithersburg, MD) for 2 h at room temperature. Nuclei were visualized by Hoechst 33258 staining at a 1:3000 dilution. Confocal images were collected at 488 nm excitation from a krypton/argon laser using a Zeiss LSM 510 confocal microscope (Thornwood, NY). Images were representative of experiments performed at least four times. The number of PAR-positive cells and γ-H2AX foci/cell were quantified by counting 60 or more cells from four independent experiments (means ± S.E.).

Formation of ROS was monitored by the conversion of non-fluorescent 6-carboxy-2′7′-dichlorodihydrofluorescin diacetate, di(acetoxymethyl ester) to fluorescent 6-carboxy-2′,7′-dichlorofluorescein diacetate di(acetoxymethyl ester) (DCF) as previously described (11, 12). Briefly, MCF-7 cells were seeded

at 2–3 × 10^5 cells in 35-mm glass bottom Petri dishes (MatTek Corp., Ashland, MA) and allowed to attach overnight. Cells were loaded with 5 μM DCF in media for 30 min at 37 °C. After loading, cells were washed twice with phosphate-buffered saline, and incubated for an additional 20 min at 37 °C to allow for dye de-esterification. Confocal images of DCF fluorescence were collected using 488-nm excitation from an argon/krypton laser, 560-nm dichroic mirror, and a 500–550 nm band pass filter. Three basal images were collected before drug addition (5–8 μM β-lap, +5 μM BAPTA-AM or 40 μM dicoumarol). Subsequent images were taken after the indicated treatments at 15-s intervals and similar results were found at 37 °C or rm. temp. BAPTA-AM was co-loaded with DCF where indicated. Mean pixel intensities were determined in regions of interest for at least 40 individual cells at each time point. Shown are representative traces of at least three independent experiments (means ± S.E.).

Single Cell Gel Electrophoresis (Alkaline Comet) Assays—DNA damage was assessed after different drug treatments by evaluating DNA "comet" tail area and migration distance (13). MCF-7 cells were pretreated with BAPTA-AM (5 μM, 30 min) or Me_2SO (1:1000 dilution), and then exposed to H_2O_2 (500 μM, 1 h), β-lap (4 μM, various times), or vehicle alone, and harvested at various times. Cell suspensions (3 × 10^5/ml cold PBS) were mixed with 1% low melting temperature agarose (1:10 (v/v)) at 37 °C and immediately transferred onto a CometSlide™ (Trevigen). After solidifying (30 min at 4 °C), slides were submerged in prechilled lysis buffer (2.5 M NaCl, 100 mM EDTA pH 10, 10 mM Tris Base, 1% sodium lauryl sarcosinate, and 1% Triton X-100) at 4 °C for 45 min, incubated in alkaline unwinding solution (300 mM NaOH, and 1 mM EDTA) for 45 min at room temperature and washed twice (5 min) in neutral 1× TBE (89.2 mM Tris Base, 89 mM boric acid, and 2.5 mM EDTA disodium salt). Damaged and undamaged nuclear DNA was then separated by electrophoresis in 1× TBE for 10 min at 1 V/cm, fixed in 70% ethanol, and stained using SYBR-green (Trevigen). Comets were visualized using an Olympus fluorescence microscope (Melville, NY), and images captured using a digital camera. Images were analyzed using ImageJ software (14, 15) and comet tail length was calculated as the distance between the end of nuclei heads and the end of each tail. Tail moments were defined as the product of the %DNA in each tail, and the distance between the mean of the head and tail distributions in Equation 1,

$$\%DNA_{(tail)} = TA \times TAI \times 100/(TA \times TAI) + [HA \times HAI] \quad \text{(Eq. 1)}$$

where TA is the tail area, TAI is the tail area intensity, HA is the head area, and HAI is the head area intensity. Importantly, tail moment and tail area calculations yielded similar experimental results. Each datum point represented the average of 100 cells ± S.E., and data are representative of experiments performed three times.

Determination of NAD^+ and ATP Levels—Intracellular NAD^+ levels were measured as described (16) with modification. Briefly, cells were seeded at 1 × 10^6 and allowed to attach overnight. Cells were pretreated for 2 h with 3-AB (25 mM), DPQ (20 μM), BAPTA-AM (5 μM), or Me_2SO and then exposed to β-lap (2–20 μM) for the indicated times. Cell extracts were prepared in 0.5 M perchloric acid, neutralized (1 M KOH, 0.33 M KH_2PO_4/K_2HPO_4 (pH 7.5)), and centrifuged to remove $KClO_4$ precipitates. Supernatants or NAD^+ standards were incubated 4:1 (v/v) for 20 min at 37 °C with NAD^+ reaction mixture as described (17). Measurements from extracts were taken at an absorbance of 570 nm and intracellular NAD^+ levels were normalized to 1 × 10^6 cells. Data were expressed as %NAD^+ ± S.E., for T/C samples from nine individual experiments.

ATP levels were analyzed using a luciferase-based bioluminescence assay as described (18). Data were graphed as means ± S.E. of experiments performed at least three times. Results were compared using the two-tailed Student's *t* test for paired samples.

NQO1 Enzyme Activity Assays—NQO1 enzymatic assays were performed as described (19) using cytochrome *c* (practical grade, Sigma) in Tris-HCl buffer (50 mM, pH 7.5). NADH (200 μM) was the immediate electron donor, and menadione (10 μM) the electron acceptor. Changes in absorbance were monitored using a Beckman DU 640 spectrophotometer (Beckman Coulter, Fullerton, CA). Dicoumarol (10 μM) inhibitable NQO1 levels were calculated as nmol of cytochrome *c* reduced/min/μg protein based on initial rate of change in absorbance at 550 nm and an extinction coefficient for cytochrome *c* of 21.1 nmol/liter/cm (20). Results were expressed as means ± S.E. of three or more separate experiments.

Flow Cytometry and Apoptotic Measurements—Flow cytometric analyses of TUNEL-positive cells were performed as described using APO-DIRECT™ (BD Pharmingen) (5). Samples were analyzed in an EPICS Elite ESP flow cytometer using an air-cooled argon laser at 488 nm, 15 milliwatt (Beckman Coulter Electronics, Miami, FL) and Elite acquisition software. Experiments were performed a minimum of five times, and data expressed as means ± S.E. Statistical analyses were performed using a two-tailed Student's *t* test for paired samples.

Glutathione Measurements—Disulfide glutathione and total glutathione (GSH + GSSG) levels were determined using a spectrophotometric recycling assay (21, 22). Following indicated treatments, pellets were thawed and whole cell homogenates prepared as described (21, 22). Data were expressed as the %GSSG normalized to protein content, as measured using the method of Lowry *et al.* (23). Shown are means ± S.E. for experiments performed at least three times.

RESULTS

Time and Ca^{2+} Dependence of β-lap-induced Cell Death—To elucidate the signaling events required for β-lap-induced cell death, log-phase human MCF-7 breast cancer cells, with high levels of endogenous NQO1 activity, were tested for their sensitivities to various concentrations of β-lap at various times. The purpose of these experiments was to determine the minimal time of β-lap exposure required to kill the entire cell population. Cells exposed to doses of ≤3 μM β-lap required ≥4 h to elicit cell death, whereas 2 h exposures of β-lap at ≥4 μM killed all MCF-7 cells (Fig. 1*A*).

Prior data from our laboratory demonstrated that Ca^{2+} was released within 2–5 min from endoplasmic reticulum (ER)

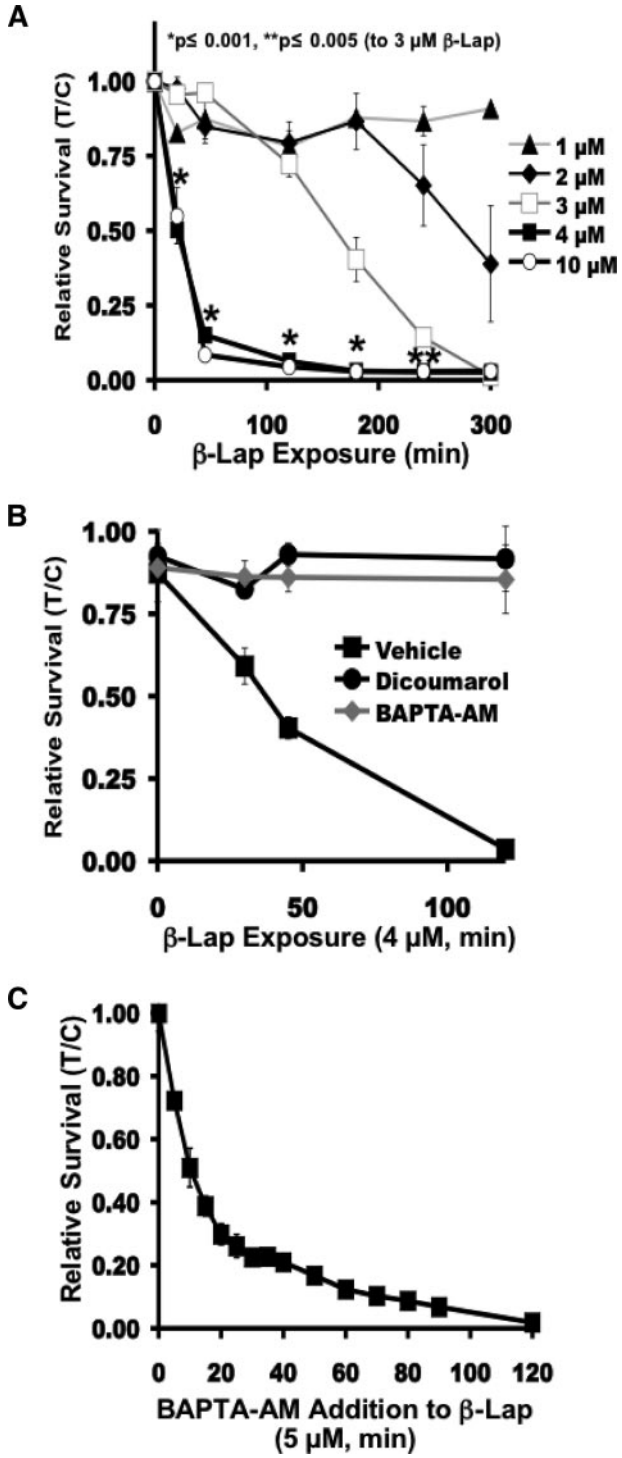

FIGURE 1. **β-lap-induced cell death is time- and Ca^{2+}-dependent.** *A–C,* cell death was examined using relative survival assays in NQO1+ MCF-7 cells. *A,* cells were exposed to various doses of β-lap for different lengths of time to determine the minimal exposure time required for cell death. After drug exposure, media were removed and drug-free media added. Cells were then allowed to grow for an additional 6 days and relative survival, based on DNA content was determined by Hoechst 33258 staining as described under "Experimental Procedures." Student's *t* test for paired samples, experimental group compared with 3 μM β-lap (*, $p \leq 0.001$; **, $p \leq 0.005$). Prior studies using β-lap showed that relative survival assays directly correlated with colony forming ability. *B,* relative survival assays using MCF-7 cells treated with 4 μM β-lap alone, or in combination with 40 μM dicoumarol or 5 μM BAPTA-AM. *C,* MCF-7 cells were treated with 5 μM β-lap at $t = 0$. BAPTA-AM (5 μM) was then added to β-lap-treated cells at various times afterwards as indicated.

Ca^{2+} stores after β-lap treatment (24), suggesting that this was a required initiating factor in β-lap-induced cell death (24). To test this, MCF-7 cells were pretreated with the intracellular Ca^{2+} chelator BAPTA-AM (5 μM, 30 min), then exposed to 4 μM β-lap for various times (Fig. 1*B*). Under these conditions, we previously demonstrated that BAPTA-AM pretreatment was sufficient to block the rise in cytosolic Ca^{2+} caused by β-lap treatment (24). BAPTA-AM abrogated β-lap-induced cytotoxicity and nuclear condensation (Fig. 1*B* and supplemental Fig. S1*A*). To determine the kinetics of Ca^{2+}-dependent cell death, MCF-7 cells were treated with 5 μM β-lap, and 5 μM BAPTA-AM was added at various times thereafter, up to 2 h. A time-dependent decrease in survival was observed with delayed addition of BAPTA-AM (Fig. 1*C*), indicating that Ca^{2+} release was a necessary event, occurring before cells were committed to death. Abrogation of β-lap cytotoxicity by BAPTA-AM was equivalent to that noted with NQO1 inhibition by dicoumarol (Fig. 1*B*). Addition of BAPTA-AM also prevented β-lap-induced, atypical proteolysis (*e.g.* ~60 kDa PARP-1 and p53 cleavage fragments), in a manner as effective as dicoumarol (supplemental Fig. S1*B*, *lanes 3* and *4*). Interestingly, Z-VAD-fmk (50 μM), a pan-caspase inhibitor, did not block atypical PARP-1 and p53 proteolysis in β-lap-treated MCF-7 cells (*lane 7*). As expected, Z-VAD-fmk inhibited STS (1 μM)-induced caspase-mediated proteolysis (25). However, BAPTA-AM did not affect STS-induced apoptotic proteolysis (supplemental Fig. S1*C*). These data, in conjunction with our prior data showing β-lap-induced ER Ca^{2+} release (24), support a role for Ca^{2+} in the initiation of cell death induced by this drug.

PARP-1 Hyperactivation after β-lap Treatment Is NQO1-dependent and BAPTA-AM-sensitive—Because β-lap-induced cell death was accompanied by a ≥80% loss of ATP within 1 h (24), we suspected PARP-1 hyperactivation played a role in the mode of action for this drug. To investigate this, we generated 231 NQO1-proficient (231-NQ+) cells that are sensitive to β-lap (LD_{50}: ~1.5 μM), after a 2-h pulse, and compared these cells to vector alone, 231 NQO1-deficient (231-NQ-) cells, that are resistant to the drug (LD_{50}: 17.5 μM). Only β-lap-treated, 231-NQ+ cells exhibited an increase in PAR-modified proteins, mostly PARP-1, consistent with the role of PARP-1 as the predominant poly(ADP-ribosyl)ated species. This response peaked ~30 min during β-lap exposure (Fig. 2*A*). In contrast, treatment of 231-NQ- cells with equal or significantly higher doses of β-lap did not induce PAR accumulation (data not shown). In contrast, both 231-NQ+ and 231-NQ- cells hyperactivated PARP-1 in response to H_2O_2. The NQO1-dependence of PARP-1 hyperactivation after β-lap exposure was confirmed in a number of other cell lines (*e.g.* breast, prostate, and lung cancers) that have elevated NQO1 activity demonstrating that the responses to β-lap were not cell type-specific. In all cases, dicoumarol suppressed β-lap-induced PAR formation (supplemental Fig. S2, *A–C*).

We then examined a possible connection between the involvement of Ca^{2+} in lethality and PARP-1 hyperactivation. MCF-7 cells were pretreated with 5 μM BAPTA-AM, then exposed to 5 μM β-lap for the indicated times (Fig. 2*B*). The kinetics of PAR accumulation were faster in MCF-7 cells than in 231-NQ+ cells, (10 min *versus* 20 min Figs. 2, *B* and *A*,

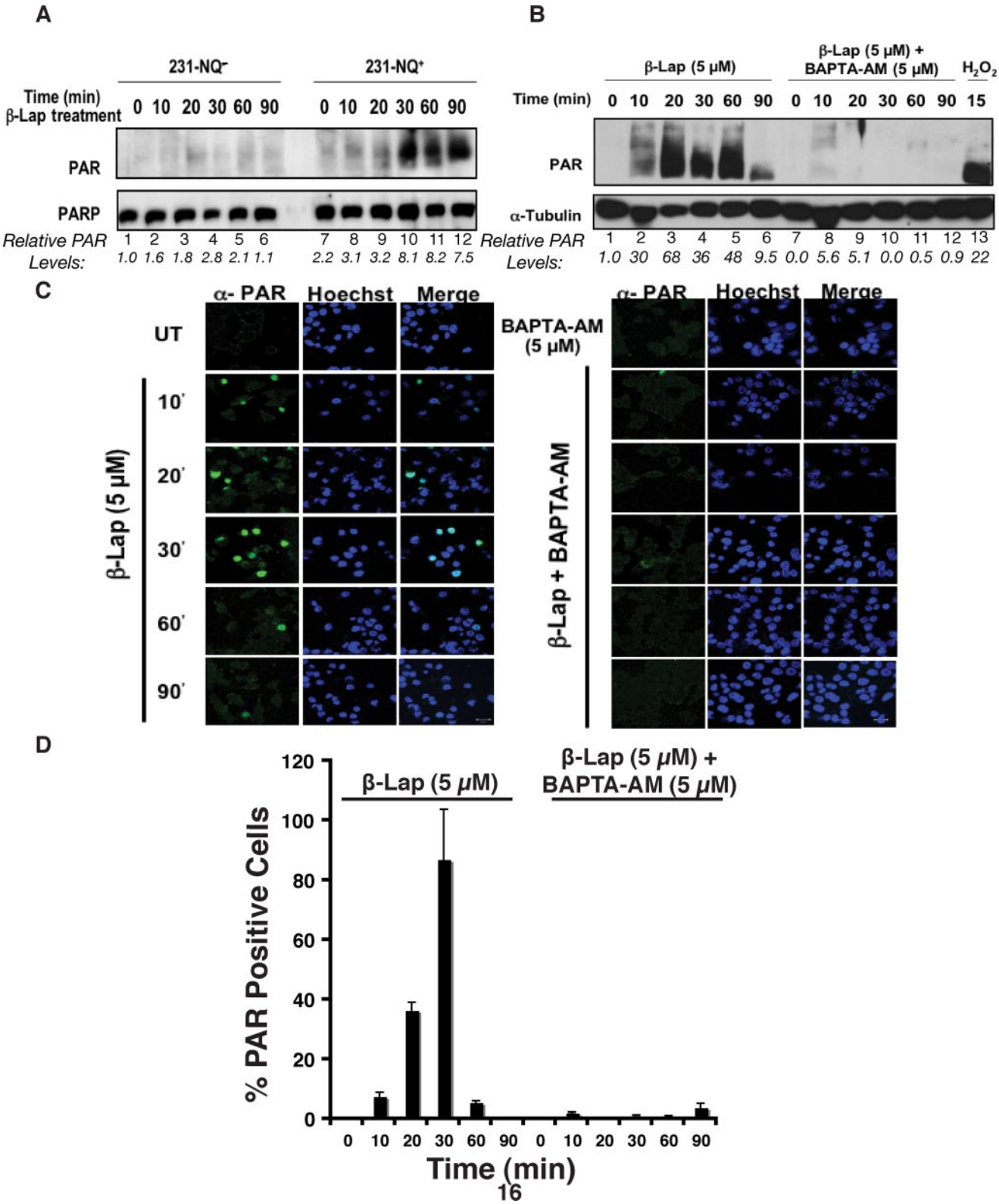

FIGURE 2. **β-lap induces NQO1- and Ca^{2+}-dependent PARP-1 hyperactivation.** *A*, immunoblots of PAR formation as a measure of PARP-1 hyperactivation, and steady-state PARP-1 protein levels from whole cell extracts of isogenic 231-NQ+ and 231-NQ− cells treated with 6 μM β-lap for 10–90 min. Relative PAR levels were calculated by densitometric analyses by NIH ImageJ using PARP loading controls wherein controls were set to 1.0. *B*, immunoblots of PAR formation and steady state α-tubulin expression in extracts from MCF-7 cells treated with β-lap or H_2O_2 (2 mM, control for PARP-1 hyperactivation). Other cells were pretreated with BAPTA-AM with or without β-lap (5 μM). Samples were harvested at the indicated times. Relative PAR levels were calculated by densitometric analyses by NIH ImageJ using α-tubulin loading controls wherein controls were set to 1.0. *C*, assessment of PARP-1 hyperactivation, measured by PAR formation, in MCF-7 cells treated with β-lap alone or in cells pretreated with BAPTA-AM for 30 min prior to β-lap exposure. PAR formation was visualized using confocal microscopy. *D*, quantified percentages of PAR-positive cells from confocal microscopy analyses of at least 60 cells from four independent experiments (means ± S.E.).

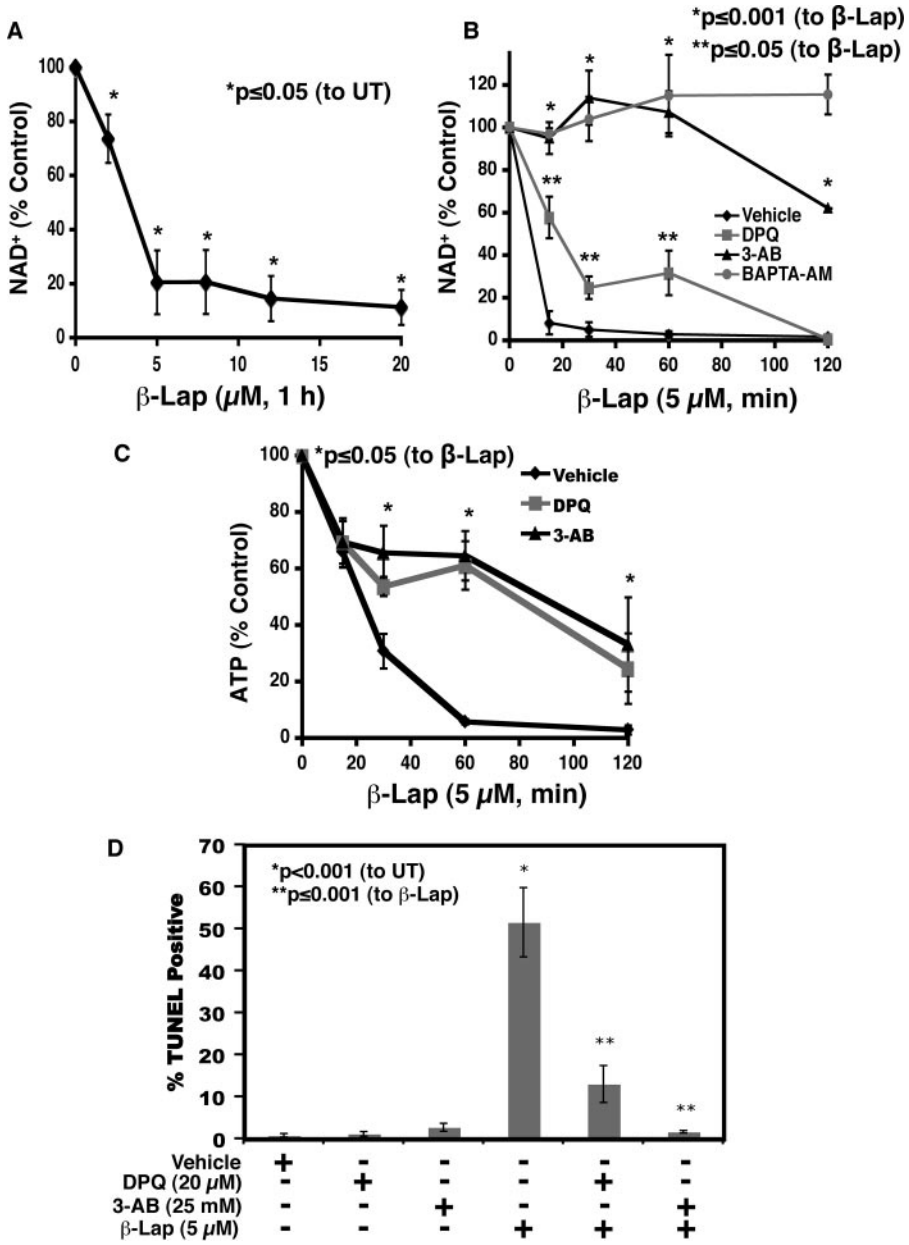

FIGURE 3. **PARP-1-dependent NAD^+ and ATP pool depletion leads to cell death after β-lap exposure in MCF-7 cells.** *A* and *B*, NAD^+ pool depletion occurs immediately after β-lap treatment in MCF-7 cells. *A*, MCF-7 cells were exposed to varying concentrations of β-lap for 1 h, or *B*, 5 μM β-lap alone with or without pre- and co-treatment of PARP inhibitors, (20 μM DPQ or 25 mM 3-AB) or 5 μM BAPTA-AM for various times and harvested for NAD^+ content. Student's *t* test for paired samples, comparing experimental groups containing β-lap + 3-AB or DPQ *versus* β-lap alone are indicated (*, $p \leq 0.001$; **, $p \leq 0.05$, respectively). *C*, intracellular ATP levels were monitored using a luciferase-based bioluminescence assay in MCF-7 cells treated with β-lap, or in cells pre- and co-treated with 20 μM DPQ, or 25 mM 3-AB 2 h prior to β-lap addition. Differences were compared using two-tailed Student's *t* test. Groups having *, $p \leq 0.05$ values compared with β-lap alone are indicated. *D*, apoptotic DNA fragmentation was assessed using TUNEL assays in β-lap-exposed, log-phase MCF-7 cells with or without pre- and co-treatment with DPQ or 3-AB.

respectively), consistent with higher NQO1 levels in MCF-7 cells. PAR levels decreased after 90 min, corresponding to auto-(ADP-ribosyl)ation of PARP-1, and efficient PAR hydrolysis by poly(ADP-ribose) glycohydrolase (PARG) (26). Interestingly, BAPTA-AM pretreatment abrogated PARP-1 hyperactivation induced by β-lap (Fig. 2*B*) as confirmed by confocal microscopy (Fig. 2*C*). Robust and extensive poly(ADP-ribosyl)ation occurred within 30 min (87% ± 17 PAR-positive cells) of drug exposure and dissipated between 60–90 min (Fig. 2, *C* and *D*). However, in the presence of BAPTA-AM PAR accumulation in β-lap-treated MCF-7 cells was prevented (Fig. 2, *C* and *D*). To determine the global nature of this response, other cancer cell lines such as NQO1+ PC-3 human prostate cancer cells were examined and similar responses noted (supplemental Fig. S2*D*). Collectively, these data suggested a role for Ca^{2+} in the modulation of PARP-1 hyperactivation after β-lap exposure.

β-lap-induced PARP-1 Hyperactivation Alters Cellular Energy Dynamics Causing Cell Death—PARP-1 hyperactivation can elicit depletion of cellular NAD^+ levels and cause cell death in situations of extreme DNA damage or ischemia-reperfusion (27, 28). Treatment of MCF-7 cells with doses of β-lap ≥5 μM resulted in decreases (>80%) in NAD^+ and ATP levels 1 h during treatment (Fig. 3, *A–C*). To determine if NAD^+ and ATP losses were attributable to PARP-1 hyperactivation, MCF-7 cells were pretreated for 2 h with PARP inhibitors (*i.e.* 3-AB or DPQ), prior to 5 μM β-lap exposure. Similar to pretreatment with BAPTA-AM, NAD^+ and ATP losses in β-lap-treated MCF-7 cells were abrogated by 3-AB or DPQ (Fig. 3, *B* and *C*). 3-AB was more effective at preventing nucleotide loss than DPQ presumably because it has two distinct modes of PARP-1 inhibition, preventing NAD^+ binding to the catalytic site and competing with the PARP-1 DNA binding domain (29), whereas DPQ is a competitive inhibitor of NAD^+ (30). Similar effects of DPQ on NAD^+ and ATP losses after DNA damage have been reported (31). Neither 3-AB nor DPQ (used at >2-fold higher doses than in the above experiments) altered NQO1 activity in enzyme assays *in vitro*. Finally, 3-AB did not affect β-lap-induced ROS formation (data not shown).

To confirm that the energetic consequences of PARP-1 hyperactivation (*e.g.* NAD^+ and ATP losses) were necessary and sufficient for β-lap-induced cell death, the effects of 3-AB or DPQ, on apoptosis, was measured by TUNEL assay. Pretreatment with either inhibitor resulted in a reduction in apoptosis (2% and 15% total apoptosis, respectively for 3-AB and DPQ) compared with 55% in β-lap-treated cells (Fig.

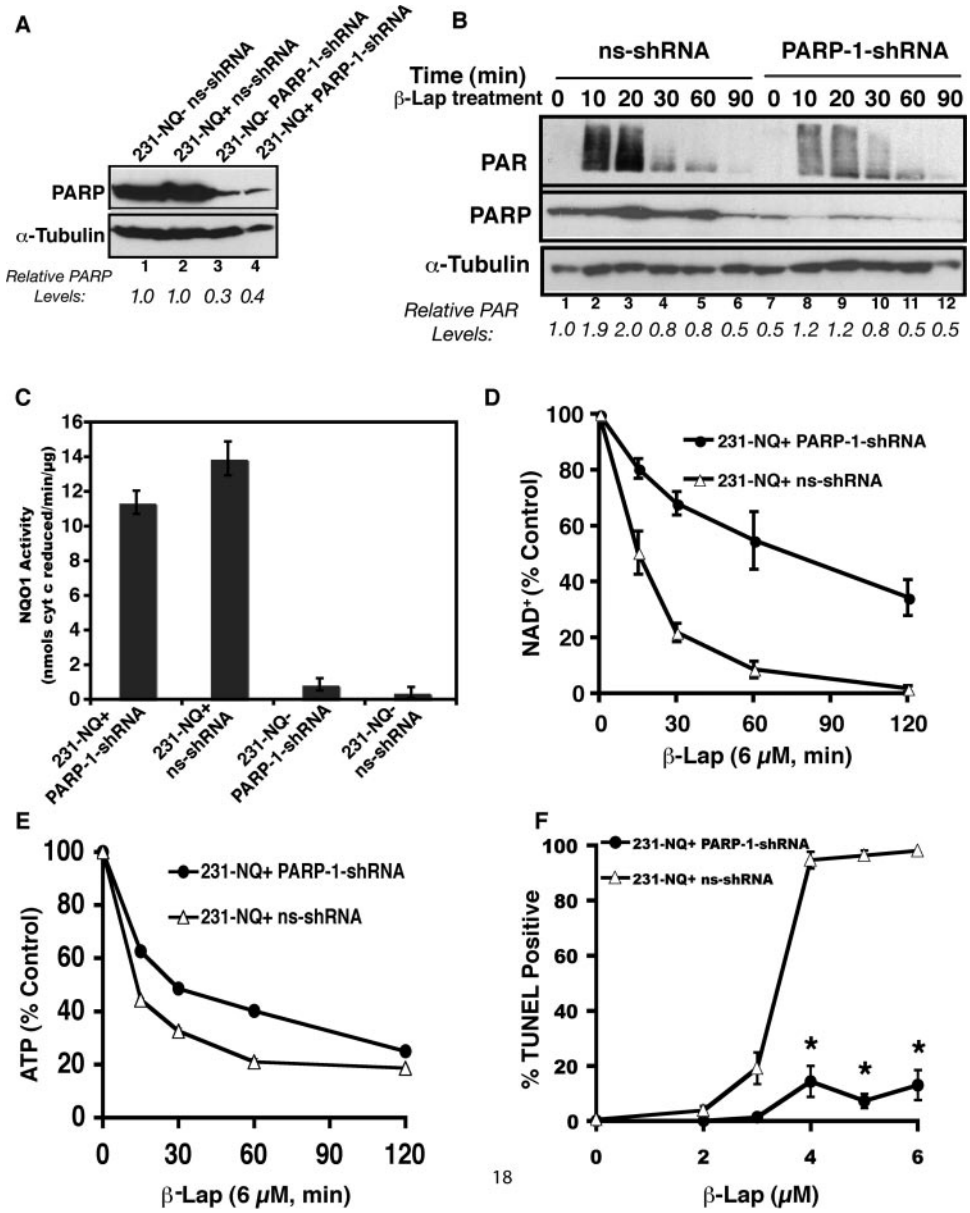

FIGURE 4. **PARP-1 plays an essential role in β-lap-induced apoptotic cell death as monitored by TUNEL.** *A*, immunoblots of steady state PARP-1 and α-tubulin protein levels from whole cell extracts of 231-NQ+ ns-shRNA, 231-NQ+ PARP-1-shRNA, 231-NQ- ns-shRNA, and 231-NQ- PARP-1-shRNA cell lines. Relative PARP-1 protein levels were calculated by densitometry analyses using α-tubulin loading controls by NIH ImageJ wherein controls were set to 1.0. *B*, immunoblots of PAR, PARP-1, and α-tubulin protein levels from control and β-lap (6 μM, 10–90 min)-exposed 231-NQ+ ns-shRNA or PARP-1-shRNA cells. Relative PAR levels were calculated by densitometry analyses using α-tubulin loading controls by NIH ImageJ. *C*, PARP-1 protein knock-down does not alter NQO1 enzymatic activity. NQO1 enzyme activities were determined for 231-NQ+ ns-shRNA, 231-NQ+ PARP-1-shRNA, 231-NQ- ns-shRNA, and 231-NQ- PARP-1-shRNA cells. NQO1 enzyme activities were calculated as nmol of cytochrome *c* reduced/min/μg protein. *D*, PARP-1 is necessary for NAD^+ loss after β-lap exposure. 231-NQ+ ns-shRNA and 231-NQ+ PARP-1-shRNA cells were treated with 6 μM β-lap for 0–120 min at which times NAD^+ content was determined as previously described. *E*, β-lap-induced ATP loss is PARP-1-dependent. ATP levels were monitored in 231-NQ+ ns-shRNA or PARP-1-shRNA cells after exposure to β-lap (6 μM, 0–120 min). Student's *t* test for paired samples, comparing experimental groups 231-NQ+ ns-shRNA *versus* 231-NQ+ PARP-1-shRNA are indicated (*, $p \leq 0.05$; **, $p \leq 0.001$). *F*, knock-down of PARP-1 protein protects cells from β-lap-induced cell death. 231-NQ+ ns-shRNA, and 231-NQ+ PARP-1-shRNA cells were exposed to a 2-h pulse of β-lap and monitored for apoptosis 24-h later. Students's *t* test for paired samples, experimental group compared with vehicle control (*, $p \leq 0.001$).

3*D*). Thus, PARP-1 inhibition by 3-AB or DPQ spared β-lap-induced apoptosis in NQO1+ MCF-7 cells, consistent with the effects of these inhibitors to prevent NAD^+ and ATP losses. Cumulatively, these data strongly suggest that Ca^{2+}-dependent PARP-1 hyperactivation caused NAD^+ and ATP loss in NQO1+ human cancer cell lines after β-lap treatment.

PARP-1 Hyperactivation Is Required for β-lap Cytotoxicity—Because the use of PARP inhibitors was only partially effective at preventing nucleotide loss after β-lap treatment, we confirmed the above findings using a genetic system. NQO1-expressing 231 breast cancer cells were chosen, since they have lower NQO1 levels than MCF-7 cells. PARP-1 protein in 231-NQ+ and 231-NQ− cells was suppressed by stable PARP-1-shRNA expression. Both 231-NQ+ and 231-NQ− cells infected with PARP-1-shRNA showed 3-fold knockdown of PARP-1 protein levels compared with cells containing a non-silencing shRNA sequence (ns-shRNA) (Fig. 4*A*). Poly-(ADP-ribosyl)ation was decreased in 231-NQ+ PARP-1-shRNA cells after β-lap exposure compared with 231-NQ+ ns-shRNA cells (Fig. 4*B*). The remaining PAR-modified proteins noted in cell extracts from β-lap-treated 231-NQ+ PARP-1-shRNA cells were caused by residual PARP-1 activity, since NQO1 activity was not altered after viral knock-down (Fig. 4*C*). PARP-1 protein knock-down spared 231-NQ+ cells from β-lap-induced NAD^+ and ATP losses compared with 231-NQ+ ns-shRNA cells (Fig. 4, *D* and *E*, respectively). Importantly, PARP-1 protein knock-down in 231-NQ+ PARP-1-shRNA cells was sufficient to abrogate β-lap-induced apoptosis at concentrations that killed all 231-NQ+ ns-shRNA cells (Fig. 4*F*). In contrast, without NQO1 activity, nominal PAR accumulation, NAD^+ or ATP losses were observed in 6 μM β-lap-treated 231-NQ- cells containing PARP-1-shRNA or ns-shRNA (data not shown). These cells remained resistant to β-lap independent of altered PARP-1 levels.

NQO1-dependent DNA Damage after β-lap Treatment—To date, there is little direct evidence that β-lap treatment causes DNA damage as assessed by alkaline or neutral filter elution, p53 induction, or covalent complex protein-DNA formation (8, 32, 33). However, many of these prior studies were performed in cells expressing little to no NQO1 (34). PARP-1 hyperactivation typically requires DNA damage,

therefore, we examined NQO1-positive cells exposed to β-lap for DNA breaks, by measuring γ-H2AX. H2AX contains a highly conserved serine residue (Ser^{139}), that is rapidly phosphorylated upon DNA damage (35). Significant γ-H2AX foci formation was observed in 30 min, similar to that seen 15 min following 5 Gy (Fig. 5*A*). In contrast, total H2AX and α-tubulin levels remained unchanged. These results were confirmed by confocal microscopy (Fig. 5*B*).

Because Ca^{2+} chelation blocked both β-lap-induced PARP-1 hyperactivation and cell death, we tested the effects of BAPTA-AM on γ-H2AX foci formation. Similar to the immunoblot analyses and the PAR formation kinetics (Fig. 2*C*), β-lap-treated MCF-7 cells showed γ-H2AX foci in 10 min (~17 foci/cell) of exposure, with peak levels at 60 min (~40 foci/cell) (Fig. 5*C*). Importantly, β-lap-induced γ-H2AX foci formation was partially abrogated by BAPTA-AM addition, with fewer γ-H2AX foci noted in 30–90 min (~5–25 foci/cell respectively) (Fig. 5*C*). These results were confirmed by immunoblot analyses (Fig. 5*D*).

Ca^{2+} Chelation Modulates DNA Repair after β-lap Treatment—We postulated that metabolism of β-lap by NQO1 would generate superoxide, peroxide, and other ROS (36). We directly monitored intracellular ROS formation, using the conversion of non-fluorescent 6-carboxy-2′,7′-dichlorodihydrofluorescin to fluorescent 6-carboxy-2′,7′-dichlorodihydrofluorescein (DCF). Indeed, exposure of MCF-7 cells with 5 or 8 μM β-lap treatment, caused an increase in fluorescence within 5 min compared with Me_2SO-treated cells (Fig. 6*A, left panel*). Region-of-interest analyses showed an ~2000-fold increase in fluorescence with β-lap alone over control cells, which could be abrogated by inhibiting NQO1 activity with dicoumarol (Fig. 6*A*, *right panel*). Because BAPTA-AM has moderate affinity for divalent cations other than Ca^{2+}, we explored the possibility that BAPTA-AM may protect cells from DNA damage and subsequent cell death by interfering with Fenton chemistry. Cells pretreated with 5 μM BAPTA-AM and then exposed to 5 or 8 μM β-lap exhibited no significant difference in the rate or extent of ROS formation compared with β-lap alone-treated cells (Fig. 6*A*). These results were confirmed by examining the oxidative state of MDA-MB-468-NQ+ cells after treatment with 4 μM β-lap in the presence or absence of 5 μM BAPTA-AM. β-lap treatment caused an ~65% rise in disulfide glutathione (GSSG) levels, that persisted during drug exposure (Fig. 6*B*). Addition of BAPTA-AM did not alter the kinetics or levels of GSSG formation during β-lap exposure (Fig. 6*B*). These data suggest that the protective effects of BAPTA-AM on β-lap-treated NQO1+ cells were not caused by interference with β-lap-induced ROS formation. Similar results were found in 231-NQ+ cells (data not shown).

To assess the effects of Ca^{2+} on DNA damage and repair, β-lap-treated MCF-7 cells were analyzed by alkaline comet assays to monitor total DNA strand breaks with or without BAPTA-AM addition. β-lap-treated cells exhibited significant DNA strand breakage by 10 min, resembling the positive control (H_2O_2), and after 30 min, β-lap-induced DNA damage exceeded those levels (Fig. 6*C* and supplemental Fig. S3). Cells pretreated with BAPTA-AM exhibited less DNA damage compared with β-lap alone, and their repair of DNA damage correlated well with their ability (or lack thereof) to survive (Figs. 6*C* and 1*B*).

We then examined the kinetics of repair in MCF-7 cells following a 2-h β-lap exposure with or without BAPTA-AM pretreatment. After β-lap exposure, DNA damage persisted and gradually increased over time (Fig. 6*C*), indicative of inhibition of DNA repair and consistent with the drop in NAD^+ and ATP levels (Fig. 3, *B* and *C*). Although cells treated with β-lap and BAPTA-AM at 2 h exhibited equivalent damage to 10 min of β-lap exposure alone (4.6 ± 0.2 *versus* 4.7 ± 0.4, $p > 0.5$ comet microns, respectively), BAPTA-AM pretreated cells were protected from PARP-1 hyperactivation (Fig. 2*B*), as well as decrements in NAD^+ levels (Fig. 3*B*). BAPTA-AM-pretreated cells showed a time-dependent recovery from DNA damage (Fig. 6*C* and supplemental Fig. S3). In contrast, β-lap-exposed cells showed extensive DNA damage with no signs of DNA repair. Collectively, these data suggest that NQO1-mediated metabolism of β-lap leads to the generation of ROS and subsequent DNA damage that hyperactivates PARP-1.

H_2O_2 Causes Ca^{2+}-dependent PARP-1 Hyperactivation—To examine the universality of Ca^{2+}-modulated PARP-1 function in response to other DNA damaging agents, we examined responses to H_2O_2 or MNNG. Unlike β-lap, H_2O_2 treatment caused PARP-1 hyperactivation in both 231-NQ+ and 231-NQ− cells (Fig. 7*A*). However, expression of NQO1 required higher doses of H_2O_2 to cause PAR formation in 231 cells (Fig. 7*A*). These data suggest that NQO1 has a broader antioxidant role by protecting against ROS-induced damage as previously proposed (37–39). Consistent with β-lap, however, was the abrogation of H_2O_2-induced PAR formation by BAPTA-AM in 231 cells independent of NQO1 activity (Fig. 7*B*).

H_2O_2 treatment also caused a dose-dependent increase in apoptosis in both 231-NQ− and 231-NQ+ cells that was blocked by BAPTA-AM (Fig. 7*C*). However, 231-NQ+ cells were much less sensitive to H_2O_2 than 231-NQ- cells. ATP loss was seen within minutes of H_2O_2 exposure in 231-NQ−, but not in NQO1-positive 231-NQ+ cells (supplemental Fig. S4). In addition, PARP-1 hyperactivation and cell death in response to equivalent doses of H_2O_2 in 231-NQ- cells was much more robust than in 231-NQ+ cells (Fig. 7, *B* and *C*). Interestingly, as noted with β-lap exposure, treatment of MCF-7 cells with ≥200 μM H_2O_2 for 2 h resulted in formation of a 60-kDa PARP-1 and 40-kDa p53 fragments. This atypical proteolysis was effectively inhibited by BAPTA-AM pretreatment (supplemental Fig. S5).

Finally, BAPTA-AM had no effect on PARP-1 hyperactivity or cytotoxicity caused by treatment with the monofunctional DNA-alkylating agent, MNNG (Fig. 7*E*). Because MNNG does not cause Ca^{2+} release like β-lap or H_2O_2, these data suggest that Ca^{2+} modulation of PARP-1 hyperactivation is unique to ROS-producing agents.

DISCUSSION

The regulatory mechanisms controlling PARP-1 function to either promote cell survival or cell death in response to DNA damage remain enigmatic. PARP-1 facilitates DNA repair and cell survival in response to a variety of DNA-damaging agents. However, it also mediates programmed necrosis (17), as well as caspase-inde-

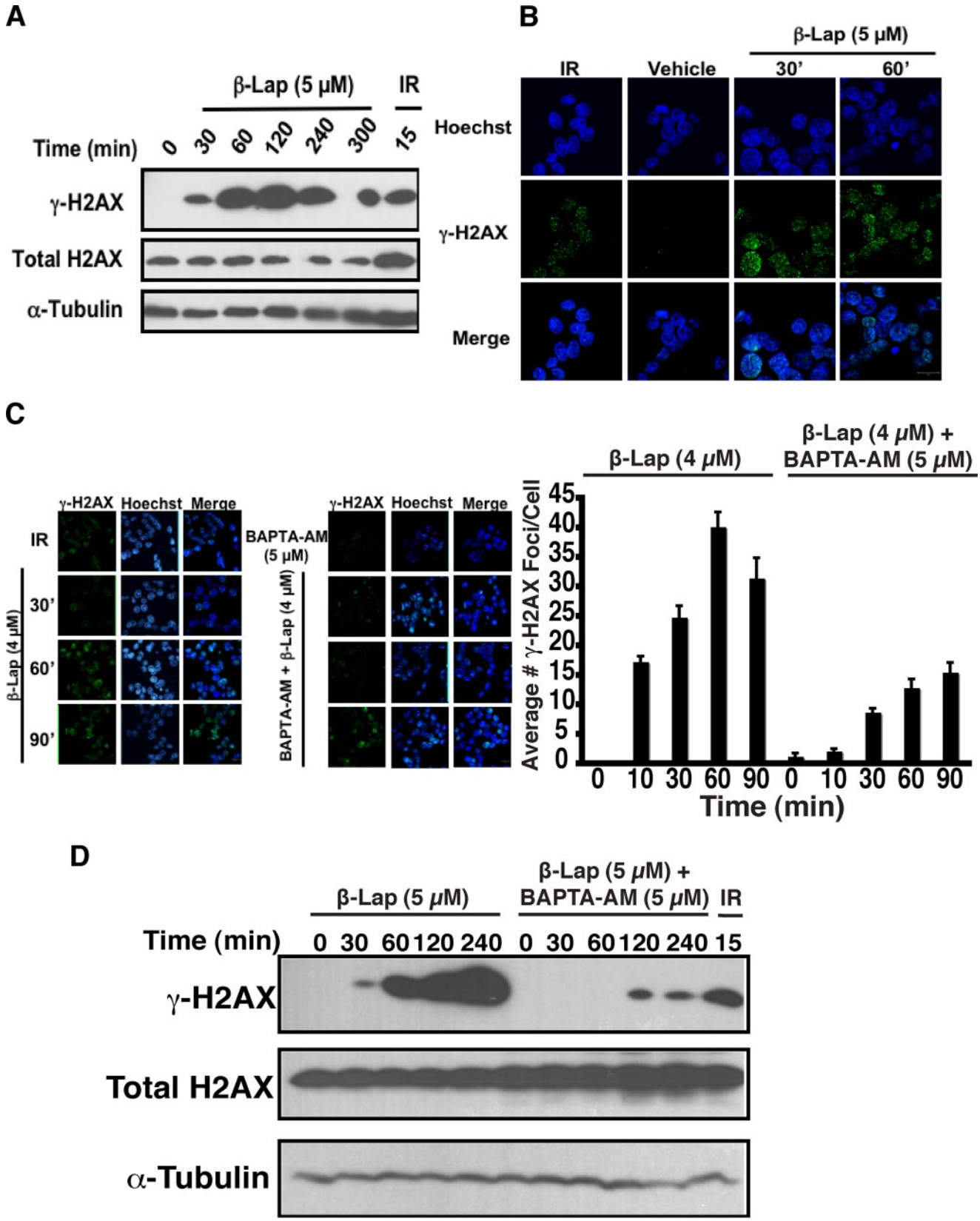

FIGURE 5. **β-lap-induced γ-H2AX foci formation is abrogated by BAPTA-AM pretreatment.** *A*, immunoblot analyses of γ-H2AX, total H2AX, and α-tubulin protein levels in whole cell extracts from MCF-7 cells exposed to β-lap for various times, or IR (5 Gy) harvested after 15 min. *B*, visualization of γ-H2AX foci in MCF-7 cells at various times after treatment with 5 μM β-lap or 15 min post-IR (5 Gy) by confocal microscopy. *C*, BAPTA-AM pretreatment followed by β-lap exposure abrogates γ-H2AX foci formation in MCF-7 cells as visualized by confocal microscopy. The number of γ-H2AX foci per cell was determined from at least 60 cells for each treatment group from four independent confocal experiments (means ± S.E.). *D*, immunoblot of γ-H2AX, total H2AX, and α-tubulin protein levels in whole cell extracts from MCF-7 cells exposed to β-lap for various times with or without BAPTA-AM (5 μM) pretreatment, or IR (5 Gy) harvested after 15 min.

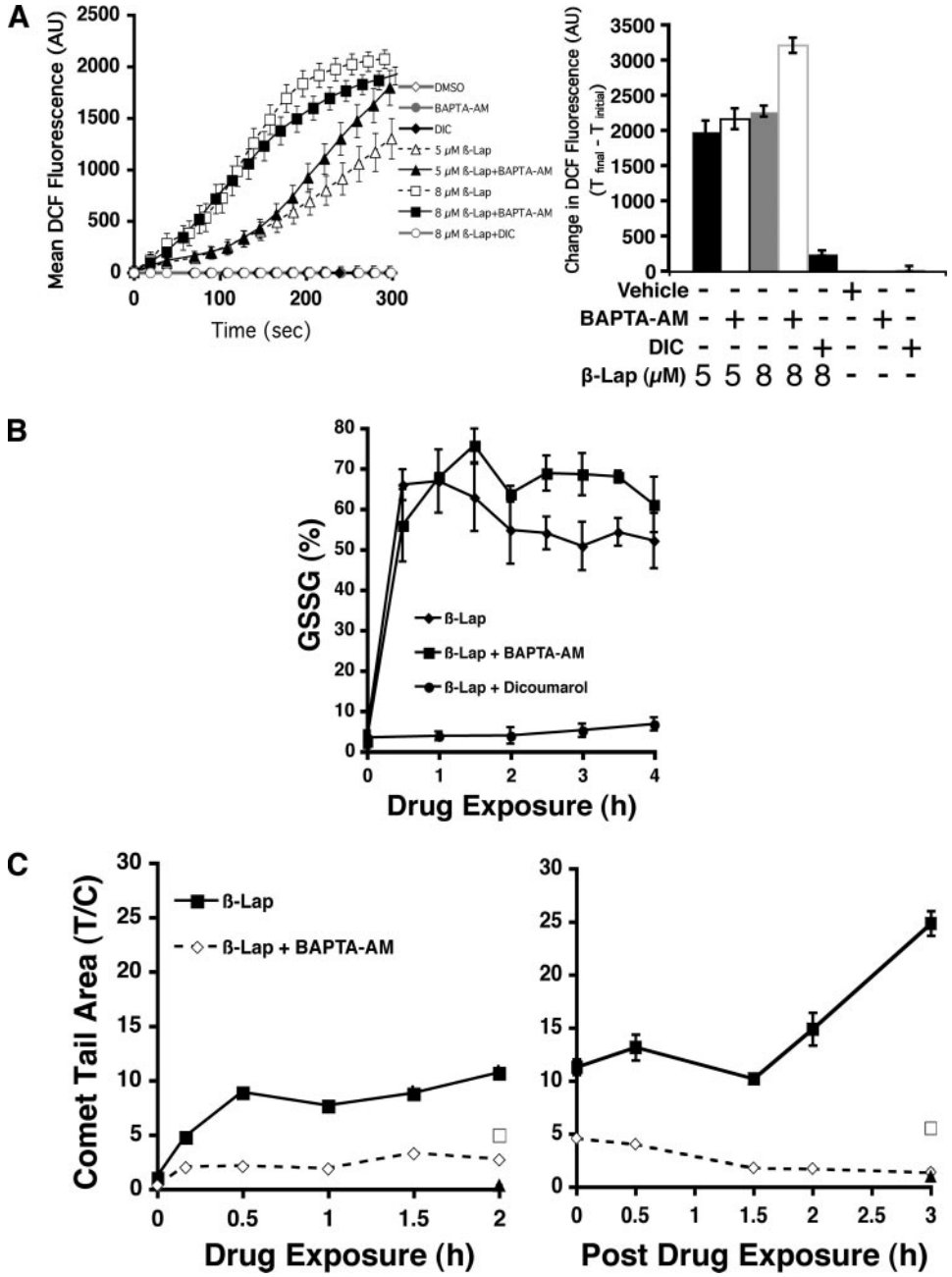

FIGURE 6. **Ca^{2+} modulates DNA repair in β-lap-treated cells.** *A*, β-lap treatment causes the formation of ROS that is not blocked by BAPTA-AM pretreatment. MCF-7 cells were loaded with DCF as described under "Experimental Procedures." Images were collected before drug treatment (0 min) and every 15 s during treatment up to 5 min. Cells were treated with β-lap (5 or 8 μM) with or without BAPTA-AM pretreatment or cotreatment with dicoumoral. Values represent the average of total cellular DCF fluorescence expressed as arbitrary units (AU) from 0–5 min (*left panel*). X-fold changes in fluorescence were calculated as the difference in fluorescence at 5 min minus the initial fluorescence obtained at the time of drug addition (*right panel*). Results are expressed as means ± S.E. from 20–30 cells per treatment group. Shown are representative data from three independent experiments. *B*, BAPTA-AM does not block β-lap-induced ROS production in NQO1+ MDA-MB-468 cells as monitored by changes in levels of disulfide glutathione (%GSSG) following treatment with 4 μM β-lap alone, or in cells pretreated for 30 min with 5 μM BAPTA-AM and then exposed to 4 μM β-lap. *C*, DNA damage in MCF-7 cells during (*left*) or following (*right*) vehicle (Me_2SO) alone, 500 μM H_2O_2 (□), 4 μM β-lap, 5 μM BAPTA-AM (▲) or in MCF-7 cells pretreated with 5 μM BAPTA-AM prior to β-lap (4 μM) exposure. DNA damage was assessed by alkaline comet assays at the indicated times. The comet tail area of 100 cells (means ± S.E.) for each time and condition were quantified with NIH ImageJ software and normalized to untreated cells. Similar results were obtained by analyzing comet tail length.

pendent apoptotic cell death following severe levels of DNA damage (40). The downstream pathways essential for the execution of cell death in response to PARP-1-mediated metabolic alterations remain poorly understood.

In elucidating the cell death pathway after exposure to β-lap, we uncovered a novel mechanism of PARP-1-mediated cell death. Our data suggest that this mechanism occurred selectively in response to ROS-generating agents. We demonstrated, for the first time, that Ca^{2+}-mediated PARP-1 hyperactivation commits cells to death as a consequence of metabolic starvation without the involvement of caspases.

PARP-1 hyperactivation in response to β-lap treatment was not cell type-specific and has been observed in all cells that express elevated NQO1 levels (Fig. 2*A*, and supplemental Fig. S2, *A–C*). As a result, cells exposed to β-lap exhibited depletion of NAD^+ and ATP, occurring 30–60 min during drug exposure. NAD^+ and ATP losses were, in part, PARP-1-mediated since PARP inhibitors (*e.g.* 3-AB and DPQ) partially abrogated nucleotide loss (Fig. 3, *B* and *C*). Chemical inhibition of PARP-1, or PARP-1 protein knock-down, not only prevented NAD^+ and ATP losses, but also abrogated β-lap-induced apoptosis (Figs. 3*D* and 4, *D–F*). These data established PARP-1-mediated NAD^+ and ATP losses as crucial upstream events in β-lap-mediated cell death.

PARP-1-mediated alterations in cellular metabolism caused by β-lap reported in NQO1-expressing cells in this study explain many of its purported effects *in vitro* and *in vivo*. These include, but are not limited to: (i) inhibition of NFκB activation via inhibition of IKK-α (41), (ii) lack of caspase activation (6) and p53 stabilization (8), and (iii) inhibition of Topoisomerase (Topo) I and Topo II-β (42). Furthermore, β-lap can initiate cell death independently from Bax and/or Bak activation as changes in mitochondrial outer membrane permeabilization (MOMP) can occur via PARP-1-mediated NAD^+ loss.[3] Thus, the results reported here appear to explain all prior phenomena reported in cells exposed to β-lap.

[3] W. X., Zong, E. A. Bey, and D. A. Boothman, unpublished data.

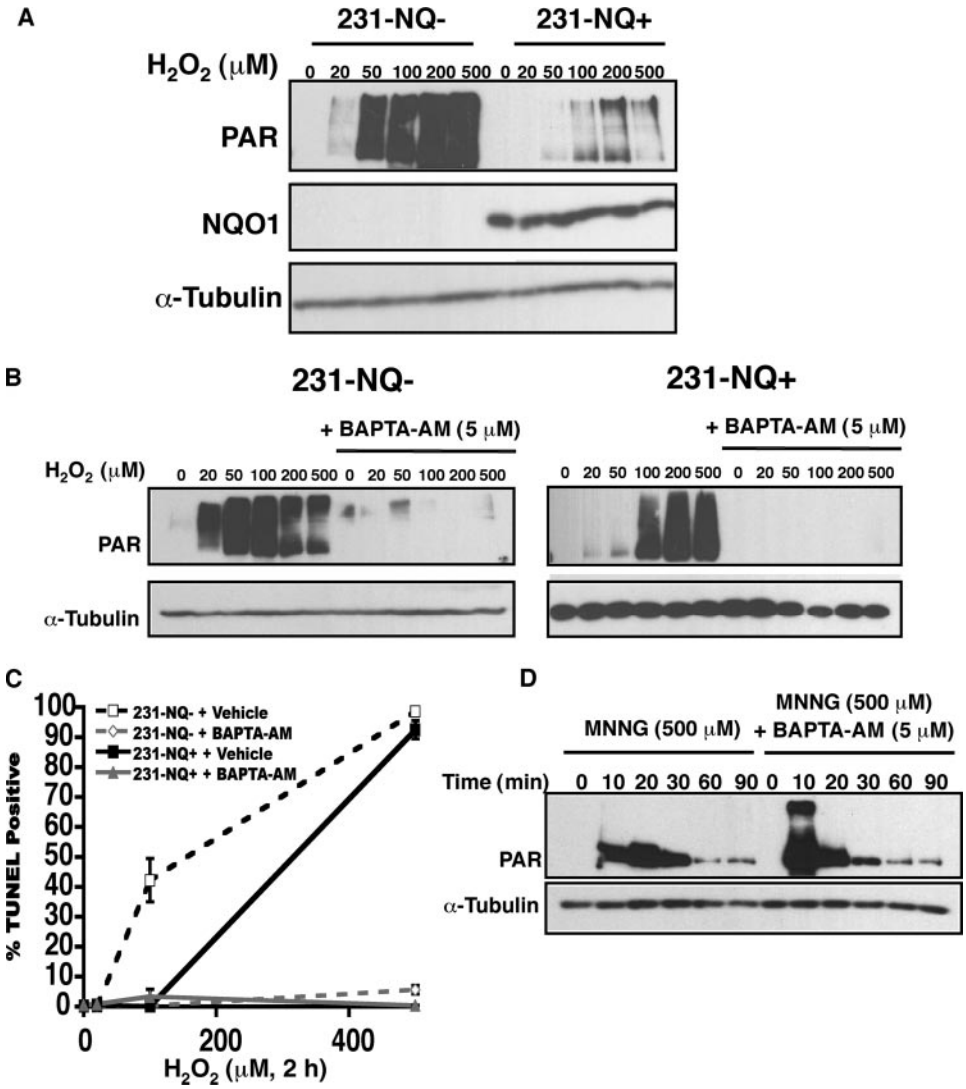

FIGURE 7. **H_2O_2 causes Ca^{2+}-dependent PARP-1 hyperactivation and cell death.** *A*, PARP-1 hyperactivation after H_2O_2 exposure occurs regardless of NQO1 status. Immunoblot analyses of PAR, NQO1, and α-tubulin protein levels in whole cell extracts from 231-NQ- and 231-NQ+ cells after exposure to varying doses of H_2O_2 for 15 min. *B*, PARP-1 hyperactivation after H_2O_2 treatment is Ca^{2+}-dependent. 231-NQ- (*left*) and 231-NQ+ cells (*right*) were pretreated with BAPTA-AM or vehicle alone for 30 min and then treated with varying doses of H_2O_2 and harvested after 15 min. Immunoblots of PAR, and α-tubulin protein levels from whole cell extracts were then analyzed. *C*, Ca^{2+} chelation protects 231-NQ- and 231-NQ+ cells from H_2O_2-induced apoptosis. TUNEL assays were performed in H_2O_2-exposed, log-phase 231-NQ- and 231-NQ+ cells, with or without pretreatment with 5 μM BAPTA-AM. *D*, MNNG-induced PARP-1 hyperactivation is not blocked by Ca^{2+} chelation. Immunoblots of PAR and α-tubulin protein levels from whole cell extracts of MCF-7 cells treated with MNNG or in cells pretreated for 30 min with BAPTA-AM and then exposed to MNNG are shown. Cells were treated for the indicated times and immediately harvested.

A unique feature of PARP-1-mediated cell death stimulated by β-lap was that administration of BAPTA-AM abrogated PARP-1 hyperactivation (Fig. 2*B*, supplemental Fig. S2*D*), nucleotide pool loss (Fig. 3*B*), atypical proteolyses (assessed by p53 and 60 kDa PARP-1 cleavage) (supplemental Fig. S1*B*), and cell death (Fig. 1, *B* and *C*). When BAPTA-AM was added >20 min after β-lap treatment, cells were not protected from cell death (Fig. 1*C*), suggesting that events occurring within the first 20 min of drug exposure committed cells to death. BAPTA (free acid form) did not alter NQO1 activity *in vitro* (24). This appears to be confirmed by the inability of BAPTA-AM to prevent ROS generation, which arises from NQO1-mediated metabolism of β-lap. Instead, our data suggest that the ability of BAPTA-AM to prevent β-lap-induced lethality in NQO1+ cancer cells was caused by the specific prevention of PARP-1 hyperactivation. The observed differences in the amount of DNA damage and γ-H2AX foci formation between β-lap alone and that of β-lap co-administered with BAPTA-AM suggest that preventing PARP-1 hyperactivation and subsequent changes in cellular metabolism can allow for cell recovery, noted by more rapid and extensive DNA damage repair (Figs. 5*C* and 6*C*). Recent data suggest that protein phosphatase 2A (PP2A) dephosphorylates γ-H2AX and is required for DSB repair (43). It is possible that Ca^{2+} chelation not only prevents PARP-1 hyperactivation, but also augments γ-H2AX dephosphorylation through PP2A activity. ROS-induced ER Ca^{2+} release may poison PP2A. However, we favor the theory that NQO1-mediated β-lap-induced ER Ca^{2+} release has its predominant affect on PARP-1 hyperactivation, thereby inhibiting DNA repair and cell recovery.

The mechanism of cell death induced by β-lap could be recapitulated by treatment with high doses of ROS-generating agents, such as H_2O_2 (Fig. 7, *A–D*). Notable similarities included: H_2O_2-mediated PARP-1 hyperactivation, Ca^{2+}-dependent proteolytic cleavage of PARP-1 and p53, and apoptotic DNA fragmentation. Furthermore, H_2O_2-induced lethality was abrogated by BAPTA-AM (Fig. 7, *A–D* and supplemental Fig. S5). Although β-lap and H_2O_2 initiate a similar downstream death pathway, the compounds differed in their lethality in cells with respect to NQO1 expression. β-lap lethality was enhanced in cells that express NQO1, whereas H_2O_2 caused greater cytotoxicity in NQO1-deficient cells (Fig. 7*C*). We noted striking similarities between β-lap- or H_2O_2-induced cell death and the caspase-independent cell death induced by ischemia-reperfusion. ROS produced during ischemia-reperfusion induces DNA strand breaks beyond a normal threshold that lead to PARP-1 hyperactivation, metabolic catastrophe, and an increase in intracellular Ca^{2+} levels leading to μ-calpain activation (44). These data suggest that programmed PARP-1-mediated cell death is a global response to these types of cellular insults.

PARP-1 hyperactivation was also observed following high doses of MNNG, however, this response was not affected by BAPTA-AM (Fig. 7*D*). These data highlight two separate PARP-1 regulatory mechanisms. First, ROS-induced, PARP-1-mediated cell death appears to require Ca^{2+} as a cofactor, whereas alkylation-mediated PARP-1-induced cell death does not. We propose that Ca^{2+} release following ROS-induced stress directly influences PARP-1 and PARG function. Both Mg^{2+} and Ca^{2+} exert significant (≥3-fold increases) allosteric activation of PARP-1 auto(ADP-ribosyl)ation *in vitro* that is inhibited by EDTA addition (45). We, therefore, speculate that Ca^{2+} chelation modulates PAR synthesis by dampening PARP-1 auto(poly-ADP)-ribosylation. Furthermore, since increases in [Ca^{2+}] can inhibit PARG function by up to 50% *in vitro*, maintenance of homeostatic Ca^{2+} levels after drug treatment would, thereby, restore the normal turnover of PAR by PARG, lifting PARP-1 self-inhibition (46). Our data are consistent with the hypothesis that both PAR synthesis and degradation can be modulated by BAPTA-AM to spare the cell from metabolic catastrophe via Ca^{2+}-mediated NAD^+ and ATP losses (Figs. 2*B*, and 3, *B* and *C*) (47). The remaining PARP-1 activity would be necessary for DNA break repair, ultimately providing a survival advantage to damaged cells (Figs. 1*B*, 5*C*, 6*C*, and 7*C*). We are currently exploring the mechanism by which Ca^{2+} modulates PARP-1 hyperactivation and subsequent DNA repair after H_2O_2 or β-lap treatments *versus* MNNG.

There appears to be some disagreement as to the role of Ca^{2+} in PARP-1-dependent cell death. Ca^{2+} can hyperactivate PARP-1 in the absence of DNA breaks (48). In neuronal cells, glutamate caused Ca^{2+}-mediated ROS production through mitochondrial dysfunction, leading to DNA damage, PARP-1 hyperactivation, and cell death. Furthermore, Ca^{2+} chelators, such as BAPTA-AM, EGTA-AM, and Quin-2-AM, protected against other oxidative stress-induced apoptotic and necrotic cell death mechanisms (49, 50). In these studies, Ca^{2+} chelation did not directly inhibit PARP-1 activity, but rather prevented DNA damage by inhibiting ROS. Contrary to these observations, in our system BAPTA-AM did not alter the direct production of ROS or oxidative stress in H_2O_2- or β-lap-exposed cells (Fig. 6*A*). Therefore, there does not appear to be an interference with transition metal-mediated oxidant production by BAPTA-AM (*e.g.* Fenton reaction) as previously suggested after H_2O_2 treatment (51, 52). In fact, our data demonstrate that β-lap caused equivalent ROS production in both β-lap alone and β-lap + BAPTA-AM treated cells. In contrast to β-lap alone-treated cells, cells pretreated with BAPTA-AM did not exhibit notable PARP-1 hyperactivation, associated NAD^+ and ATP losses, and showed a decrease in DNA damage over time (supplemental Table S1). While these data are suggestive of ongoing DNA repair in the presence of Ca^{2+} chelators, we cannot discount that these observations could also be the result of a decrease in the initial amount of DNA damage created in NQO1+ cells in response to β-lap. Initial DNA damage and active DNA repair would be indistinguishable in these experiments. Thus, although we believe it is unlikely, the Ca^{2+}-dependence of PARP-1 hyperactivation could be an indirect consequence of a BAPTA-AM-mediated decrease (*i.e.* protection) in the initial amount of DNA lesions created in response to β-lap. Future studies will address this issue by utilizing DNA repair-compromised NQO1+ cells.

Collectively, our data suggest that PARP-1 is necessary for the initiation of cell death caused by β-lap. To date, however, the endonuclease responsible for the execution of cell death in response to β-lap treatment remains unknown. We therefore propose, that PARP-1-mediated NAD^+ and ATP losses, in addition to PARG-liberated ADP-ribose, causes an influx of Ca^{2+} from extracellular and intracellular sources. Impairment of ATP-dependent membrane/organelle transporters (*e.g.* plasma membrane Ca^{2+} ATPases (PMCA) and sarcoplasmic/endoplasmic reticulum Ca^{2+} ATPases (SERCA)) by ATP loss, and activation of plasma membrane cation channels (*e.g.* transient receptor potential-melastatin-like (TRMP)) by ADP-ribose, leads to high intracellular Ca^{2+} levels (53) sufficient to activate the Ca^{2+}-dependent protease μ-calpain and commit the cell to death. Previous studies from our laboratory have demonstrated that β-lap causes the downstream activation of μ-calpain resulting in its translocation to the nucleus concomitant with nuclear proteolytic cleavage of p53 and PARP-1 (7). Studies from our laboratory indicate that β-lap treatment causes apoptosis-inducing factor (AIF) translocation from the mitochondria to the nucleus, leading to nuclear condensation following μ-calpain activation.[4] To date, the mechanism responsible for PARP-1-mediated AIF release remains unclear. We speculate that AIF release under conditions of DNA damage may be mediated through a concerted effort of both μ-calpain and PARP-1. Disruption of the mitochondrial membrane potential through PARP-1-dependent NAD^+ and ATP losses, in conjunction with μ-calpain-mediated cleavage of Bid or of AIF itself, may mediate its release from the mitochondria (54, 55).

In conclusion, our studies offer new insights into the signal transduction pathways necessary for PARP-1-mediated cell death, providing a connection between PARP-1 hyperactivation and cell death via fluctuations in Ca^{2+} homeostasis. Knowledge of this pathway may be used to understand, and effectively treat, a large number of human pathologies (*e.g.* ischemia-reperfusion during heart attacks and stroke, and diabetes), as well as to enhance current cancer chemotherapeutic agents through modulation of PARP-1 hyperactivation.

Acknowledgments—We thank Drs. John J. Pink (Case Western Reserve University), Craig Thompson (U. of Pennsylvania), Wei-Xing Zong (State University of New York), and Ying Dong (University of Texas Southwestern Medical Center) for helpful discussions.

REFERENCES

1. Green, D. R., and Evan, G. I. (2002) *Cancer Cell* **1,** 19–30
2. Calabrese, C. R., Almassy, R., Barton, S., Batey, M. A., Calvert, A. H., Canan-Koch, S., Durkacz, B. W., Hostomsky, Z., Kumpf, R. A., Kyle, S., Li, J., Maegley, K., Newell, D. R., Notarianni, E., Stratford, I. J., Skalitzky, D., Thomas, H. D., Wang, L. Z., Webber, S. E., Williams, K. J., and Curtin, N. J. (2004) *J. Natl. Cancer Inst.* **96,** 56–67
3. Kim, M. Y., Zhang, T., and Kraus, W. L. (2005) *Genes Dev.* **19,** 1951–1967
4. Jagtap, P., and Szabo, C. (2005) *Nat. Rev. Drug. Discov.* **4,** 421–440

[4] E. A. Bey and D. A. Boothman, unpublished observations.

5. Pink, J. J., Planchon, S. M., Tagliarino, C., Varnes, M. E., Siegel, D., and Boothman, D. A. (2000) *J. Biol. Chem.* **275,** 5416–5424
6. Pink, J. J., Wuerzberger-Davis, S., Tagliarino, C., Planchon, S. M., Yang, X., Froelich, C. J., and Boothman, D. A. (2000) *Exp. Cell Res.* **255,** 144–155
7. Tagliarino, C., Pink, J. J., Reinicke, K. E., Simmers, S. M., Wuerzberger-Davis, S. M., and Boothman, D. A. (2003) *Cancer Biol. Ther.* **2,** 141–152
8. Wuerzberger, S. M., Pink, J. J., Planchon, S. M., Byers, K. L., Bornmann, W. G., and Boothman, D. A. (1998) *Cancer Res.* **58,** 1876–1885
9. Ross, D., Kepa, J. K., Winski, S. L., Beall, H. D., Anwar, A., and Siegel, D. (2000) *Chem. Biol. Interact.* **129,** 77–97
10. Siegel, D., Franklin, W. A., and Ross, D. (1998) *Clin. Cancer Res.* **4,** 2065–2070
11. Nieminen, A. L., Byrne, A. M., Herman, B., and Lemasters, J. J. (1997) *Am. J. Physiol.* **272,** C1286–C1294
12. Dawson, T. L., Gores, G. J., Nieminen, A. L., Herman, B., and Lemasters, J. J. (1993) *Am. J. Physiol.* **264,** C961–C967
13. Olive, P. L., Banath, J. P., and Durand, R. E. (1990) *Radiat. Res.* **122,** 86–94
14. Abramoff, M. D., Magelhaes, P. J., and Ram, S. J. (2004) *Biophotonics Int.* **11,** 36–42
15. Rasband, W. (1997–2005) *Image J. Int.,* Bethesda, MD
16. Jacobson, E. L., and Jacobson, M. K. (1997) *Methods Enzymol.* **280,** 221–230
17. Zong, W. X., Ditsworth, D., Bauer, D. E., Wang, Z. Q., and Thompson, C. B. (2004) *Genes Dev.* **18,** 1272–1282
18. Beigi, R. D., and Dubyak, G. R. (2000) *J. Immunol.* **165,** 7189–7198
19. Fitzsimmons, S. A., Workman, P., Grever, M., Paull, K., Camalier, R., and Lewis, A. D. (1996) *J. Natl. Cancer Inst.* **88,** 259–269
20. Hollander, P. M., and Ernster, L. (1975) *Arch. Biochem. Biophys.* **169,** 560–567
21. Lee, Y. J., Galoforo, S. S., Berns, C. M., Chen, J. C., Davis, B. H., Sim, J. E., Corry, P. M., and Spitz, D. R. (1998) *J. Biol. Chem.* **273,** 5294–5299
22. Blackburn, R. V., Spitz, D. R., Liu, X., Galoforo, S. S., Sim, J. E., Ridnour, L. A., Chen, J. C., Davis, B. H., Corry, P. M., and Lee, Y. J. (1999) *Free Radic. Biol. Med.* **26,** 419–430
23. Lowry, O. H., Rosebrough, N. J., Farr, A. L., and Randall, R. J. (1951) *J. Biol. Chem.* **193,** 265–275
24. Tagliarino, C., Pink, J. J., Dubyak, G. R., Nieminen, A. L., and Boothman, D. A. (2001) *J. Biol. Chem.* **276,** 19150–19159
25. Jacobsen, M. D., Weil, M., and Raff, M. C. (1996) *J. Cell Biol.* **133,** 1041–1051
26. D'Amours, D., Desnoyers, S., D'Silva, I., and Poirier, G. G. (1999) *Biochem. J.* **342,** 249–268
27. Szabo, C., and Dawson, V. L. (1998) *Trends Pharmacol. Sci.* **19,** 287–298
28. Pieper, A. A., Verma, A., Zhang, J., and Snyder, S. H. (1999) *Trends Pharmacol. Sci.* **20,** 171–181
29. McLick, J., Hakam, A., Bauer, P. I., Kun, E., Zacharias, D. E., and Glusker, J. P. (1987) *Biochim. Biophys. Acta* **909,** 71–83
30. Southan, G. J., and Szabo, C. (2003) *Curr. Med. Chem.* **10,** 321–340
31. Cipriani, G., Rapizzi, E., Vannacci, A., Rizzuto, R., Moroni, F., and Chiarugi, A. (2005) *J. Biol. Chem.* **280,** 17227–17234
32. Boothman, D. A., and Pardee, A. B. (1989) *Proc. Natl. Acad. Sci. U. S. A.* **86,** 4963–4967
33. Boothman, D. A., Wang, M., Schea, R. A., Burrows, H. L., Strickfaden, S., and Owens, J. K. (1992) *Int. J. Radiat. Oncol. Biol. Phys.* **24,** 939–948
34. Boothman, D. A., Meyers, M., Fukunaga, N., and Lee, S. W. (1993) *Proc. Natl. Acad. Sci. U. S. A.* **90,** 7200–7204
35. Rogakou, E. P., Pilch, D. R., Orr, A. H., Ivanova, V. S., and Bonner, W. M. (1998) *J. Biol. Chem.* **273,** 5858–5868
36. Reinicke, K. E., Bey, E. A., Bentle, M. S., Pink, J. J., Ingalls, S. T., Hoppel, C. L., Misico, R. I., Arzac, G. M., Burton, G., Bornmann, W. G., Sutton, D., Gao, J., and Boothman, D. A. (2005) *Clin. Cancer Res.* **11,** 3055–3064
37. Siegel, D., Gustafson, D. L., Dehn, D. L., Han, J. Y., Boonchoong, P., Berliner, L. J., and Ross, D. (2004) *Mol. Pharmacol.* **65,** 1238–1247
38. Lewis, A., Ough, M., Li, L., Hinkhouse, M. M., Ritchie, J. M., Spitz, D. R., and Cullen, J. J. (2004) *Clin. Cancer Res.* **10,** 4550–4558
39. Cullen, J. J., Hinkhouse, M. M., Grady, M., Gaut, A. W., Liu, J., Zhang, Y. P., Weydert, C. J., Domann, F. E., and Oberley, L. W. (2003) *Cancer Res.* **63,** 5513–5520
40. Yu, S. W., Wang, H., Poitras, M. F., Coombs, C., Bowers, W. J., Federoff, H. J., Poirier, G. G., Dawson, T. M., and Dawson, V. L. (2002) *Science* **297,** 259–263
41. Manna, S. K., Gad, Y. P., Mukhopadhyay, A., and Aggarwal, B. B. (1999) *Biochem. Pharmacol.* **57,** 763–774
42. Pardee, A. B., Li, Y. Z., and Li, C. J. (2002) *Curr. Cancer Drug. Targets* **2,** 227–242
43. Chowdhury, D., Keogh, M. C., Ishii, H., Peterson, C. L., Buratowski, S., and Lieberman, J. (2005) *Mol. Cell* **20,** 801–809
44. van Wijk, S. J., and Hageman, G. J. (2005) *Free Radic Biol. Med.* **39,** 81–90
45. Kun, E., Kirsten, E., Mendeleyev, J., and Ordahl, C. P. (2004) *Biochemistry* **43,** 210–216
46. Tanuma, S., Kawashima, K., and Endo, H. (1986) *J. Biol. Chem.* **261,** 965–969
47. Ogata, N., Ueda, K., Kawaichi, M., and Hayaishi, O. (1981) *J. Biol. Chem.* **256,** 4135–4137
48. Homburg, S., Visochek, L., Moran, N., Dantzer, F., Priel, E., Asculai, E., Schwartz, D., Rotter, V., Dekel, N., and Cohen-Armon, M. (2000) *J. Cell Biol.* **150,** 293–307
49. Virag, L., Scott, G. S., Antal-Szalmas, P., O'Connor, M., Ohshima, H., and Szabo, C. (1999) *Mol. Pharmacol.* **56,** 824–833
50. Barbouti, A., Doulias, P. T., Zhu, B. Z., Frei, B., and Galaris, D. (2001) *Free Radic Biol. Med.* **31,** 490–498
51. Jornot, L., Petersen, H., and Junod, A. F. (1998) *Biochem. J.* **335,** 85–94
52. Britigan, B. E., Rasmussen, G. T., and Cox, C. D. (1998) *Biochem. Pharmacol.* **55,** 287–295
53. Fonfria, E., Marshall, I. C., Benham, C. D., Boyfield, I., Brown, J. D., Hill, K., Hughes, J. P., Skaper, S. D., and McNulty, S. (2004) *Br. J. Pharmacol.* **143,** 186–192
54. Polster, B. M., Basanez, G., Etxebarria, A., Hardwick, J. M., and Nicholls, D. G. (2005) *J. Biol. Chem.* **280,** 6447–6454
55. Takano, J., Tomioka, M., Tsubuki, S., Higuchi, M., Iwata, N., Itohara, S., Maki, M., and Saido, T. C. (2005) *J. Biol. Chem.* **280,** 16175–16184

Non-homologous end joining is essential for cellular resistance to the novel antitumor agent β-lapachone[*†]

Melissa S. Bentle[1], Kathryn E. Reinicke[2] Ying Dong[3], and David A. Boothman[1,2,3§]

From the Departments of [1]Pharmacology and [2]Biochemistry, Case Western Reserve University, Cleveland, Ohio, 44106, the [3]Department of Pharmacology, Laboratory of Molecular Stress Responses, and the Simmons Comprehensive Cancer Center, University of Texas Southwestern Medical Center, Dallas, Texas, 75390

Running Title: NHEJ mediates resistance to β-lapachone

Key Words: Non-homologous end joining, homologous recombination, β-Lapachone, carcinogenesis, caspase-independent cell death, DNA damage

Footnotes to the title page:

*This work was supported in part by National Institutes of Health/NCI Grant CA10279201 (to D.A.B.), CWRU Core Grant P30CA43703-12 and Department of Defense Breast Cancer Program Predoctoral Fellowships W81XWH-04-1-0301 and W81XWH-05-1-0248 (to M.S.B. and K.E.R. respectively)

[§]Request for reprints: David A. Boothman, Ph.D., Departments of Pharmacology, Oncology and Radiation Oncology, Laboratory of Molecular Stress Responses Program in Cell Stress and Nanomedicine, and the Simmons Comprehensive Cancer Center, UT Southwestern Medical Center, 5323 Harry Hines Blvd, Dallas, Texas 75390, Tel. 214 648-9255; Fax. 214 648-0264; E-Mail: David.Boothman@UTSouthwestern.edu

[†]This is manuscript CSCN 011 from the Cell Stress and Cancer Nanomedicine Program, Simmons Comprehensive Cancer Center at the University of Texas Southwestern Medical Center at Dallas.

Footnotes to the text:

[1]http://clinicaltrials.gov/ct/show/NCT00102700?order=4 and http://clinicaltrials.gov/ct/show/NCT00358930?order=5

[2]Reinicke, K.E., Bentle, M.S., Bey, E.A., Dong, Y., Bornmann, W., Spitz, D.R., and Boothman, D.A. NAD(P)H:quinone oxidoreductase 1-dependent reactive oxygen species are necessary, but not sufficient, for β-lapachone-mediated cell death.

Abstract

Many popular antitumor agents, such as Toposiomerase II poisons, kill cancer cells by creating non-repaired DNA double-strand breaks (DSBs). To repair DSBs, error-free homologous recombination (HR) and/or error-prone non-homologous end joining (NHEJ) are activated. These processes are mediated by the phosphatidylinositol 3′-kinase related kinase (PIKK) family of serine/threonine protein kinases: ataxia telangiectasia mutated (ATM), ataxia telangiectasia and Rad3-related (ATR) for HR, and DNA-dependent protein kinase catalytic subunit (DNA-PKcs) for NHEJ. Alterations in these repair processes can cause drug/radiation resistance and increase genomic instability.

β-Lapachone (β-Lap; aka ARQ 501), currently in Phase II clinical trials for the treatment of pancreatic cancer, causes a novel casapse- and p53-independent cell death in cancer cells over-expressing NAD(P)H:quinone oxidoreductase-1 (NQO1). NQO1 catalyzes a futile oxidoreduction of β-lap leading to reactive oxygen species (ROS) generation, DNA breaks, γ-H2AX foci formation, and the hyperactivation of poly(ADP-ribose) polymerase-1 (PARP-1) which is required for cell death. Here, we report that β-lap exposure results in the NQO1-dependent activation of the Mre11-Rad50-Nbs-1 (MRN) complex. In addition, ATM serine 1981, DNA-PKcs threonine 2609, and Chk1-serine 345 phosphorylation were noted; indicative of simultaneous HR and NHEJ activation. However, inhibition of NHEJ, but not HR, by genetic or chemical means potentiated β-lap cytotoxicity. These studies give insight into the mechanism by which β-lap radiosensitizes cancer cells and suggests NHEJ as a potent target for enhancing the therapeutic efficacy of β-lap alone or in combination with other agents in cancer cells that express elevated NQO1 levels.

Introduction

Many cancer chemotherapeutic agents, such as ionizing radiation (IR), and DNA-damaging chemotherapeutic compounds cause cell death by creating DNA double-strand breaks (DSBs) (1, 2). DSBs can occur from endogenously produced reactive oxygen species (ROS) or conversion of single-strand breaks (SSBs) to DSBs by advancing replication forks (3). Although cells maintain the capability to survive low levels of DNA damage, as little as one non-repaired DNA DSB can kill a cell (4).

Therefore, to combat the deleterious effects of DSBs, an array of evolutionary conserved detection and repair pathways have evolved. Homologous recombination (HR) and non-homologous end joining (NHEJ) are two distinct, yet complementary mechanisms for mammalian DSB repair that can interact simultaneously even on the same DSB site (5-7). Essential to both HR and NHEJ, is the activation of one or all three related phosphatidylinositol 3′-kinase-like kinases (PI3Ks) in response to DNA damage (8). Ataxia telangiectasia mutated (ATM), and ATM- and Rad3-related (ATR) are associated with HR and are typically activated during S/G_2 phase by DNA breaks (e.g. ATM) or after replication fork arrest (e.g. ATR activation after ultraviolet radiation (UV) exposure). In contrast, DNA-protein kinase catalytic subunit (DNA-PKcs; part of the DNA-PK complex including the Ku70/Ku80 heterodimer) is involved in NHEJ which operates throughout the cell cycle in response to DSBs. These kinases operate as transducer proteins that relay and amplify damage signals to mediator proteins. A common substrate of all PI3Ks is histone variant, H2AX. Formation of γ-H2AX has been identified to be an early marker of DNA damage, in particular DSBs (9, 10). Shortly after DSB damage detection and PI3K activation, H2AX becomes phosphorylated on serine 139 in a 2-Mb region surrounding the break. Microscopically, this phosphorylation event occurs on a multitude of H2AX molecules leading to the production of foci that are visible when labeled with an antibody specific for phosphorylated serine 139 of H2AX (γ-H2AX). γ-H2AX foci facilitate the recruitment of DNA-damage regulating protein complexes to the sites of damage (11), while γ-H2AX de-phosphorylation assists DNA damage repair (12). The MRE11/Rad50/Nbs-1 (MRN) complex serves as the initial protein complex to participate in both NHEJ and HR pathways (13). In the NHEJ pathway, the MRN complex modifies DSB ends by its

endo- and exo-nuclease activity (14). In HR, the complex acts as an exonuclease to produce 3′ single-strand overhangs that are bound by Rad52 (13).

β-lapachone (β-lap; a.k.a. ARQ 501) is currently in Phase II clinical trials for the treatment of pancreatic adenocarcinoma in combination with gemcitabine[1]. β-Lap is a novel antitumor agent that is bio-activated by the two-electron oxidoreductase NAD(P)H quinone oxidoreductase-1 (NQO1) (E.C. 1.6.99.2). Since NQO1 is highly expressed in many human cancers (e.g. breast, lung, pancreatic, and prostate cancer) it is an attractive target for selective cancer chemotherapy by β-lap alone or in combination with IR (15-17). We previously reported that the initiation of β-lap-induced cell death is triggered by the NQO1-dependent oxidoreduction of β-lap (15). NQO1-mediated metabolism of β-lap results in a futile cycling event wherein β-lap is reduced to an unstable hydroquinone that reverts spontaneously back to its parent structure, using two molecules of oxygen (18). As a result, ROS are generated causing DNA damage, γ-H2AX foci formation, poly(ADP-ribose) polymerase-1 (PARP-1) hyperactivation, and subsequent loss of ATP and NAD^+ (19). This loss of ATP and NAD^+ was proposed to be the mechanism by which β-lap could enhance the sensitivities of a variety of chemotherapeutic therapies as well as IR (20). β-lap-induced cell death was unique in that PARP-1 and p53 were cleaved concomitant with μ-calpain activation, consistent with the fact that global caspase inhibitors had little effect on β-lap-induced proteolysis and lethality (15, 21). Interestingly, β-lap-mediated cell death exhibited classical features of apoptosis (e.g. DNA condensation, and terminal deoxynucleotidyl transferase-mediated dUTP nick-end labeling (TUNEL)-positive cells), but was not dependent on standard apoptotic mediators such as p53, Bax/Bak, or caspases (22).

Previous information from our laboratory demonstrated that β-lap caused DNA damage, γ-H2AX focus formation and PARP-1 hyperactivation selectively in NQO1-positive cells. To date, however, studies have not explored the contribution of DNA DSB repair in β-lap-induced cell death. We investigated whether β-lap exposure of NQO1-positive cancer cells activated HR and/or NHEJ, and explored the extent to which each of these repair systems influences drug resistance. To examine this, we utilized a variety of cell model systems with altered ATM, ATR, and DNA-PKcs functions as well as the use

of selective inhibitors to these kinases. β-lap caused the delayed (10-15 min) but dose-dependent activation of the MRN complex, ATM, DNA-PKcs, as well as ATR monitored by Chk1-pSer345. Importantly, only inhibition of DNA-PKcs enhanced the potency of β-lap, indicating a predominant role for NHEJ in the repair of DSBs and resistance of cancer cells after sub-lethal doses of β-lap. Information gathered from these studies warrants the combinatorial usage of DNA repair inhibitors, particularly of NHEJ components, to enhance the toxicity of this agent in the treatment of human cancers that express elevated NQO1 levels.

Materials and Methods

Reagents. β-Lap was synthesized by Dr. William G. Bornmann (MD Anderson), dissolved in dimethyl sulfoxide (DMSO) at 40 mM, and the concentration verified by spectrophotometry (19). Hoechst 33258, etoposide (ETO), and dicoumarol (DIC) were obtained from Sigma (St. Louis, MO). The DNA-PKcs inhibitor, Nu7026 (2-(Morpholin-4-yl)-benzo[h]chromen-4-one) and ATM/ATR kinase inhibitor (AAI) were obtained from Calbiochem (La Jolla, CA). They were dissolved in DMSO and used at 10 μM unless otherwise stated. 2-morpholin-4-yl-6-thianthren-1-yl-pyran-4-one (KU-55933) was synthesized by KuDOS Pharmaceuticals Ltd. (Cambridge, UK), dissolved in DMSO and used at 10 μM.

Cell culture. MCF-7 breast cancer cells were maintained and used as described (15). Human MO59K and MO59J cells which are proficient and deficient in both DNA-PK activity and p350 protein, respectively (23) were obtained from the American Type Culture Collection (Manassas, VA). U2OS-derived stable cell lines that can conditionally regulate either wild-type (WT) or kinase-dead ATR (KD-ATR) levels by doxycylin (dox) were a generous gift from Dr. Paul Nghiem/Dr. Stuart L. Schreiber (Harvard University) (24). Recombinant ATM was stably expressed in immortalized human A-T cells using an episomal expression vector, were obtained from Dr. Yosef Shiloh and described elsewhere (25). Cells are designated as follows: A-T cells ($ATM^{-/-}$) and A-T cells ectopically expressing ATM ($ATM^{+/+}$). NQO1-deficient MO59K, MO59J, $ATM^{-/-}$, and $ATM^{+/+}$ cells were stably infected using a puromycin-selectable pLPCX

retroviral vector alone or one containing the NQO1 cDNA packaged in Phoenix-Ampho cells (26). Uninfected cells were removed by selection in puromycin (0.5 μg/mL) containing media, however, all experiments were performed in the absence of selection. NQO1 expression was evaluated in all cells as described elsewhere (15). Unless otherwise defined, all cells were grown in high glucose-containing DMEM tissue culture medium containing 10% fetal bovine serum (FBS) or tetracycline-free FBS (U2OS cells), 2 mM L-glutamine, penicillin (100 units/mL), and streptomycin (100 mg/mL) at 37°C in a 5% CO_2, 95% air humidified atmosphere (27). MCF-7 cells were grown as described above, except in high-glucose containing RPMI medium. All tissue culture components were purchased from Invitrogen (Carlsbad, CA) unless otherwise stated. All cells were routinely tested and found free of mycoplasma contamination.

Relative Survival Assays. Relative survival assays were performed as described (15). MCF-7, MO59K, and MO59J cells were pretreated for 1 h with 10 μM Nu7026 or KU-55933 prior to co-treatment with β-lap at the indicated doses for 2-4 h. After β-lap treatment, medium containing Nu7026 or KU-55933 alone was added and then removed after 16 h. Drug-free medium was added and survival after 6 days was assessed. U2OS WT or KD-ATR cells were treated with 1 μg/mL of dox 48 h prior to treatment with various concentrations of β-lap, with or without DIC (40 μM) for 2-4 h, then replaced with drug-free media. Cells were allowed to grow for an additional 5-6 days and relative survival determined (15). Prior studies using β-lap demonstrated that relative survival assays correlated directly with colony forming ability assays (15). Data were expressed as means, $\pm$ S.E.M. for treated/control (T/C) from separate triplicate experiments, and comparisons analyzed using a two-tailed Student's *t* test for paired samples.

Cell irradiation. For ultraviolet light C (UVC) exposures, U2OS WT and KD-ATR culture medium was removed and reserved. Cell cultures were washed once in room temp. 1 X PBS and then placed uncovered under a UV lamp emitting primarily 254 nm radiation at a fluency rate of 2.2 $J/m^2/s$. Following UVC exposure, reserved medium was replaced and the cultures were incubated for the indicated periods of time. Other cells were treated with 10 μM β-lap, or 500 μM H_2O_2 and harvested for immunoblotting 2 h after treatment. For exposure to IR, cells were irradiated using a ^{137}Cs source as described and analyzed for foci formation (see below) (28).

Immunoblotting. Western blots were prepared as described (22) with modifications. To examine Chk1 and p53 phosphorylation, whole cell extracts were prepared using lysis buffer (50 mM Tris, pH 8.0, 150 mM NaCl, 1 mM EDTA, 1 mM EGTA, 1% NP-40, 10 μl/ml protease inhibitor mixture, and 1 mM sodium metavanadate). Protein levels were determined by the Bradford method. Total α-Chk-1 and the α-phospho-Ser345 Chk-1 (Chk1-pSer345) antibody were used at a dilution of 1:100 (Cell Signaling Technology, Danvars, MA) and α-tubulin was used at a dilution of 1:5000 (Calbiochem). An NQO1 antibody was generously provided to us by Dr. David Ross (Univ. of Colorado Health Science Center) and used at a 1:2000 dilution (29).

Confocal microscopy. MCF-7 cells were treated with 1-5 μM β-lap for various times with or without pre- and co-treatment with Nu7026, KU-55933 or DMSO alone. As a positive control for the DSB damage response, cells were irradiated with 5 Gy and fixed 15 minutes later. After treatment, cells were washed once with 1 X PBS and fixed in methanol/acetone (1:1) for 10 minutes at 4°C, then blocked with 5% bovine serum albumin (BSA)/PBST for 30 minutes at room temperature. Cells were incubated with primary antibodies: α-MRE11, α-Rad50 (GeneTex, San Antonio, TX), α-Nbs-1 phospho-ser343 (Abcam, Cambridge, MA), α-ATM phospho-ser1981, α-DNA-PKcs phospho-Thr2609 (Rockland, Gilbertsville, PA), or α-γ-H2AX (Trevigen, Gaithersburg, MD; Upstate, Charlottesville, VA) overnight at 4°C at 1:100-500 dilutions. Alexa Fluor fluorescent secondary antibodies (Molecular Probes, Eugene, OR) were then added for 2 h at room temperature. Nuclei were visualized by Hoechst 33258 staining at 1:3000 dilution. Coverslips were mounted in fluoromount-G (Southern Biotech, Birmingham, AL). Confocal images were collected using a X63 N.A. 1.4 oil immersion planapochromat objective at 488 nm and 594 nm from a krypton/argon laser using a Zeiss LSM 510 confocal microscope (Thornwood, NY). Images shown were representative of experiments performed at least three times. The average number of foci/1 μM slice was calculated as means, $\pm$ S.E.M. by counting 30 or more cells from three independent experiments. Student's *t* tests were used for comparision.

Alkaline and Neutral Comet Assays. Single cell gel electrophoretic comet assays were performed under alkaline or neutral conditions as described (19). MCF-7 cells were treated with 5 μM β-lap, 100 μM ETO, 500 μM H_2O_2, or vehicle alone and harvested at

various times. For neutral comet assays, after cellular lysis, slides were immersed in neutral buffer (1 X TBE, pH 7.0) for 60 min at room temperature in the dark. Comets were visualized using an Olympus fluorescence microscope (Melville, NY), and images captured using a digital camera. Images were analyzed using ImageJ software (30, 31) and comet tail length was calculated as the distance between the end of the nuclei heads and the end of each tail, as well as the distance between the mean of the head and tail distributions. $\%DNA_{tail}$=TA X TAI X 100/(TA/TAI) + [HA X HAI] where TA is the tail area, TAI is tail intensity, HA the head area, and HAI the head area intensity. Each datum point represents the average of 100 cells $\pm$ S.E.M., and data are representative of experiments performed in duplicate.

Results

The MRE11/Rad50/Nbs-1 (MRN) complex is activated by β-Lap. Previously, we showed that exposure of NQO1-expressing cancer cells to β-lap caused ROS and DNA damage, measured by alkaline comet assay and γ-H2AX formation (19). Furthermore, activation of the MRN complex following β-lap exposure was recently reported in the yeast system *Saccharomyces cerevisiae* (32). Therefore, we wanted to determine if and which DSB repair pathways were activated in response to this agent by examining MRN complex recruitment to the break sites. Although the true nature of damage-induced foci has not been elucidated, these protein complexes are suggested to be a visual indication of DNA repair centers (11). Since the MRN complex is central to both HR and NHEJ, we examined foci formation in MCF-7 cells after various times of β-lap exposure. Mock- or β-lap treated cells were stained with antibodies complementary to MRE-11, Rad50, and phosphorylated Nbs-1 (Nbs-1-p). A marked increase in the organized localization of MRE-11 and Rad50 were observed in the nuclei of β-lap treated cells at 15 min and foci persisted through 60 min (Fig. 1*A* and Fig. 1*B*). Similarly, nuclear foci for Nbs-1-p were also visible beginning at 15 minutes after drug exposure, similar to the kinetics of γ-H2AX (Fig. 1*A* and Fig. 1*B*); both proteins are downstream targets of ATM activation (33). The appearance of these foci was delayed compared to foci observed after IR exposure, where prior studies have demonstrated γ-H2AX foci formation within 1-5 mins post-IR (34). Interestingly, with IR treated cells MRN foci randomly appeared

throughout the nucleus, whereas with β-lap treated cells all components of the MRN formed foci that was predominantly perinuclear (Fig. 1*A* and Supplementary Fig. 1*A-C*). The appearance of perinuclear MRN foci appears to be consistent with the fact that NQO1 is largely cytoplasmic (35) and is where β-lap is metabolized to form ROS. We theorize that H_2O_2 would diffuse through the nucleus, mediating Fenton reactions leading to SSBs, which may then be converted to DSBs at a later time.

Dose-dependent activation of ATM and DNA-PK following β-lap treatment.

Since the MRN complex was recruited after exposure to β-lap, we tested for the activation of ATM; an HR-associated PI3K. After interacting with a DNA DSB, ATM autophosphorylates itself at serine 1981, causing dissociation of the ATM homodimer (36). The now activated ATM monomer can phosphorylate a number of downstream proteins, including Nbs-1 (33). To test for ATM activation, MCF-7 cells were mock-treated or exposed to varying doses of β-lap. Fixed cells were stained with a serine 1981 phospho-specific antibody to ATM (ATM-pSer1981). The activation of ATM occurred in a dose-dependent manner after β-lap treatment. Doses of β-lap (0-3 μM), resulted in few activated ATM molecules, consistent with the low level of DNA damage detected at these doses (Supplementary Fig. 2 and Fig. 2*A*). In contrast, lethal doses of (≥4 μM) β-lap caused considerable ATM activation with an ~8 fold increase in the number of foci/cell, corresponding to the net increase in total damage (Supplemental Fig. 2 and Fig 2*A* and 2*C*). These data suggest that the accumulation of large numbers of β-lap-induced SSBs leads to the creation of DSBs. These DSBs cause the activation of the canonical HR DSB repair pathway involving the MRN complex and ATM.

Due to the cell-cycle independence of NQO1-mediated bioactivation of β-lap (27) and generation of DNA damage, we examined DNA-PK activation, which is known to also be activated in a cell-cycle independent manner (22). Previous work indicated that DNA-PKcs was autophosphorylated at Thr2609 (DNA-PKcs-pThr2609) *in vivo* in response to IR, and DNA-PKcs-pThr2609 co-localizes with γ-H2AX after DNA damage (37, 38). MCF-7 cells were mock-treated or exposed to 1-5 μM β-lap for 30 min. Similar to ATM activation, DNA-PKcs-pThr2609 foci formed in a dose-dependent manner, wherein non-toxic doses of drug caused little DNA-PKcs-pThr2609 foci over

background, whereas cytotoxic doses led to increases in DNA-PKcs-pThr2609 foci that co-localized with γ-H2AX (37) (Fig. 2*B*). Importantly, at 3 μM β-lap (the approximate LD_{50}), DNA-PKcs was significantly activated (9 ± 0.2 foci/cell) while ATM and γ-H2AX were not as robustly activated (3.9 foci/cell ± 1.98 and 3.0 foci/cell ± 0.12 respectively). These data suggest that both HR and NHEJ are activated after β-lap treatment, but the predominant DNA repair pathway activated is NHEJ (Fig. 2*C*).

NHEJ is necessary for β-lap-induced cell death. Due to the robust activation of DNA-PK, we examined the consequences of its inhibition on β-lap lethality. Glioblastoma cell lines, MO59K cells that contain DNA-PKcs and MO59J cells that lack DNA-PKcs were used (39). After generating NQO1-expressing cell lines for each, NQO1-proficient MO59K (MO59K-NQ^+) and MO59J (MO59J-NQ^+), which expressed equivalent levels of NQO1 enzymatic activity (790 ± 20 vs. 690 ± 10 μmols/cyt c reduced/μg protein; respectively) were used in subsequent studies. MO59J-NQ^+ and MO59K-NQ^+ were mock-treated or exposed to various doses of β-lap for 2 h, with or without DIC cotreatment; a selective NQO1 inhibitor. DNA-PKcs-deficient MO59J-NQ^+ cells were significantly more sensitive to β-lap than their DNA-PKcs-proficient counterparts, MO59K-NQ^+ cells (Fig. 3*A*). MO59J-NQ^+ cells required doses of ≥ 5 μM β-lap to elicit cell death whereas MO59K-NQ^+ cells were resistant to the drug, with only 30% cytotoxicity by 12 μM β-lap. In both cell lines, cytotoxicity was abrogated by inhibiting NQO1 activity with 40 μM DIC (Fig. 3*A*). To assess the functionality of DNA-PKcs in the MO59K-NQ^+ cell line, we pretreated both MO59J-NQ^+ and MO59K-NQ^+ with the DNA-PKcs selective inhibitor Nu7026 prior to β-lap treatment. Nu7026 is a potent radiosensitizer in both proliferating and quiescent cells (40). As anticipated, Nu7026 had little effect on cell death in MO59J-NQ^+ cells, since they are devoid of DNA-PKcs activity. However, Nu7026 significantly sensitized MO59K-NQ^+ cells to β-lap (Fig. 3*B*). Treatment with Nu7026 and 12 μM β-lap resulted in an ~80% ± 3.4 reduction in cell viability compared to ~5% ± 1.0 loss of survival in MO59K-NQ^+ cells that were not pretreated with Nu7026 (Fig. 3*B*).

To confirm that DNA-PK was essential in β-lap-induced cell death, MCF-7 cells were treated with sub-lethal doses of β-lap with or without pre- and co-treatment with 30 μM Nu7026 for 2 h. Relative survival was determined 6-7 days later. Doses of β-lap ≤ 2 μM had little to no cellular toxicity alone, whereas doses of β-lap 2.5 μM and higher caused significant lethality. When MCF-7 cells were treated in combination with Nu7026, β-lap-induced cytotoxicity was potentiated (Fig. 3*C*). The most significant difference in cell death was noted between 2-2.5 μM β-lap, where cotreatment with an otherwise non-toxic dose of Nu7026 resulted in an > 80% reduction in survival compared to cells treated with β-lap alone (Fig. 3*C*). To confirm that the effect of Nu7026 was specific for DNA-PKcs and not ATM *per se*, MCF-7 cells were treated with 5 μM β-lap alone with or without pre- and co-treatment with 30 μM Nu7026 and effects on DNA-PKcs versus ATM foci formation were assessed. After 30 min of β-lap exposure, cells were fixed and stained with antibodies to both DNA-PKcs-pThr2609 and ATM-pSer1981 and the average number of foci/cell were examined by confocal microscopy. MCF-7 cells exposed to β-Lap alone resulted in 14 $\pm$ 0.1 DNA-PKcs-p-Thr2609 foci/cell, which was reduced to 3 $\pm$ 1.0 foci/cell upon coadministration with Nu7026 (Fig. 3*D*). Alternatively, ATM-pSer1981 was not altered with Nu7026 treatment versus β-lap alone treated cells (4.7 $\pm$ 2.9 *v.* 4.5 $\pm$ 0.7, respectively) indicating that DNA-PKcs was the predominate PI3K inhibited after treatment with this agent (Fig. 3*D*).

We previously demonstrated that β-lap-induced cell death was mediated by the hyperactivation of PARP-1 (19). Since a deficiency in DNA-PKcs, potentiated β-lap-induced cell death, we examined whether inhibition of NHEJ was accompanied by hyperactivation of PARP-1 at normally sub-lethal doses of β-lap. PARP-1 is associated with both DNA SSB and DSB repair. After binding to DNA breaks, PARP-1 converts β-NAD^+ into polymers of branched or linear poly(ADP-ribose) (PAR) units and attaches them to various nuclear receptor proteins, including PARP-1 itself as part of its autoregulation (41). MO59J-NQ^+ and MO59K-NQ^+ cells were treated with varying doses of β-lap and cell extracts were taken after 20 min. Lethal doses of β-lap in MO59J-NQ^+ cells resulted in considerable PAR accumulation, while the same dose that was found to be non-toxic in the MO59K-NQ^+ cells resulted in little PAR accumulation (Fig.

3*E*). Increasing amounts of PAR polymers were noted in the MO59K-NQ^+ cells with increasing ≥5 μM β-lap doses (Fig. 3*E*). In addition, only treatment of MCF-7 cells with Nu7026, but not with the ATM and ATR inhibitors, KU55933 and AAI resulted in PAR formation (data not shown). These results suggest that although activation of all three PI3Ks occurs after β-lap treatment, only components of NHEJ, namely DNA-PKcs are necessary for β-lap cell death mediated by PARP-1 hyperactivation.

The HR-associated PI3K ATM is not necessary for β-lap-induced cell death. Since ATM autophosphorylation was also observed following β-lap treatment in NQO1-proficient cancer cells, we investigated whether loss of ATM would alter β-lap-mediated cytotoxicity. Isogenic NQO1-positive human immortalized fibroblasts from A-T patients deficient in ATM ($AT^{-/-}$) or proficient via ectopic ATM expression ($AT^{+/+}$) were used (25). $AT^{+/+}$ and $AT^{-/-}$ cells were mock-treated or exposed to varying doses of β-lap in the presence or absence of DIC for 4 h. There was no observable difference in β-lap-induced lethality between NQO1-proficient $AT^{+/+}$ or $AT^{-/-}$ cells. Furthermore, both cells were protected from lethality via DIC cotreatment (Fig. 6*A*).

To corroborate these findings, MCF-7 cells were mock-treated or exposed to sub-lethal-to-lethal doses of β-lap in the presence or absence of the ATM kinase inhibitor KU55933 or the general ATM/ATR inhibitor AAI for 2 h or 4 h (42). KU55933 inhibited ATM-p-Ser1981 after β-lap or IR treatments and as with Nu7026, KU55933 did not affect NQO1 enzymatic activity (Fig. 3*D* and data not shown). Although weak ATM activation was observed after sub-lethal doses of β-lap, inhibition of ATM by KU55933 or AAI had little effect on the lethality of β-lap when treated for either 2 h or 4 h (Fig. 2*A* and 4*B*-*C*).

ATR activation after β-lap exposure. In addition to ATM, HR can also be mediated via ATR, which is recruited to single-stranded DNA regions, which primarily arise in response to replication fork arrest or during the processing of bulky lesions such as UV photoproducts (43). Since β-lap causes ROS generation, we postulate that the DNA SSBs are the primary lesions formed. However, because of the robust DNA DSB damage

responses, DSBs could be formed as a result of stalled replication forks. Therefore, we wanted to examine the activation of ATR in response to β-lap treatment by utilizing a set of stable cell lines derived from U2OS cells (human osteosarcoma). These cells are wild-type for p53, have an intact G_1 DNA-damage checkpoint, and allow the doxycycline inducible expression of either wild-type ATR or a dominant negative (kinase-dead) ATR point mutant (24). ATR activation after β-lap treatment was confirmed by monitoring Chk1-pSer345 levels in WT U2OS cells after treatment with both UVC or β-lap (Fig. 5*A*). However, in U2OS KD-ATR cells, Chk1-pSer345 was muted after both UVC and β-lap exposure (Fig. 5*A*). Furthermore, neither expression of wild-type ATR nor inhibition of ATR (by KD-ATR expression) affected the survival of NQO1-proficient U2OS cells following β-lap exposure (Fig. 5*B*). Furthermore, administration of DIC abrogated β-lap-induced lethality in both cells lines; confirming its role as the key determinant in β-lap-mediated cytotoxicity (Fig. 5*B*).

To confirm our findings that HR was not necessary for β-lap-induced cell death, we treated MCF-7 cells with an inhibitor to both ATM and ATR prior to β-lap exposure. Inhibition of both enzymes was not sufficient to enhance β-lap-mediated cytotoxicity compared to the 80% enhancement observed after inhibition of DNA-PKcs (Fig. 3*C* and Fig. 4*C*). These data indicate that ATR signaling is activated but not the predominant pathway required for the repair of DNA lesions created after treatment with this agent.

ATR activation argues for the presence of DNA SSBs at arrested replication forks. To elucidate the type of DNA damage created by β-lap, NQO1-positive MCF-7 cells were treated with lethal (5 μM) as well as sub-lethal (0-2 μM) doses of β-lap and the formation of total DNA strand breaks (measured by alkaline comet assays) as well as DSBs (monitored by neutral comet assays) were assessed. Sub-lethal doses of β-lap resulted in little to no strand breakage over time, consistent with their survival at these same doses (Supplementary Fig. 2) (19). In contrast, lethal doses of β-lap resulted in a significant increase in total DNA breaks, occurring minutes after drug exposure (Fig. 5*C*) and surpassing the positive control, 500 μM H_2O_2 30 min thereafter (Supplementary Fig. 4). Further analyses indicated that ROS formation and DNA damage were detected within ≤ 5 min after drug addition (19). The amount of DNA strand breaks increased over

time after 5 μM β-lap treatment, suggesting that the lethal event may be related to the total amount of DNA breaks generated[2]. Interestingly, when cells were analyzed using neutral conditions, under the same conditions, little to no DSBs were observed, in contrast to ETO treatment (Fig. 5*C* and Supplemental Fig. 4). As expected, H_2O_2 treatment caused few DNA DSBs, similar to what was observed after β-lap exposure (Supplemental Fig. 4). The formation of DNA breaks after β-lap exposure was NQO1-dependent as coadminstration with DIC prevented any damage (19). These studies indicate that the majority of DNA damage caused by the NQO1-mediated metabolism of β-lap was SSBs, consistent with the genesis of "long-lived" ROS (e.g. H_2O_2).

Discussion

β-Lap, a natural product-based antitumor agent, elicits a unique cell death pathway selectively in cancer cells that express elevated levels of NQO1. The drug is currently in phase I/II clinical trials for the treatment of pancreatic as well as other cancers[1]. We recently demonstrated that β-lap-induced cell death was dependent upon PARP-1 hyperactivation, but not on typical apoptotic mediators such as p53, Bax/Bak or caspases (18). Data from others suggested that β-lap does not cause DNA damage (44). However, we recently showed that β-lap-induced cell death was initiated by the NQO1-dependent generation of ROS, subsequent formation of DNA damage, and calcium-dependent hyperactivation of PARP-1. Once stimulated, PARP-1 hyperactivation depletes ATP/NAD^+ pools inhibiting DNA repair. Therefore, once a threshold level of DNA breaks are formed, PARP-1 hyperactivation appears to be the dominant factor, dictating downstream responses that lead to cell death (19). Since reaching the threshold level of DNA breaks required to hyperactivate PARP-1 is critical for the lethal effects of this drug, understanding the mechanism(s) by which cells resist this threshold (e.g. amplified DNA repair) is important for improving its efficacy. As a first step, we set out to elucidate the DNA damage repair pathways activated by β-lap in NQO1-proficient cancer cells.

We examined by immunofluorescence a number of proteins involved in DNA DSB repair, due to their very rapid and specific localization and modification at double-stranded breaks before and after β-lap exposure (11). Of these proteins, the MRN

complex is activated in a time- and dose-dependent manner (Fig. 1*A*, Fig. 1*B*, and Supplemental Fig. 1). Simultaneously, we noted the activation of ATM and DNA-PK as monitored by their autophosphorylation products, which only occurred in cells with NQO1 enzymatic activity (Fig. 2*A*-*C*, Supplementary Fig. 4). Although low levels of γ-H2AX and DNA-PKcs-pThr2609 foci were evident in NQO1-deficient cells, this may be due to the metabolism of β-lap by one-electron oxidoreductases such as P450 and b5R reductases (45). Overall, these data support a role for NQO1 in amplifying the toxic effects of β-lap exposure via its two-electron oxidoreduction (Supplementary Fig. 4). Activation of ATM, DNA-PK, and the MRN complex were dose-dependent (Fig. 4*A*-*C*). Evidence from our laboratory has suggested that this may be due to a minimal threshold of DNA damage created after β-lap treatment, and after which point the cell is committed to death via PARP-1 hyperactivation[2] (Supplementary Fig. 2).

NHEJ is the primary mechanism by which mammalian cells repair DNA. However, as it does not require a sister strand to serve as a DNA template during repair, it therefore has a higher infidelity rate (18). As such, we tested the hypothesis that NHEJ was not only activated after β-lap treatment, but was necessary to protect cells from β-lap-induced lethality at sub-lethal doses. DNA-PKcs is known to be a direct player in DSB repair by acting as a key component of the NHEJ repair pathway, as defects in kinase activity result in radiosensitivity (39). We noted a ~2-fold increase in the number of DNA-PKcs-pThr2609 versus ATM-pSer1981-induced foci after β-lap exposure (Fig. 2*C*). Further examination of MO59K-NQ$^+$ and MO59J-NQ$^+$ cells revealed that NHEJ was essential for the survival of cells after β-lap treatment (Fig. 5*A*). Importantly, co-treatment of β-lap with the DNA-PKcs inhibitor, Nu7026 sensitized MO59K-NQ cells as well as MCF-7 cells to β-lap (Fig. 3*B*-*C*), indicating a major role for NHEJ in repair following β-lap-induced DNA damage.

To determine if inhibition of NHEJ causes PARP-1-mediated cell death at sub-lethal doses of β-lap we examined PAR accumulation after treatment with β-lap in MO59J-NQ$^+$ and MO59K-NQ$^+$ cells. In DNA-PKcs-deficient MO59J-NQ$^+$ cells, doses of β-lap ≥ 5 μM alone caused significant PAR-modification (Fig. 3*E*). However, proficiency of NHEJ in the MO59K-NQ$^+$ cell line muted PAR accumulation, consistent with their cellular resistance to β-lap (Fig. 3*E*). Furthermore, coadministration of

Nu7026 in MCF-7 cells reverted a sub-lethal dose of β-lap to a toxic event accompanied by the accumulation of PAR polymers that was not seen with ATM or ATR inhibitors (Fig. 3*C*, Fig. 4*B*-*C*, and data not shown). These data indicate that interruption of NHEJ during β-lap treatment commits cells to PARP-1-mediated cell death as we have previously reported (19). An interplay between DNA-PK and PARP-1 has been clearly established and inhibition of both PARP-1 and DNA-PK were able to increase net DSB levels over time after chemically-induced damage (46, 47). Therefore the combined use of β-lap and NHEJ inhibitors would be an ideal "two-hit" cancer therapy by inhibiting mechanistically diverse DNA repair enzymes and thereby retarding DSB rejoining.

In addition to DNA-PKcs-pThr2609, ATM-pSer1981 was also noted after β-lap treatment (Fig. 2*A*). There is some discrepancy as to the exact role ATM plays in HR. It has been shown to be pivotal in general damage signaling and cell cycle regulation (48), but more evidence shows that ATM has a specific role in the slow component of DSB repair (49, 50). In particular, after biologically relevant doses of IR, A-T cells fail to show recovery, and experiments using reverse genetics failed to see any potentiation in phenotype arising from the conditional loss of RAD54 in $ATM^{-/-}$ cells suggesting an inherent HR defect in $ATM^{-/-}$ cells (51). In addition, it has been suggested that the interplay between ATM and DNA-PKcs may be important for the proper initiation of DSB signaling and the processing of DSBs to ensure repair and maintenance of genomic integrity after damage (52). Using cells deficient in ATM we tested whether the loss of ATM and therefore HR-mediated repair, would alter β-lap-mediated cell death similar to what was observed with the loss of NHEJ. Data from our studies revealed no significant difference between $ATM^{+/+}$ and $ATM^{-/-}$ cells in terms of sensitivity to β-lap (Fig. 4*A*). To corroborate these findings we utilized a selective ATM kinase inhibitor, KU55933. As expected, inhibition of ATM in MCF-7 cells showed no difference in lethality to β-lap (Fig. 4*B*). The dose of KU55933 used in these studies was sufficient to inhibit ATM-pSer1981 after IR or β-lap-induced DNA damage (Fig. 3*D*). Interestingly, inhibition of ATM-pSer1981 by this inhibitor also abrogated DNA-PKcs-pThr2609, a response recently noted by Chen *et. al.* supporting a role for ATM in DNA-PKcs-pThr2609 in response to DNA damage (Fig. 3*D*) (52). In contrast, inhibition of DNA-PKcs with Nu7026 blocked ATM-mediated DNA-PKcs-pThr2609 (Fig. 3*D*). These data suggested

that the ATM-mediated DNA-PKcs-pThr2609 was a component of an amplification scheme whereby autophosphorylation of DNA-PKcs at Thr2609 was required prior to signal amplification via ATM.

Since β-lap treatment results in the generation of ROS and possibly other reactive species[2] it is likely that the activation of the DNA DSB repair machinery is a result of DSBs formed as a consequence of stalled replication forks encountering the numerous DNA SSBs (53, 54). As such, we also examined the activation of the PI3K ATR, that is normally involved in the signaling and repair of DNA DSB caused by these abnormalities. To test this, we utilized a human osteosarcoma cell line that contained a kinase-dead form of ATR under the control of a dox inducible promoter. In the absence of dox, these cells showed an increase in Chk1-pSer345 (a downstream substrate of ATR) after UVC, as well as after β-lap treatment whereas this response was muted in the presence of dox (Fig. 5*A*). The levels of total Chk1 and NQO1 were relatively unchanged under either treatment condition (Fig. 5*A* and data not shown). Since ATR was activated, we then tested the sensitivity of these cells to β-lap. U2OS KD-ATR cells treated with or without dox showed no differential β-lap toxicity (Fig. 5*B*). In addition, we utilized an ATM and ATR inhibitor (AAI) to determine if blocking both PI3Ks would enhance β-lap-induced toxicity. Inhibiting both enzymes had no apparent effect on β-lap-induced cytotoxicity in MCF-7 cells (Fig. 4*C*).

ATR is recruited by ATR-interacting protein (ATRIP) to replication protein A (RPA)-coated single-stranded DNA that accumulate at stalled DNA replication forks or is generated by processing of the initial DNA damage (33). Therefore, ATR activation would be consistent with stalled replication forks and could indicate the formation of DSBs from SSBs in response to β-lap exposure in NQO1-proficient cancer cells. We determined the primary lesion generated after β-lap exposure was DNA SSBs, which is consistent with the creation of ROS, in particular H_2O_2 (Fig. 5*C*). Alternatively, the lack of detectable DSBs could be a result of the low sensitivity of the neutral comet assay with respect to γ-H2AX to detect the minor population of DSBs. However, despite the predominance of SSBs, extensive formation of γ-H2AX-induced foci, as well as activation of the MRN complex, ATM, DNA-PK, and ATR were noted albeit in a delayed manner to the initial generation of SSBs (within 5 min *v*. 10-15 min,

respectively) (19). Therefore these data support the hypothesis that DSBs are formed as a secondary DNA lesion after initial SSBs were generated likely as a result from stalled replication forks thereby activating the DNA damage response pathways.

A number or current cancer chemotherapeutic DNA damaging agents function primarily as non-selective inducers of DNA DSBs in highly proliferative cells. A major problem with many of these agents is their lack of selectivity, in which both normal and cancerous tissues are targeted. In contrast, β-lap, which is currently under investigation in PhaseI/II clinical trials, selectively targets cancer cells that express elevated levels of NQO1 resulting in DNA damage and cell death mediated by PARP-1. Here, we demonstrate that in addition to SSB-induced DNA repair pathways, β-lap causes the activation of a variety of DSB repair pathways. In particular, NEHJ was found to be key to the survival of cells exposed to β-lap, since inhibition of NHEJ caused a PARP-1-mediated cell death after treatment with sub-lethal doses of β-lap. In summary, these data warrant the combinatorial use of β-lap with inhibitors of NHEJ thereby increasing the therapeutic efficacy of this compound by targeting two distinct repair mechanisms.

References

1. Krasin, F. and Hutchinson, F. Repair of DNA double-strand breaks in Escherichia coli, which requires recA function and the presence of a duplicate genome. J Mol Biol, *116:* 81-98, 1977.

2. D'Andrea, A. D. and Haseltine, W. A. Modification of DNA by aflatoxin B1 creates alkali-labile lesions in DNA at positions of guanine and adenine. Proc Natl Acad Sci U S A, *75:* 4120-4124, 1978.

3. Kuzminov, A. Single-strand interruptions in replicating chromosomes cause double-strand breaks. Proc Natl Acad Sci U S A, *98:* 8241-8246, 2001.

4. Rich, T., Allen, R. L., and Wyllie, A. H. Defying death after DNA damage. Nature, *407:* 777-783, 2000.

5. van Gent, D. C., Hoeijmakers, J. H., and Kanaar, R. Chromosomal stability and the DNA double-stranded break connection. Nat Rev Genet, *2:* 196-206, 2001.

6. Richardson, C. and Jasin, M. Coupled homologous and nonhomologous repair of a double-strand break preserves genomic integrity in mammalian cells. Mol Cell Biol, *20:* 9068-9075, 2000.

7. Frank-Vaillant, M. and Marcand, S. Transient stability of DNA ends allows nonhomologous end joining to precede homologous recombination. Mol Cell, *10:* 1189-1199, 2002.

8. Khanna, K. K. and Jackson, S. P. DNA double-strand breaks: signaling, repair and the cancer connection. Nat Genet, *27:* 247-254, 2001.

9. Rogakou, E. P., Pilch, D. R., Orr, A. H., Ivanova, V. S., and Bonner, W. M. DNA double-stranded breaks induce histone H2AX phosphorylation on serine 139. J Biol Chem, *273:* 5858-5868, 1998.

10. Foster, E. R. and Downs, J. A. Histone H2A phosphorylation in DNA double-strand break repair. Febs J, *272:* 3231-3240, 2005.

11. Paull, T. T., Rogakou, E. P., Yamazaki, V., Kirchgessner, C. U., Gellert, M., and Bonner, W. M. A critical role for histone H2AX in recruitment of repair factors to nuclear foci after DNA damage. Curr Biol, *10:* 886-895, 2000.

12. Chowdhury, D., Keogh, M. C., Ishii, H., Peterson, C. L., Buratowski, S., and Lieberman, J. gamma-H2AX Dephosphorylation by Protein Phosphatase 2A Facilitates DNA Double-Strand Break Repair. Mol Cell, *20:* 801-809, 2005.

13. Jackson, S. P. Sensing and repairing DNA double-strand breaks. Carcinogenesis, *23:* 687-696, 2002.

14. Trujillo, K. M., Yuan, S. S., Lee, E. Y., and Sung, P. Nuclease activities in a complex of human recombination and DNA repair factors Rad50, Mre11, and p95. J Biol Chem, *273:* 21447-21450, 1998.

15. Pink, J. J., Planchon, S. M., Tagliarino, C., Varnes, M. E., Siegel, D., and Boothman, D. A. NAD(P)H:Quinone oxidoreductase activity is the principal determinant of beta-lapachone cytotoxicity. J Biol Chem, *275:* 5416-5424, 2000.

16. Boothman, D. A. and Pardee, A. B. Inhibition of radiation-induced neoplastic transformation by beta-lapachone. Proc Natl Acad Sci U S A, *86:* 4963-4967, 1989.

17. Suzuki, M., Amano, M., Choi, J., Park, H. J., Williams, B. W., Ono, K., and Song, C. W. Synergistic effects of radiation and beta-lapachone in DU-145 human prostate cancer cells in vitro. Radiat Res, *165:* 525-531, 2006.

18. Bentle, M. S., Bey, E. A., Dong, Y., Reinicke, K. E., and Boothman, D. A. New tricks for old drugs: the anticarcinogenic potential of DNA repair inhibitors. J Mol Histol, *37:* 203-218, 2006.

19. Bentle, M. S., Reinicke, K. E., Bey, E. A., Spitz, D. R., and Boothman, D. A. Calcium-dependent modulation of poly(ADP-ribose) polymerase-1 alters cellular metabolism and DNA repair. J Biol Chem, *281:* 33684-33696, 2006.

20. Wang, A., Li, C. J., Reddy, P. V., and Pardee, A. B. Cancer chemotherapy by deoxynucleotide depletion and E2F-1 elevation. Cancer Res, *65:* 7809-7814, 2005.

21. Tagliarino, C., Pink, J. J., Reinicke, K. E., Simmers, S. M., Wuerzberger-Davis, S. M., and Boothman, D. A. Mu-calpain activation in beta-lapachone-mediated apoptosis. Cancer Biol Ther, *2:* 141-152, 2003.

22. Wuerzberger, S. M., Pink, J. J., Planchon, S. M., Byers, K. L., Bornmann, W. G., and Boothman, D. A. Induction of apoptosis in MCF-7:WS8 breast cancer cells by beta-lapachone. Cancer Res, *58:* 1876-1885, 1998.

23. Lees-Miller, S. P., Godbout, R., Chan, D. W., Weinfeld, M., Day, R. S., 3rd, Barron, G. M., and Allalunis-Turner, J. Absence of p350 subunit of DNA-activated protein kinase from a radiosensitive human cell line. Science, *267:* 1183-1185, 1995.

24. Nghiem, P., Park, P. K., Kim Ys, Y. S., Desai, B. N., and Schreiber, S. L. ATR is not required for p53 activation but synergizes with p53 in the replication checkpoint. J Biol Chem, *277:* 4428-4434, 2002.

25. Ziv, Y., Bar-Shira, A., Pecker, I., Russell, P., Jorgensen, T. J., Tsarfati, I., and Shiloh, Y. Recombinant ATM protein complements the cellular A-T phenotype. Oncogene, *15:* 159-167, 1997.

26. Patton, J. T., Mayo, L. D., Singhi, A. D., Gudkov, A. V., Stark, G. R., and Jackson, M. W. Levels of HdmX expression dictate the sensitivity of normal and transformed cells to Nutlin-3. Cancer Res, *66:* 3169-3176, 2006.

27. Pink, J. J., Wuerzberger-Davis, S., Tagliarino, C., Planchon, S. M., Yang, X., Froelich, C. J., and Boothman, D. A. Activation of a cysteine protease in MCF-7 and T47D breast cancer cells during beta-lapachone-mediated apoptosis. Exp Cell Res, *255:* 144-155, 2000.

28. Boothman, D. A., Meyers, M., Fukunaga, N., and Lee, S. W. Isolation of x-ray-inducible transcripts from radioresistant human melanoma cells. Proc Natl Acad Sci U S A, *90:* 7200-7204, 1993.

29. Siegel, D., Franklin, W. A., and Ross, D. Immunohistochemical detection of NAD(P)H:quinone oxidoreductase in human lung and lung tumors. Clin Cancer Res, *4:* 2065-2070, 1998.

30. Abramoff, M. D., Magelhaes, P.J., Ram, S.J. Image Processing with ImageJ. Biophotonics International, *11:* 36-42, 2004.

31. Rasband, W. ImageJ. . Bethesda, Maryland, USA, 1997-2005.

32. Menacho-Marquez, M. and Murguia, J. R. beta-lapachone Activates a Mre11p-Tel1p G1/S Checkpoint in Budding Yeast. Cell Cycle, *5*, 2006.

33. Kurz, E. U. and Lees-Miller, S. P. DNA damage-induced activation of ATM and ATM-dependent signaling pathways. DNA Repair (Amst), *3:* 889-900, 2004.

34. Rothkamm, K. and Lobrich, M. Evidence for a lack of DNA double-strand break repair in human cells exposed to very low x-ray doses. Proc Natl Acad Sci U S A, *100:* 5057-5062, 2003.

35. Winski, S. L., Koutalos, Y., Bentley, D. L., and Ross, D. Subcellular localization of NAD(P)H:quinone oxidoreductase 1 in human cancer cells. Cancer Res, *62:* 1420-1424, 2002.

36. Bakkenist, C. J. and Kastan, M. B. DNA damage activates ATM through intermolecular autophosphorylation and dimer dissociation. Nature, *421:* 499-506, 2003.

37. Chan, D. W., Chen, B. P., Prithivirajsingh, S., Kurimasa, A., Story, M. D., Qin, J., and Chen, D. J. Autophosphorylation of the DNA-dependent protein kinase catalytic subunit is required for rejoining of DNA double-strand breaks. Genes Dev, *16:* 2333-2338, 2002.

38. Ding, Q., Reddy, Y. V., Wang, W., Woods, T., Douglas, P., Ramsden, D. A., Lees-Miller, S. P., and Meek, K. Autophosphorylation of the catalytic subunit of the DNA-dependent protein kinase is required for efficient end processing during DNA double-strand break repair. Mol Cell Biol, *23:* 5836-5848, 2003.

39. Allalunis-Turner, M. J., Barron, G. M., Day, R. S., 3rd, Dobler, K. D., and Mirzayans, R. Isolation of two cell lines from a human malignant glioma specimen differing in sensitivity to radiation and chemotherapeutic drugs. Radiat Res, *134:* 349-354, 1993.

40. Veuger, S. J., Curtin, N. J., Richardson, C. J., Smith, G. C., and Durkacz, B. W. Radiosensitization and DNA repair inhibition by the combined use of novel inhibitors of DNA-dependent protein kinase and poly(ADP-ribose) polymerase-1. Cancer Res, *63:* 6008-6015, 2003.

41. Kim, M. Y., Zhang, T., and Kraus, W. L. Poly(ADP-ribosyl)ation by PARP-1: 'PAR-laying' NAD+ into a nuclear signal. Genes Dev, *19:* 1951-1967, 2005.

42. Hickson, I., Zhao, Y., Richardson, C. J., Green, S. J., Martin, N. M., Orr, A. I., Reaper, P. M., Jackson, S. P., Curtin, N. J., and Smith, G. C. Identification and characterization of a novel and specific inhibitor of the ataxia-telangiectasia mutated kinase ATM. Cancer Res, *64:* 9152-9159, 2004.

43. Cortez, D., Guntuku, S., Qin, J., and Elledge, S. J. ATR and ATRIP: partners in checkpoint signaling. Science, *294:* 1713-1716, 2001.

44. Pardee, A. B., Li, Y. Z., and Li, C. J. Cancer therapy with beta-lapachone. Curr Cancer Drug Targets, *2:* 227-242, 2002.

45. Byczkowski, J. Z. and Gessner, T. Inhibition of the redox cycling of vitamin K3 (menadione) in mouse liver microsomes. Int J Biochem, *20:* 1073-1079, 1988.

46. Boulton, S., Kyle, S., and Durkacz, B. W. Interactive effects of inhibitors of poly(ADP-ribose) polymerase and DNA-dependent protein kinase on cellular responses to DNA damage. Carcinogenesis, *20:* 199-203, 1999.

47. Ruscetti, T., Lehnert, B. E., Halbrook, J., Le Trong, H., Hoekstra, M. F., Chen, D. J., and Peterson, S. R. Stimulation of the DNA-dependent protein kinase by poly(ADP-ribose) polymerase. J Biol Chem, *273:* 14461-14467, 1998.

48. Shiloh, Y. The ATM-mediated DNA-damage response: taking shape. Trends Biochem Sci, *31:* 402-410, 2006.

49. Kuhne, M., Riballo, E., Rief, N., Rothkamm, K., Jeggo, P. A., and Lobrich, M. A double-strand break repair defect in ATM-deficient cells contributes to radiosensitivity. Cancer Res, *64:* 500-508, 2004.

50. Riballo, E., Kuhne, M., Rief, N., Doherty, A., Smith, G. C., Recio, M. J., Reis, C., Dahm, K., Fricke, A., Krempler, A., Parker, A. R., Jackson, S. P., Gennery, A., Jeggo, P. A., and Lobrich, M. A pathway of double-strand break rejoining dependent upon ATM, Artemis, and proteins locating to gamma-H2AX foci. Mol Cell, *16:* 715-724, 2004.

51. Morrison, C., Sonoda, E., Takao, N., Shinohara, A., Yamamoto, K., and Takeda, S. The controlling role of ATM in homologous recombinational repair of DNA damage. Embo J, *19:* 463-471, 2000.

52. Chen, B. P., Uematsu, N., Kobayashi, J., Lerenthal, Y., Krempler, A., Yajima, H., Lobrich, M., Shiloh, Y., and Chen, D. J. ATM is essential for DNA-pkcs phosphorylations at T2609 cluster upon DNA double strand break. J Biol Chem, 2006.

53. Michel, B., Ehrlich, S. D., and Uzest, M. DNA double-strand breaks caused by replication arrest. Embo J, *16:* 430-438, 1997.

54. Michel, B., Grompone, G., Flores, M. J., and Bidnenko, V. Multiple pathways process stalled replication forks. Proc Natl Acad Sci U S A, *101:* 12783-12788, 2004.

Figure Legends

Figure 1. The MRN complex is activated upon β-Lap treatment. β-Lap causes the punctate localization of MRE11, Rad50, and the phosphorylation of Nbs-1. *A,* Visualization of MRE11, Rad50, phosphorylated Nbs-1 and γ-H2AX in MCF-7 cells at various times after treatment for 30 min with 5 μM β-Lap by confocal microscopy. *B*, The average number of MRE11, Rad50, Nbs-1-p, and γ-H2AX foci per cell was determined from at least 60 cells for each treatment group from three independent confocal experiments (means ± S.E.M.).

Figure 2. Dose-dependent activation of ATM and DNA-PK after β-Lap administration. MCF-7 cells were treated with 0-5 μM β-Lap for 30 min at which time samples were fixed and probed with antibodies to *A*, phosphorylated ATM at ser1981 (ATM-pSer1981) or *B*, phosphorylated DNA-PKcs at Thr2609 (DNA-Pkcs-pThr2609) and visualized by confocal microscopy. *C*, MCF-7 cells were treated with 0-5 μM β-Lap for 30 min, fixed and probed for ATM-pSer1981, DNA-PKcs-pThr2609, and Nbs-1-p after 30 min. Shown is the quanitation of the average number of foci/cell per dose of β-lap treated cells for at least 60 cells per treatment (means ± S.E.M.). Student's *t*-test for paired samples, comparing Nbs-1-p or γ-H2AX foci/cell *versus* the number of DNA-PKcs-pThr2609 foci/cell at various doses of β-lap are indicated (*, $p<0.05$).

Figure 3. Loss of DNA-PKcs activity potentiates β-lap-induced cell death. *A-C*, cell death was examined using relative survival assays in NQO1 containing cells. *A*,

MO59K-NQ$^+$ (DNA-PKcs positive) and MO59J-NQ$^+$ (DNA-PKcs negative) cells were treated with varying doses of β-lap alone or in combination with 40 μM DIC for 2 h. After drug exposure, media were removed and drug-free media added. Cells were then allowed to grow for an additional 6 days and relative survival, based on DNA content was determined by Hoechst 33258 staining as described under "Experimental Procedures." *B*, Loss of DNA-PKcs kinase activity sensitizes MO59K-NQ$^+$ cells to β-lap. Relative survival assays using MO59K-NQ$^+$ and MO59J-NQ$^+$ pre- and co-treated with the DNA-PKcs inhibitor Nu7026 (10 μM) for 1 h prior to treatment with varying doses of β-lap for 2 h. *C*, Inhibition of DNA-PKcs with Nu7026 potentiates β-lap-induced cell death in NQO1$^+$ MCF-7 cells. MCF-7 cells were treated with sub-lethal to lethal doses of β-lap alone with or without pre- and co-treatment with 30 μM Nu7026 for 2 h. Differences were compared using two-tailed Student's *t*-test. Groups having *, $p \leq 0.05$; **$p \leq 0.001$ values compared with β-lap alone are indicated. *D*, Nu7026 inhibits DNA-PKcs-pThr2609 but not ATM-pSer1981. MCF-7 cells were treated with 5 μM β-lap with or without pre- and co-treatment with 30 μM Nu7026 for 30 min. After treatment, cells were fixed and probed with antibodies to DNA-PKcs-pThr2609 and ATM-pSer1981 and foci were visualized by confocal microscopy. Shown is the quanitation of the average number of foci/cell for at least 60 cells per treatment group (means $\pm$ S.E.M.). Student's *t*-test for paired samples, experimental groups containing β-lap + KU55933 (KU) or Nu7026 (NU) *versus* β-lap alone are indicated *$p<0.001$. *E,* Lack of DNA-PKcs causes PARP-1 hyperactivation after β-lap treatment. Immunoblot analyses of PAR and α-tubulin protein levels from whole cell extracts from MO59J-NQ$^+$ and MO59K-NQ$^+$ cells that were mock treated or treated with 5 or 12 μM β-lap and harvested after 30 min.

Relative PAR levels were determined by densitometry analyses using α-tubulin loading controls by NIH ImageJ wherein controls were set to 1.0.

Figure 4. β-Lap-induced cell death is not dependent on ATM. *A-C*, Cell death was monitored using relative survival assays in $NQO1^{+}$ cells. *A*, Loss of ATM does not potentiate β-lap-induced cell death. NQO1-proficient $AT^{-/-}$ and $AT^{+/+}$ cells were treated with varying doses of β-lap alone or in combination with 40 μM DIC for 4 h. *B*, MCF-7 cells were treated with 0-4 μM β-lap alone or with pre- and co-treatment with the ATM kinase inhibitor KU55933 (10 μM) for 2 h or 4 h or *C*, the ATM and ATR kinase inhibitor AAI (10 μM) for 2 h.

Figure 5. β-Lap causes ATR activation and SSBs. *A*, Chk1-pSer345 occurs after β-lap treatment. Immunoblots of Chk1-pSer345, total Chk1, and α-tubulin protein levels from whole cell extracts of U2OS KD-ATR treated with or without 1 μg/mL of DOX for 48 h prior to treatment with 10 μM β-lap or 15 J/m^2 UVC. Cells were harvested at the indicated times after treatment. Relative Chk1-pSer345 levels were calculated by densitometric analyses by NIH ImageJ using α-tubulin wherein controls were set to 1.0. *B,* KD-ATR does not alter cell death caused by β-lap. U2OS KD-ATR cells were treated with or without 1 μg/mL of dox for 48 h to induce expression of the dox-inducible kinase-dead ATR prior to treatment with varying doses of β-lap alone or in combination with 40 μM DIC for 2 h. *C,* β-Lap causes the formation of DNA SSBs as shown by comet assay under alkaline and neutral conditions. MCF-7 cells were treated with 5 μM β-Lap for 0-120 min. At the indicated times during drug treatment, cells were harvested

for comet tail formation under both alkaline and neutral conditions. Shown are quantified comet tail lengths of 100 cells (means $\pm$ S.E.M.) for each time and condition calculated using NIH ImageJ software. *Not shown:* 100 μM ETO for 60 h under neutral and alkaline conditions had a comet tail length of roughly 81.12 $\pm$ 3.72 microns *v.* 64.42 $\pm$ 0.91 microns respectively.

Figure 6. Model of β-Lap-induced cell death after lethal and sub-lethal doses. *A,* β-Lap-induced cell death at lethal doses is PARP-1-dominated. β-Lap-mediated metabolism by NQO1 generates ROS that cause DNA SSBs. Extensive SSBs cause the hyperactivation of PARP-1, subsequent NAD^+ and ATP loss, which inhibits DNA repair and leads to cell death. *B,* Non-lethal doses of β-lap are converted to lethal events via inhibition of DNA-PK. At sub-lethal doses of compound, repairable amounts of SSBs are generated. These SSBs are transformed to DSBs possibly via replication fork arrest causing the activation of members of the PI3K family of kinases, ATM, ATR, and DNA-PKcs. NHEJ is the primary repair pathway needed to repair DSBs after drug treatment as only inhibition of DNA-PKcs by either chemical (Nu7026) or genetic (DNA-PKcs$^{-/-}$) means potentiates the toxicity of sub-lethal doses of β-lap leading to PARP-1-mediated cell death.

Bentle_Fig. 1

A.

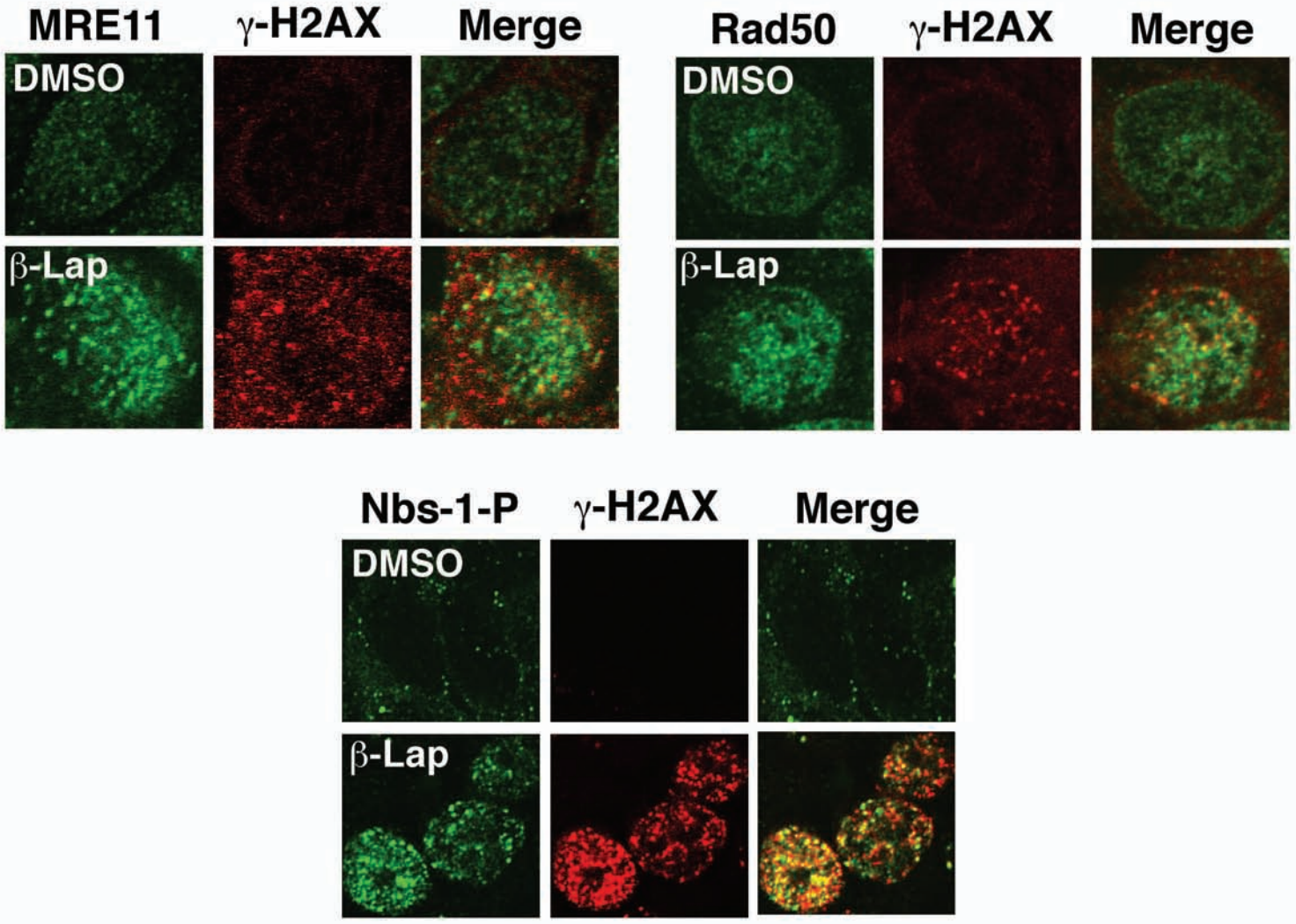

B.

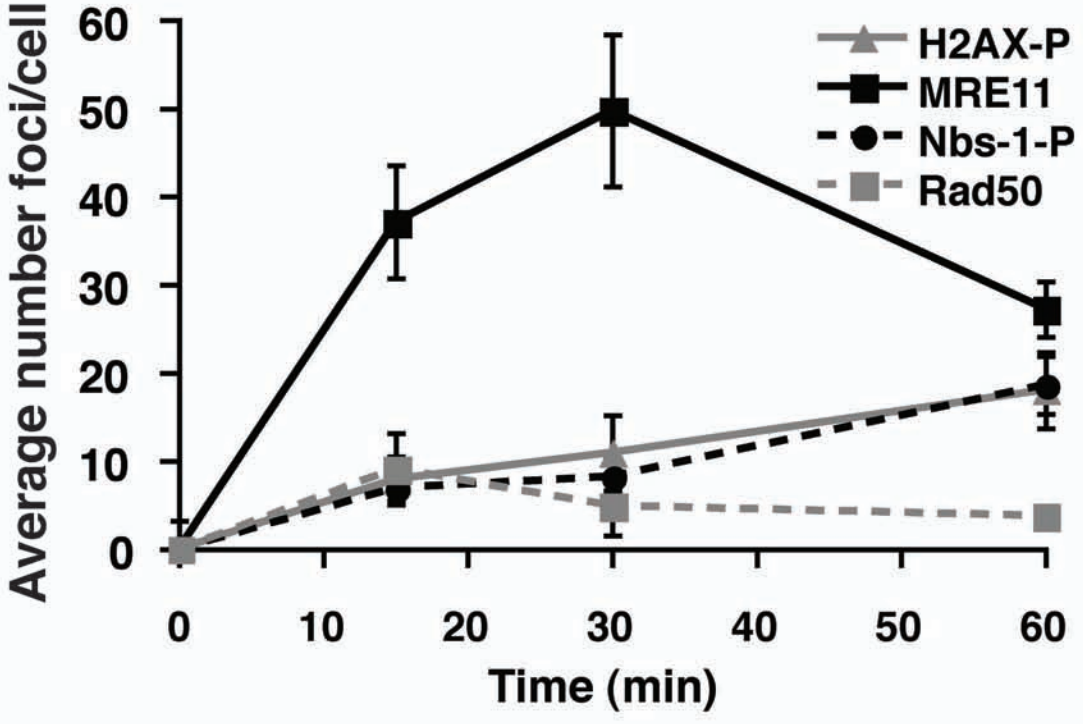

Bentle_Fig 2

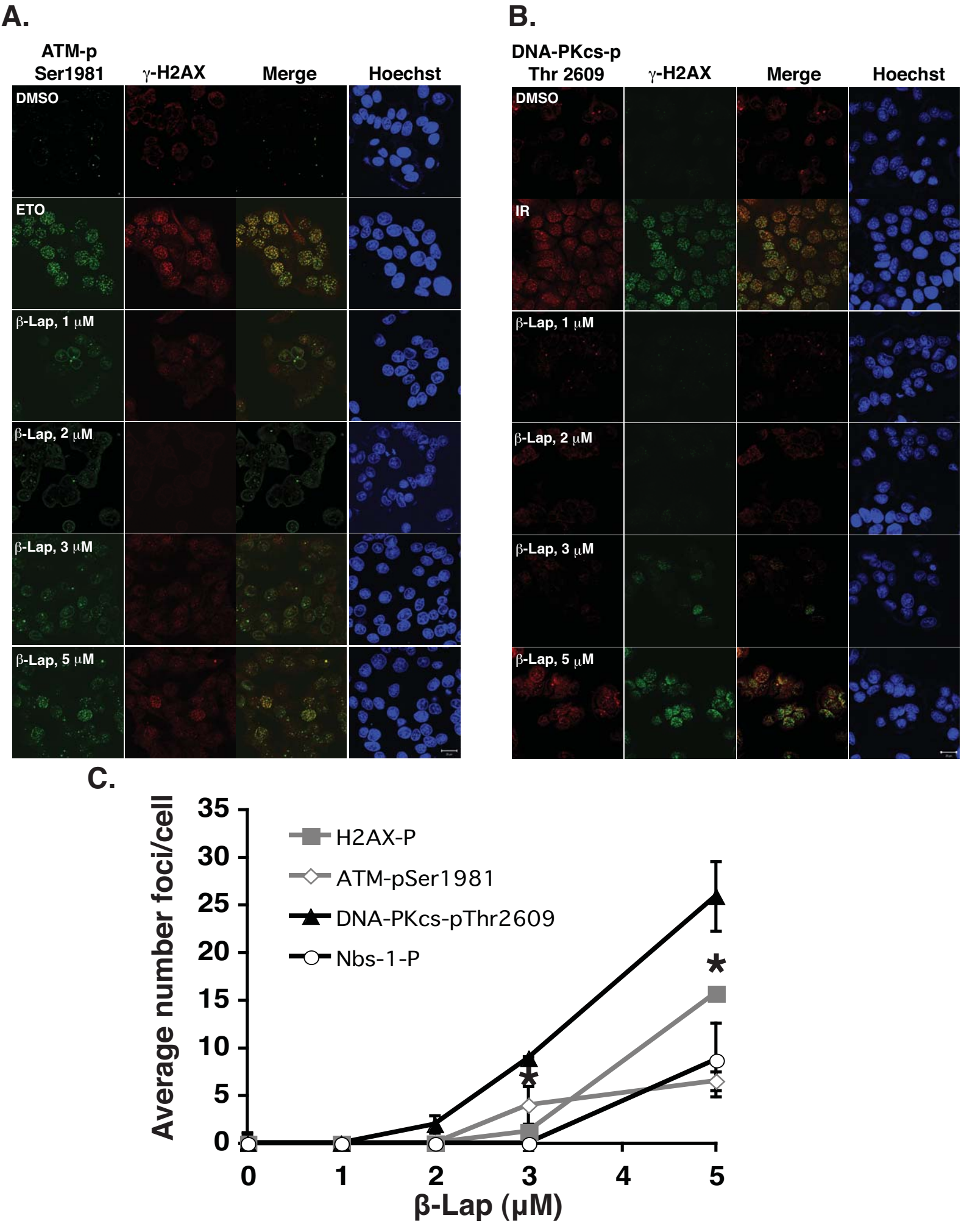
A.
ATM-p Ser1981
γ-H2AX
Merge
Hoechst
DMSO
ETO
β-Lap, 1 μM
β-Lap, 2 μM
β-Lap, 3 μM
β-Lap, 5 μM
B.
DNA-PKcs-p Thr 2609
γ-H2AX
Merge
Hoechst
DMSO
IR
β-Lap, 1 μM
β-Lap, 2 μM
β-Lap, 3 μM
β-Lap, 5 μM
C.
Average number foci/cell
35
30
25
20
15
10
5
0
H2AX-P
ATM-pSer1981
DNA-PKcs-pThr2609
Nbs-1-P
*
*
0
1
2
3
4
5
β-Lap (μM)

Bentle_Fig 3

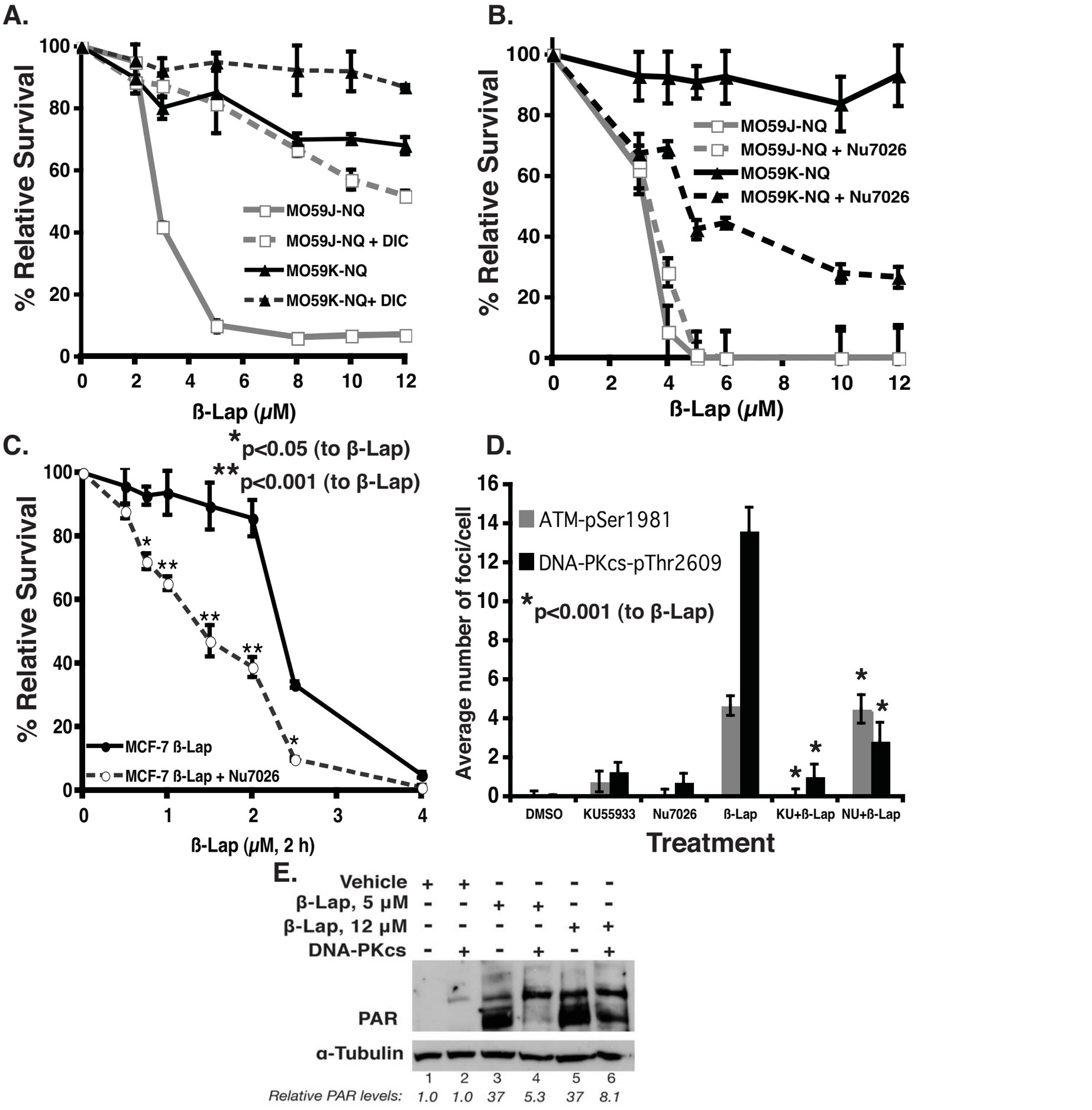
A.
% Relative Survival
MO59J-NQ
MO59J-NQ + DIC
MO59K-NQ
MO59K-NQ+ DIC
ß-Lap (μM)
B.
% Relative Survival
MO59J-NQ
MO59J-NQ + Nu7026
MO59K-NQ
MO59K-NQ + Nu7026
ß-Lap (μM)
C.
*p<0.05 (to β-Lap)
**p<0.001 (to β-Lap)
% Relative Survival
MCF-7 ß-Lap
MCF-7 ß-Lap + Nu7026
ß-Lap (μM, 2 h)
D.
Average number of foci/cell
ATM-pSer1981
DNA-PKcs-pThr2609
*p<0.001 (to β-Lap)
DMSO
KU55933
Nu7026
ß-Lap
KU+ß-Lap
NU+ß-Lap
Treatment
E.
Vehicle
β-Lap, 5 μM
β-Lap, 12 μM
DNA-PKcs
PAR
α-Tubulin
1 2 3 4 5 6
Relative PAR levels: 1.0 1.0 37 5.3 37 8.1

Bentle_Fig 4

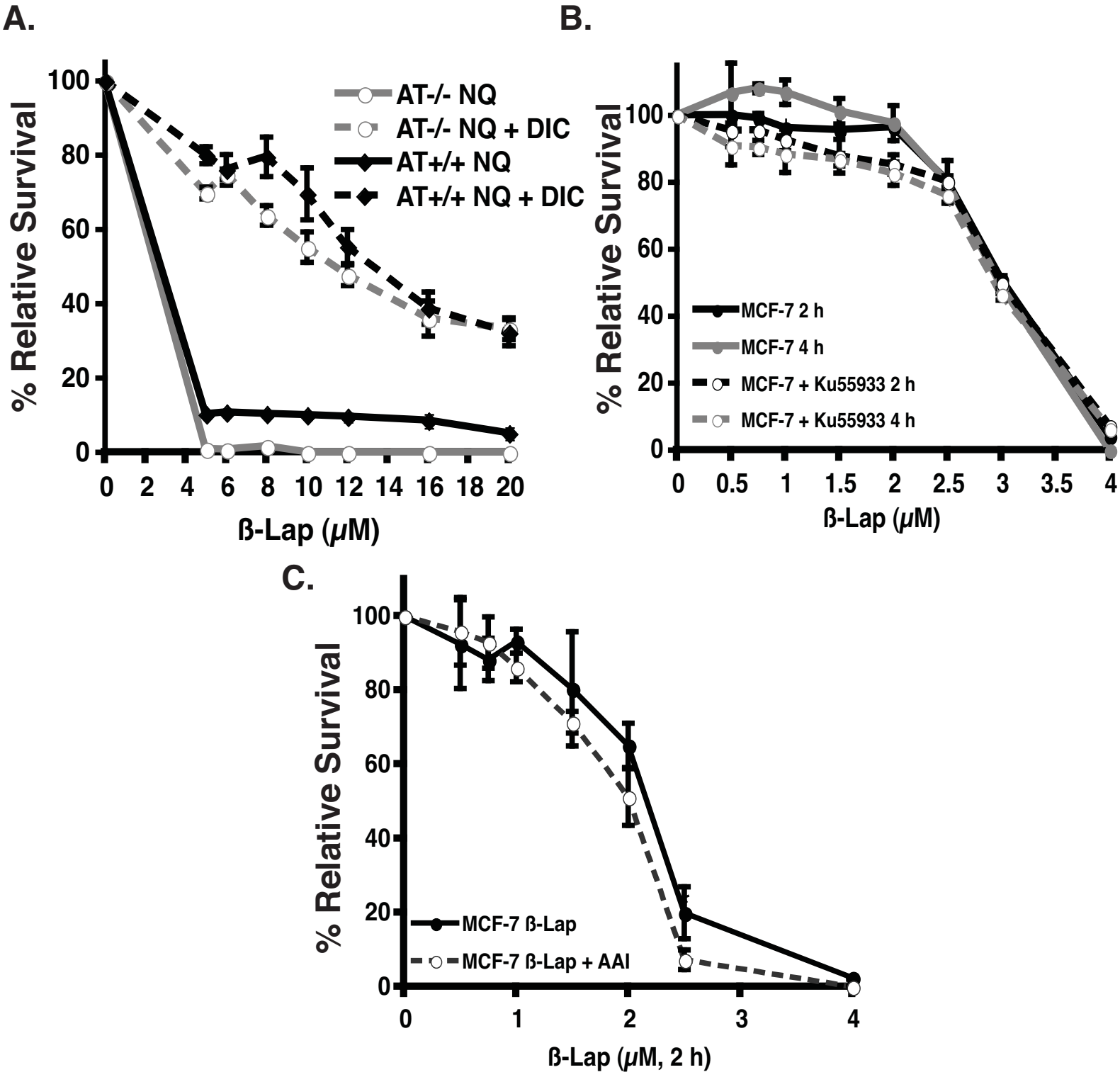
A.
% Relative Survival
AT-/- NQ
AT-/- NQ + DIC
AT+/+ NQ
AT+/+ NQ + DIC
ß-Lap (μM)
B.
% Relative Survival
MCF-7 2 h
MCF-7 4 h
MCF-7 + Ku55933 2 h
MCF-7 + Ku55933 4 h
ß-Lap (μM)
C.
% Relative Survival
MCF-7 ß-Lap
MCF-7 ß-Lap + AAI
ß-Lap (μM, 2 h)

Bentle_Fig. 5

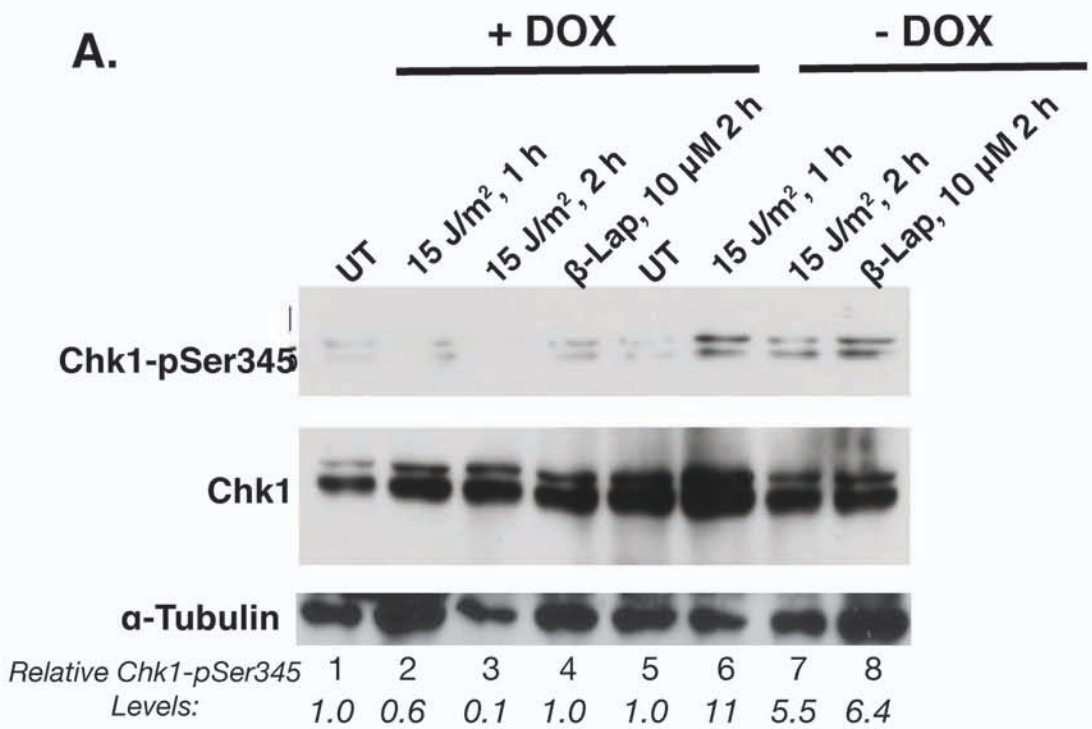
A.
+ DOX
- DOX
UT
15 J/m², 1 h
15 J/m², 2 h
β-Lap, 10 μM 2 h
UT
15 J/m², 1 h
15 J/m², 2 h
β-Lap, 10 μM 2 h
Chk1-pSer345
Chk1
α-Tubulin
Relative Chk1-pSer345 Levels:
1 2 3 4 5 6 7 8
1.0 0.6 0.1 1.0 1.0 11 5.5 6.4

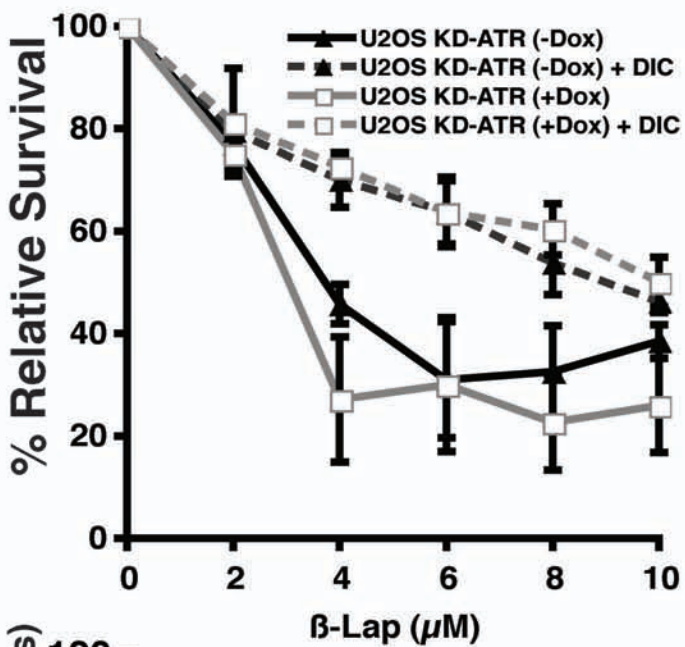
B.
% Relative Survival
U2OS KD-ATR (-Dox)
U2OS KD-ATR (-Dox) + DIC
U2OS KD-ATR (+Dox)
U2OS KD-ATR (+Dox) + DIC
100
80
60
40
20
0
0
2
4
6
8
10
ß-Lap (μM)

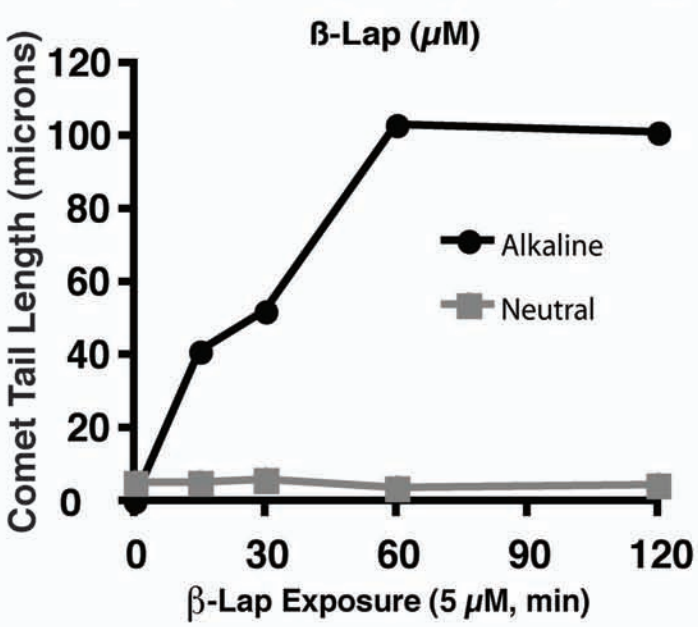
C.
Comet Tail Length (microns)
120
100
80
60
40
20
0
Alkaline
Neutral
0
30
60
90
120
β-Lap Exposure (5 μM, min)

Bentle_Fig. 6

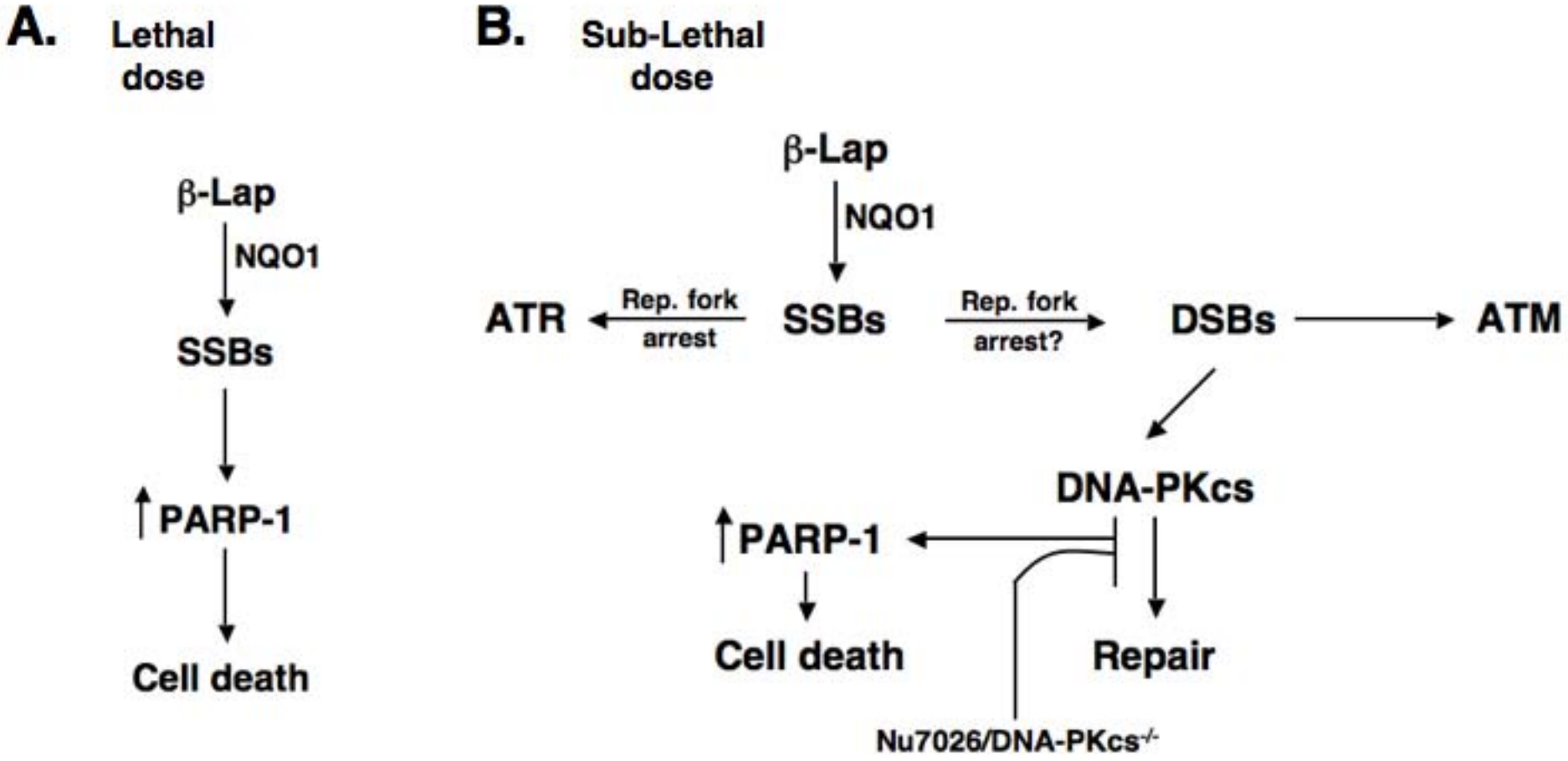
A.
Lethal dose
β-Lap
NQO1
SSBs
PARP-1
Cell death
B.
Sub-Lethal dose
β-Lap
NQO1
ATR
Rep. fork arrest
SSBs
Rep. fork arrest?
DSBs
ATM
DNA-PKcs
PARP-1
Cell death
Repair
Nu7026/DNA-PKcs-/-

Bentle_Supplementary Fig 1

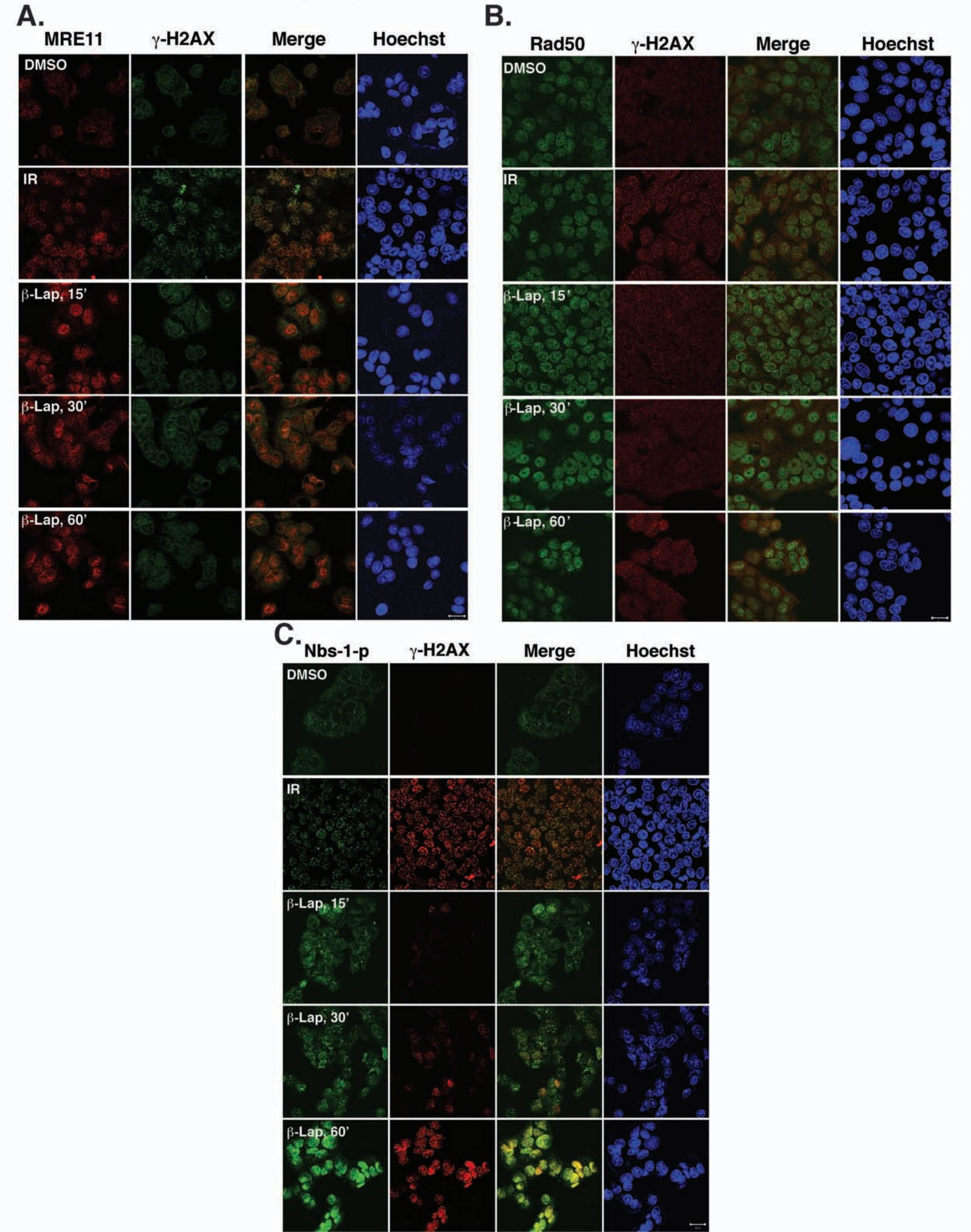

Bentle_Supplementary Fig. 2

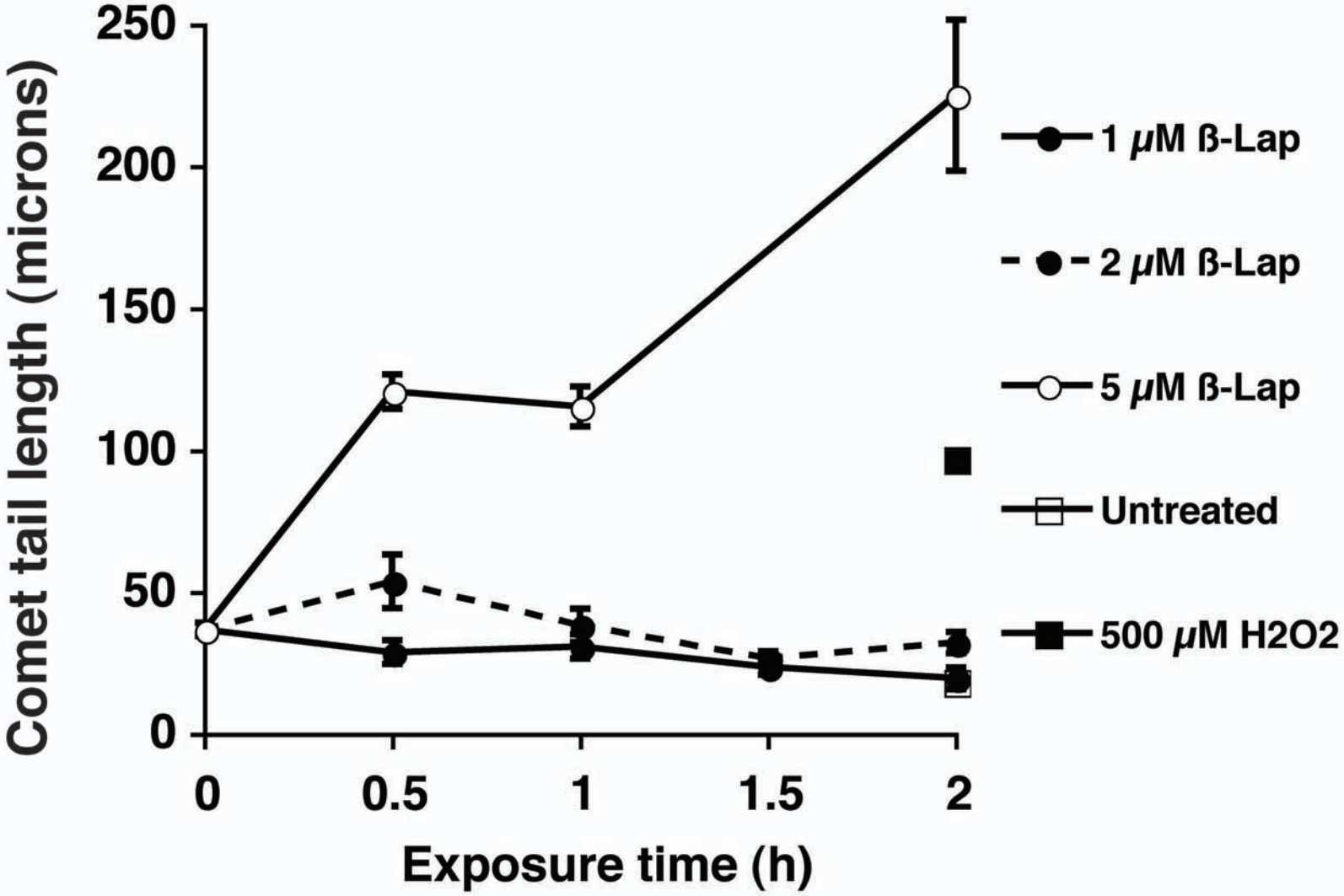

Bentle_Supplementary Fig 3

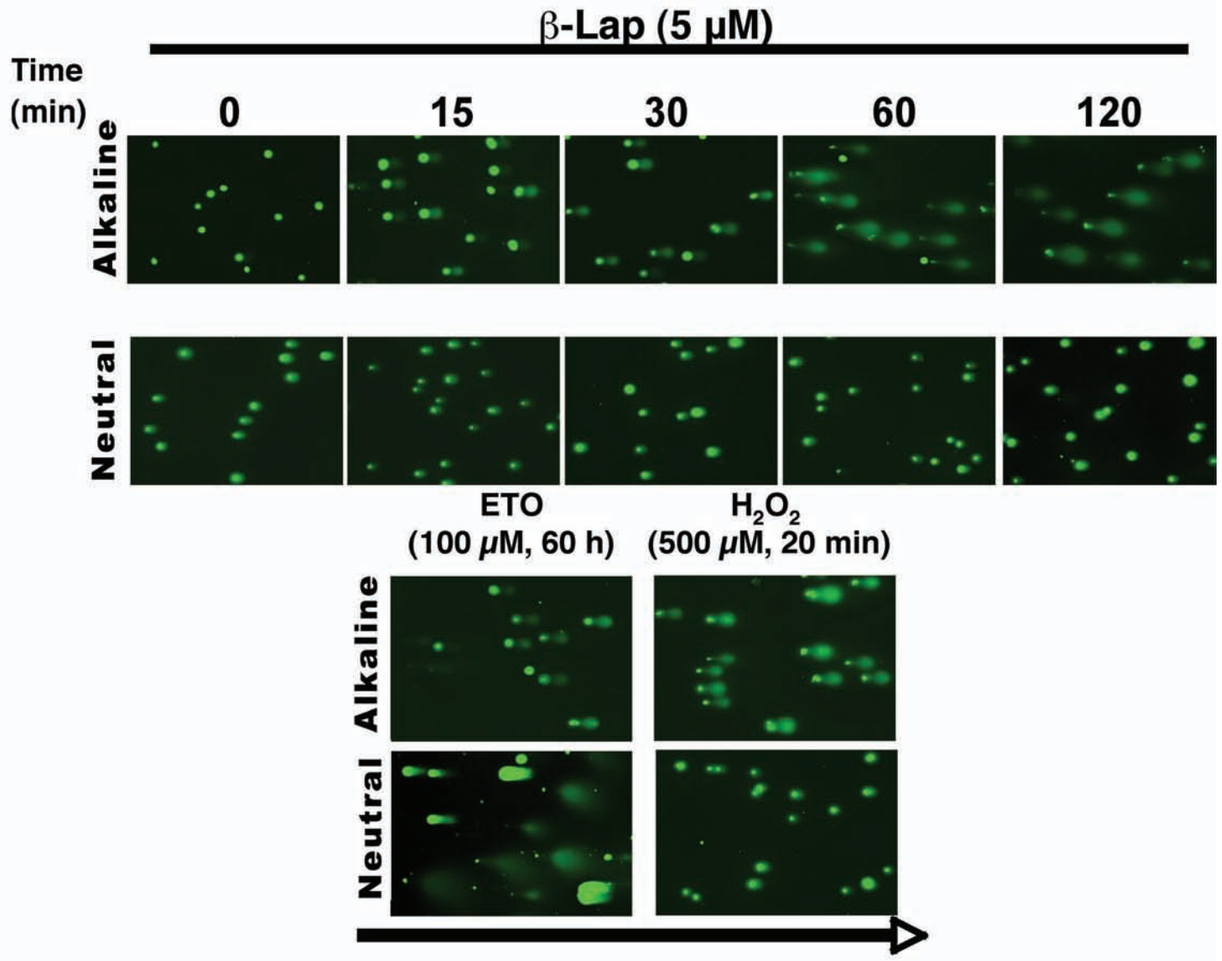

Bentle_Supplementary Fig. 4